On the Molecular Mechanisms of Functional and Dysfunction NO Signaling in Mammalian Physiology

By

Nathaniel Bernard Fernhoff

A dissertation submitted in partial satisfaction of the

requirements for the degree of

Doctor of Philosophy

in

Molecular and Cell Biology

in the

Graduate Division

of the

University of California, Berkeley

Committee in charge:

Professor Michael A. Marletta, Chair
Professor Susan Marqusee
Professor Judith P. Klinman
Professor Matthew B. Francis

Spring 2010

On the Molecular Mechanisms of Functional and Dysfunction

NO Signaling in Mammalian Physiology

Nathaniel Bernard Fernhoff

Abstract

On the Molecular Mechanisms of Functional and Dysfunction NO Signaling in Mammalian Physiology

by

Nathaniel Bernard Fernhoff

Doctor of Philosophy in Molecular and Cell Biology

University of California, Berkeley

Professor Michael A. Marletta, Chair

Nitric oxide (NO) is an important physiological mediator of vasodilation, platelet aggregation, and neurotransmission. An NO signal regulates these processes by signal transduction through the enzyme soluble guanylate cyclase (sGC), and dysfunction in this pathway manifests in human disease. NO activates sGC several hundred fold to produce the second messenger cGMP, and the mechanism of activation was previously thought to result exclusively from NO binding to the sGC heme. However, recent studies have shown that heme-bound NO only partially activates sGC and additional NO binding to a nonheme site is required for maximal NO activation. Therefore, understanding the nature the nonheme-NO coordination is crucial to understanding the mechanism of enzyme activation.

Thiol oxidation of sGC cysteines results in the loss of enzyme activity, therefore, the role of cysteines in NO-stimulated sGC activity was investigated. We found that the thiol modifying reagent methyl methanethiosulfonate specifically inhibits NO activation of sGC by blocking the non-heme site, which defines a role for sGC cysteine(s) in mediating NO binding. The nature of the NO/cysteine interaction was probed by examining the effects of redox active reagents on NO-stimulated activity. These results show that NO binding to, and dissociation from, the critical cysteine(s) does not involve a change in the thiol redox state. Evidence is provided for non-heme NO in the physiological activation of sGC in context of a primary cell culture of human umbilical vein endothelial cells. These findings have relevance to diseases involving the NO/cGMP signaling pathway.

Heme-oxidation also results in the loss enzyme activity and may play a role in the NO-desensitization of sGC in cardiovascular disease. *In vitro,* the sGC heme is typically found in the ferrous [Fe(II)] state, which is activated several hundred fold by NO. Comparatively, the ferric [Fe(III)] form of sGC is only weakly activated by NO, but the mechanism of this blunted response is not well understood. Specifically, sGC undergoes a reaction with NO termed reductive nitrosylation, where the sGC heme is reduced to the

ferrous [Fe(II)] state; but despite the recovery of the initial heme state, NO-stimulated activity does not recover. We found that the reduction of the sGC heme occurs via a coupled oxidation of an sGC cysteine to a nitrosothiol, and that the *S*-nitrosation of this key cysteine inhibits the enzymatic response to NO. The data from chapter 2 suggests the mechanism of inhibition may be the oxidation of a cysteine that constitutes the nonheme NO binding site. Thus, thiol-oxidation is at the root of the NO-desensitization of heme-oxidized sGC and the implications to human health and disease are discussed.

TABLE OF CONTENTS

LIST OF FIGURES

Chapter 1

Chapter 2

Chapter 3

LIST OF TABLES

Chapter 2

Chapter 3

LIST OF ABBREVIATIONS

ATP	adenosine 5′-triphosphate
βME	β-mercaptoethanol
cGMP	cyclic guanosine 3′,5′-monophosphate
DEAE	diethylaminoethyl
DEA/NO	diethylammonium (Z)-1-(N,N-diethylamino)diazen-1-ium-1,2-diolate
DMSO	dimethyl sulfoxide
DTT	dithiothreitol
EDTA	ethylenediamine-N,N,N′,N′-tetraacetic acid
EIA	enzyme immunoassay
EPR	electron paramagnetic spectroscopy
ESI-MS	electrospray ionization mass spectrometry
GC	guanylate cyclase
GSH	glutathione
GTP	guanosine 5′-triphosphate
HEPES	4-(2-hydroxyethyl)-1-piperazineethane sulfonic acid
HUVEC	human umbilical vein endothelial cells
H-NOX	Heme-Nitric oxide-OXygen-binding domain
IBMX	3-isobutyl-1-methylxanthine
L-NAME	Nω-nitro-L-arginine methyl ester
MALDI-TOF	matrix-assisted laser desorption/ionization-time of flight
MMTS	methyl methanethiosulfonate
MW	molecular weight
NEM	N-ethyl maleimide
NMR	nuclear magnetic resonance
NOS	nitric oxide synthase
ODQ	1H-[1, 2, 4]oxadiazolol[4, 3-*a*]quinoxalin-1-one
PAS	PER, ARNT, SIM domain
PCR	polymerase chain reaction
PROLI/NO	1-(hydroxy-NNO-azoxy)-L-proline
SDS-PAGE	sodium dodecylsulfate-polyacrylamide gel electrophoresis
sGC	soluble GC
RSNO	nitrosothiol
TCEP	tris(2-carboxyethyl)phosphine
Trx	thioredoxin
TEA	triethanolamine
UV	ultraviolet
YC-1	[3-(5′-hydroxymethyl-2′-furyl)-1-benzylindazole]

ACKNOWLEDEMENTS

Before I enrolled in graduate school, I wanted to set a reasonable expectation for the experience, and I ultimately resolved to learn enough to be able rigorously answer biochemical questions. As I reflect on the last several years, I feel both a strong sense of accomplishment for my progress towards that goal as well as a swell of gratitude to the many people who have contributed to my education. I can be stubborn, arrogant, and insolent and these winsome attributes seem to unfailingly erupt when I am engaged in scientific discussion. Therefore, I am especially grateful to those who have helped me to develop as a scientist, as they have managed to persevere through my often coarse demeanor and combative disposition. I have an enormous respect and appreciation for them.

The predominant figure in my graduate education has been my advisor Michael Marletta. From his guidance, I've learned how to transform an exciting idea into a meaningful set of experiments and to organize the results into a scientific narrative. With significant effort, he has also ingrained in me the importance of effective communication in scientific presentations in both seminars and in publications. When a project stalled and I faltered, his constructive insight, advice, and assistance reined me in and nudged me back towards progress. Additionally, Michael actively fostered a collaborative and supportive environment that has been essential to my training, education, and well-being. For all this, I am sincerely grateful to have worked in his lab.

The University of California, Berkeley is an enormous institution that is responsible, at any given time, for the education of 25,000 undergraduate and 10,000 graduate students. As such, it seems as though it would be easy for any individual student to fall through the cracks of the administration. Particularly my first year of graduate school, Susan Marqusee was instrumental in helping me navigate the graduate experience, and I am very appreciative that she has remained a central figure in my education as her advice has often proved invaluable. I am also grateful to Judith Klinman and Jack Kirsch for their advice, insight, and contagious excitement about enzymology. These four faculty members are actually the original reasons I came to UC Berkeley, and I am incredibly thankful to have been able to work with each of them.

All of my labmates have positively contributed to my experience, but a few have been particularly important in my scientific training and development. Firstly, no one has been more influential than my collaborator Emily Derbyshire. Her encyclopedic knowledge and first-hand experience with sGC enabled us to embark on an otherwise impossibly challenging course of experiments. Her detailed and meticulous approach to science is inspirational, and I will constantly aspire to imitate it. Through our joint efforts attacking a problem, I learned the value in teamwork and the time we spent working together was without a doubt the most exciting, stimulating, and edifying aspect of my academic career. I am truly indebted to her.

I am also especially thankful to have had the distinct pleasure to work along side Doug Mitchell, Jacquin Niles, and Josh Woodward. By example and through countless discussions, Doug conveyed to me the tangible benefits of developing a strong chemical intuition to address biological problems; and he showed me that it is often better to go through an obstacle than around it. Jacquin taught me both the operational imperative of grounding scientific endeavors in medically relevant systems and the utility of thorough forethought in a scientific pursuit. From my discussions with Josh, I learned to persevere through technical limitations and apparently insurmountable complications because even the most overwhelming scientific problems can often be worked out with the proper company, a pitcher[s] of beer, and a bucket of hot wings.

Finally, I am deeply grateful to my friends and family, who have genuinely shared in my experience throughout the marathon of the last six years. Their unwavering support and encouragement helped propel me through the trials and travails of graduate school. Their enthusiasm and affection made the successes and accomplishments even more rewarding.

Preface

In my time studying biochemistry, I have noticed that biologists are often hindered by their aversion to chemical terminology, but chemists are often mired in their hidebound nomenclature. Echoing the sentiments of the early Taoist philosopher Chuang Tzu, the real value in words is in conveying ideas, and once you've got the idea, you can forget about the words. Therefore, I have tried to present this technical work with accessible language, including both the exacting chemical wording and a more descriptive phrasing in the text. That said, the unifying theme of my graduate research has been following a single electron through various protein chemistries, and so I'd like to preface the text with a brief, but relevant, word on the nomenclature of nitric oxide (NO) reactions.

Nitrosation:	$R + NO^{\bullet}$	$\rightarrow$	$[RNO]^{+} + e^{-}$	formal addition of NO^{+}
Nitrosylation:	$R + NO^{\bullet}$	$\rightarrow$	$[RNO]$	formal addition of $NO^{\bullet}$
Nitroxylation:	$R + NO^{\bullet} + e^{-}$	$\rightarrow$	$[RNO]^{-}$	formal addition of NO^{-}

For example, the bimolecular association of NO to a metal center is referred to as a nitrosylation of the metal. However, the nitrosation of a thiolate ion (RS^{-}) by NO requires an electron acceptor and forms a nitrosothiol (RSNO).

As this nomenclature applies to this work, Chapter 2 concerns two tandem nitrosylation reactions that activate the NO receptor, soluble guanylate cyclase (sGC): the first is a standard nitrosylation of the heme iron and the second is an unusual nitrosylation of a protein thiol. This second reaction is importantly distinct from nitrosation, and the product differs by one critical electron. Therefore, while Chapter 2 describes sGC activation by thiol nitrosylation, Chapter 3 describes sGC inhibition by thiol nitrosation. Although the term nitrosylation is often used erroneously in reference to all three of the reactions above, it is essential to account for each electron, as the work in these pages ultimately demonstrates that the enzymatic response to an NO stimulus depends entirely on this one electron.

CHAPTER 1

INTRODUCTION

Motivation. Cardiovascular disease kills more people in the United States than any other medical condition (*1*). The diagnoses are rather broad as they refers to a vast number of conditions that adversely affect the heart or blood vessle, and this great variety of symptoms results from a great variety of molecular events. Therefore, a silver bullet therapeutic to treat all forms of cardiovascular disease is an exceedingly unlikely goal. A more manageable, albeit challenging, objective it to develop treatments for certain types of cardiovascular disease that stem from a well-defined molecular dysfunction.

Towards this end, nitric oxide (NO) signaling lies at a unique node in the vasodilatory signal transduction pathway. Many different input signals will trigger the stimulation of endothelial NO production, and cGMP is a second messenger for many different downstream effectors, and so other upstream and downstream signals can compensate for faulty signaling either before or after NO-sGC-cGMP. However, because sGC is the only point in this pathway that can transduce the NO signal into cGMP, sGC assumes a unique importance in human health and disease.

NO Signaling in Mammals

Nitric oxide (NO) is a toxic gas and for the majority of the 20th century, the biomedical community regarded NO primarily as an environmental pollutant from combustion engines or a health hazard from cigarette smoke. Then, in the 1980's, a rapid succession of reports revealed endogenous production of NO in many types of mammalian tissues and several physiological roles for NO were delineated soon thereafter (*2, 3*). The field of NO biology has developed rapidly since these early discoveries.

In eukaryotes, the enzyme nitric oxide synthase (NOS) catalyzes the formation of NO from a 5-electron oxidation of L-arginine, using NADPH and O_2 as co-substrates. The reaction is complex; NOS utilizes FAD, FMN, tetrahydrobiopterin, and heme as redox active cofactors in the reaction, but enzyme activity also requires a protein-protein interaction with Ca^{2+}-bound calmodulin and a dimerization of this entire complex, stabilized by a zinc tetrathiolate (*4*). In addition to the complicated catalytic chemistry, endogenous expression of NOS in mammals is distributed amongst three isoforms with tissue specificity: the inducible form, iNOS, and two constitutively expressed forms, eNOS and nNOS. Biochemically, iNOS is principally regulated at transcription, but eNOS and nNOS are principally regulated by their dependence on cytosolic Ca^{2+} levels (*5*).

The innate immune system produces NO as a cytotoxic agent to ward off invading microbes, and this mode of action dovetails with the potent chemical reactivity of NO. Because it is a small uncharged gas, NO rapidly diffuses across membranes and damages vital microbial biomolecules like metal centers, proteins, and DNA (*6*). Functionally,

when a macrophage engulfs a gram-negative microbe, the lipopolysaccharide component of the bacterial membrane activates the Toll-Like Receptor – 4 (TLR4) on the cell surface of the macrophage (*7*). This initiates a pro-inflammatory response that includes an induction of both the transcription of the iNOS gene and the expression of the iNOS protein. iNOS is highly active, owing to an irreversibly bound calmodulin, and translocates to outer membrane of the phagosome to generate mid- μM amounts of NO. At these relatively high local concentrations, NO reacts with O_2 to form higher order nitrogen oxides, which are substantially more reactive (*8*). Additionally, superoxide ($O_2^{\cdot-}$) is also generated by the phox family of NADPH oxidases (*9*), which combines with NO at a diffusion limited rate yielding peroxynitrite ($ONOO^-$). The reactive nitrogen species (RNS) and reactive oxygen species (ROS) effectively eliminate invading microbes and are crucial for immunity. Overproduction of NO from the immune system causes sepsis and chronic inflammation (*10*). The high concentration of NO produced in the immune system makes NO an effective cytotoxin.

NO is used in much lower amounts as a signaling molecule in the cardiovascular and nervous systems. The endothelial cells of the cardiovascular system, the cells that line the inner membrane of the vasculature, generate NO both to signal for vasodilation and to inhibit platelet aggregation (*11, 12*). Stimuli in the vasculature like bradykinin, acetylcholine, or VEGF, initiate signal transduction pathways that lead to calcium influx into the cytosol, causing calcium-bound calmodulin to bind eNOS, which activates the enzyme (*13*). In this context, stimulated output of NO is estimated to be in the mid-nM range, and at these concentrations the reactivity of NO is significantly tempered. Rather than reacting non-specifically with bulk biological material as in innate immunity, low levels of endothelium-derived NO diffuse as a paracrine hormone to neighboring smooth muscle cells (SMCs). In that tissue, NO causes SMC relaxation, which widens the caliper of the blood vessel and lowers blood pressure. Endothelium-derived NO controls another important macroscopic process in the cardiovascular system. Platelets are cell fragments that accumulate at points of injury to form a blood clot, however, inappropriate accumulation of platelets causes thrombosis and embolism (*12*). Since endothelial cells are located at the barrier between vasculature and stroma, the endothelial-derived NO has access to plasma and inhibits platelet aggregation. Because of the vital role for NO for the proper function of the cardiovascular system, the underproduction of NO causes hypertension and atherosclerosis, hallmarks of cardiovascular disease.

NO is also used as a neurotransmitter, notably in penile erection and neurons that innervate the gastrointestinal tract (*14, 15*). In the both cases, the nNOS isoform synthesizes NO in non-adrenergic, non-cholinergic neurons to transmit a vasodilatory signal to surrounding smooth muscle cells. Dysfunction in penile erection is often treated with sildenafil (Viagra®) which effectively increases the potency of NO by inhibiting downstream dampening elements of the signal transduction pathway (*16*) . Furthermore, nNOS-derived NO coordinates the peristaltic movements that push a food bolus along the gastrointestinal tract (*17*). NO is a critical effector of digestion and reproduction, and NO underproduction causes erectile dysfunction and may also have a role in neurodegenerative disorders (*18, 19*).

A sensor for the low concentrations of NO that are used in signaling necessitates a finely-tuned and highly-specific interaction for proper detection. The enzyme soluble guanylate cyclase (sGC) is the best characterized NO receptor and transduces the NO signal in the pathways discussed above. sGC catalyzes the conversion of guanosine 5'-triphosphate (GTP) to 3',5'-cyclic guanosine monophosphate (cGMP) using Mg^{2+} as a cofactor, and it also has a prosthetic heme group that is essential for allosteric activation by NO (*20, 21*). An NO signal stimulates enzymatic activity several hundred fold, causing the cellular accumulation of the second messenger cGMP, which directly activates protein kinase G (cKG), ion channels, and phosphodiesterases (PDEs) (*22*). There is significant cross-talk in these downstream pathways with overlapping stimulation and competing dampening, but the outcome is an increase in myosin phosphorylation, that causes dissociation from cytoskeletal actin, which is the biochemical underpinning of smooth muscle relaxation(*23*). Briefly, binding to cGMP activates protein kinase G to initiate a phosphorylation cascade that culminates in inhibition of myosin light chain phosphatase, increasing the amount of myosin phosphorylation. The cGMP-gated ion channels ultimately cause the influx of Ca^{2+}, and subsequently, Ca^{2+}-bound calmodulin activates myosin light chain kinase to further increase the amount myosin phosphorylation. The chief dampening effect downstream of cGMP is mediated by the cGMP activated PDEs, a class of enzyme that converts cGMP to GMP. Because cGMP activates it's own destruction, NO signaling has tight temporal regulation. In this manner, many physiological vasodilatory signals depend on the functional enzymatic activity of NOS and sGC.

Physiological NO Signaling: Genetic Deletions of NOS

Knockout mice illustrate the importance of the NO signaling pathway in mammalian physiology. Since NOS exists in three isoforms, the knockout mouse of each gene speaks to the role of that isoform *in vivo*. The iNOS knockout mice are more susceptible to microbial infection, which highlights the utility of iNOS in innate immunity (*24*). The eNOS deletion mutant causes hypertension and bradycardia, underlining the importance of NO signaling in the cardiovascular system (*25*). The data from the nNOS knockout mice actually provide a cautionary example for genetic deletion studies. The original nNOS knockout mice suffered from by pyloric stenosis and exhibited hyperaggression, but these mice were relatively healthy and unexpectedly fertile (*26, 27*). Further analysis revealed that the authors had knocked out exon 2 of nNOS, which is a coding region only for the dominantly expressed α splice variant, but the β and γ splice variants were unaffected and catalytically active. Nearly a decade, after the publication of the original mutant, the same first author of the original paper published a proper nNOS knockout as the corresponding author (*28*). The deletion of exon 6 prevents the catalytic chemistry of nNOS, since exon 6 codes for a critical portion of the heme-binding domain. Therefore, this mutant demonstrates the critically physiological role of nNOS, as these mice exhibit defective digestion and infertility.

The severity of genetic deletion of either eNOS or nNOS is mitigated by genetic compensation between the two isoforms (*29*). To examine the composite importance of NO, all three isoforms were simultaneously deleted, and the mice suffered from reduced

survival rates, reduced fertility rates, and nephrogenic diabetes insipidus (*30*). However, because these mice were generated from the original nNOS mutant of exon 2, a truly NO deficient phenotype in mammalian biology awaits experimental investigation.

Physiological NO Signaling: Genetic Deletions of sGC

sGC activity requires heterodimerization between both an α chain and a β chain, and each chain is encoded by 2 isoforms in the mammalian genome, enumerated as α1, α2, β1, and β2. Endogenously, the predominant form of sGC is α1β1, which is ubiquitously expressed. However, α2β1 is significantly expressed in brain and placenta(*31*), and expression of the β2 isoform has not been experimentally observed. Therefore, whereas genetic deletion of α1 and α2 only partially inactivates NO-stimulated sGC activity, genetic deletion of β1 fully inactivates sGC activity in the organism. Homozygous β1 deletion mutants are born with a Mendelian inheritance from heterozygotes, indicating proper development through gestation (*32*). However, a debilitating phenotype surfaces immediately and manifests as an 80% mortality rate within the first 2 days after birth. The survivors exhibit defective gastrointestinal motility and succumb shortly thereafter, unless rescued by a fiber-free diet. The surviving sGC knockout mice are hypertensive and their aggregating platelets do not disperse in response to NO. The severity of the sGC knockout phenotype highlights the importance of NO signaling in healthy mammalian physiology.

The α1 knockout mice are a striking example of residual activity masking a disease phenotype (*33*). In smooth muscle, the α1 knockout mice maintains only 6% of the NO stimulated sGC activity compared to wild-type mice, which is consistent with the dominant expression of the α1 isoform compared to the α2 isoform. Despite the overall inhibition, the partial activity from the α2 isoform is sufficient to maintain NO induced vasodilation, albeit with a slightly higher AC_{50}. Unlike the dysfunction of the total sGC knockout mice, the α1 knockout mice do not suffer from high mortality, hypertension, or gastrointestinal obstruction. Interestingly, platelets aggregation is not responsive to NO, but the α1 knockout mice are largely symptom-free. These mice emphasize functional sufficiency of even a small amount of NO stimulated sGC activity.

sGC Molecular Architecture

As discussed above, sGC senses an NO signal and transduces it into the second messenger cGMP. The enzyme has a low basal rate of cGMP synthesis that is stimulated several hundred fold in the presence of NO (*20*) and the molecular mechanism of activation bears direct relevance to human health. While there is no high resolution structure for full-length sGC, decades of biochemical research have generated detailed and practical information.

sGC is a heterodimeric protein consisting of an 80 kDa α1 subunit (690 AA [rat]) and a 70 kDa β1 subunit (619 AA [rat]). The subunits are highly homologous, but the catalytic site is comprised of residues from each chain; therefore, neither is active alone

and catalysis requires heterodimerization (*34*). Both the α1 and β1 chains may be functionally divided into 4 domains: H-NOX, PAS, coiled-coil, and catalytic domain.

The N-terminal region of β1 subunit binds to a prosthetic heme cofactor, which, in turn, binds to NO with a pM affinity. Truncation studies localized the minimally sufficient heme-binding domain of sGC to the N-terminal ~194 residues of the β1 subunit (*35, 36*), and mutational analysis identified β1 His105 as a coordinating ligand for the heme iron (*37*). Furthermore, the truncated heme domain faithfully recapitulates many of the ligand binding properties of full-length sGC and β1(1-194) is commonly used as a model for sGC. This portion of the sGC is a Heme Nitric Oxide / Oxygen (H-NOX) domain; a uniquely folded family of protein domains implicated in signaling and widely expressed in prokaryotes and eukaryotes, as described below. The N-terminal H-NOX domain of α1 does not bind heme, presumably in part, because it lacks the heme ligating histidine.

While there are structures for homologous PAS and coiled-coil domains (*38, 39*), the functional role of these domains in sGC are largely uncharacterized. These domains are generally proposed to mediate heterodimerization, orientation of the quaternary structure, and transmission of the conformational changes associated with allosteric regulation. However, the precise role of these domains awaits high-resolution structural data of full-length sGC in the basal and NO-stimulated states.

The C-terminal catalytic domains are highly homologous in sequence to adenylate cyclases, which perform a similar cyclization reaction to ATP. The individual catalytic domains α1(AA 467 - 690) and β1(414 - 619) can be recombinantly expressed, purified, and combined to recapitulate guanylate cyclase activity (*34*). A recent high-resolution structure of a guanylate cyclase catalytic domain was found to be structurally comparable to the adenylate cyclase (*20, 40*), and the active site chemistry can be inferred from these structures. The overall catalytic mechanism of the reaction simultaneously activates of the 3' hydroxyl of the ribose to a nucleophilic attack of the α phosphate group of GTP and stabilizes the developing negative charge on the pentavalent phosphate intermediate. The α1D485 and α1D529 residues coordinate 2 Mg^{2+} ions. While one Mg^{2+} coordinates the β and γ phosphate groups, the other Mg^{2+} provides the Lewis acidity to activates the 3' OH for nucleophilic attack. The ensuing covalent bond formation causes a negatively charged pentavalent phosphate intermediate which is stabilized by both a Mg^{2+} and β1R552, followed by loss of the pyrophosphate leaving group. Additionally important residues include β1N548 to orient the ribose ring, and α1R573 and to bind and orient the β and γ phosphates. Because of the high degree of homology between the α1 and β1 domains, the catalytic site is structurally related to a pseudo-symmetric site on the other side of the heterodimer. Although this site lacks catalytic residues, it is allosterically linked to the active site, as discussed below in the context of enzyme activation.

Ligand Specificity of sGC and H-NOX Domains

sGC exhibits unique ligand binding properties that are essential for an NO sensor operating in an aerobic environment. In a figurative haystack of O_2, sGC specifically

extracts the needle of NO. Moreover, sGC accomplishes this feat with a ferrous [Fe(II)] heme cofactor that has the intrinsic propensity to bind both O_2 and NO, as exemplified in globins. Even at a partial pressure of 1 atm, O_2 does not bind to or oxidize the ferrous [Fe(II)] heme of sGC and O_2 does not affect enzyme activity (*20*). NO, on the other hand, binds to the heme with a diffusion-limited on-rate and pM affinity, and activates the enzyme several hundred fold (*20, 41, 42*). Although they do not accumulate endogenously to a meaningful concentration, other heme ligands like carbon monoxide (CO), nitrosoalkanes (RNOs), and butyl-isocyanide (BIC) can bind to the sGC heme, but they show only a modest activation (4 – 5 fold) of the enzymatic activity (*20, 43-45*).

Ligand discrimination against oxygen is not only important for managing the competition of iron-coordination but it is also critical to prevent NO dioxygenation. In this reaction, the ferrous-oxy [Fe(II)-O_2] complex reacts with NO to yield a ferric [Fe(III)] heme product, which would blunt the enzymatic response of sGC to NO, as discussed in chapter 3. Because these NO dioxygenation reactions are very fast (~10^7 $M^{-1}sec^{-1}$) (*46, 47*), stable coordination of NO requires complete restriction of O_2 access to the heme. This remarkable specificity in ligand discrimination is a commonly employed feature of some H-NOX domains.

By searching genomic databases for sequences similar to the minimal heme-binding region of sGC, H-NOX domains emerged as a novel class of protein found in both prokaryotes and eukaryotes (*48*). While the H-NOX domains in eukaryotes are uniformly fused to a guanylate cyclase, the H-NOX domains in prokaryotes are found with a wider variety of partners and frequently in two-component signaling operons. In obligate anaerobes, the H-NOX domains are fused to a methyl accepting chemotaxis domain; and because these H-NOX domains also bind to O_2, they are suggested to serve as oxygen sensors that coordinate aerotaxis (*49*). In facultative aerobes, H-NOX domains have been identified in operons with a histidine kinase, in operons with a diguanylate cyclase, or as a stand-alone protein. These H-NOX domains only bind to NO but not to O_2, which suggests they are specific sensors for NO. In fact, NO has been shown to regulate such a system in *Shewanella oneidensis*, where NO binding to the H-NOX inhibits the auto-phosphorylation of the cognate histidine kinase (*50*).

H-NOX domains are a testament to the natural versatility of amino acid functionality in proteins. Employing the chemically identical ferrous [Fe(II)] heme cofactor that tightly coordinates O_2 in globins, H-NOX variants from different organism have dramatically different ligand specificities. As described above, while an H-NOX from one organism can bind both of the diatomic gasses NO and O_2, a highly homologous H-NOX from another organism can prevent O_2 from binding the heme while simultaneously permitting NO binding. The molecular mechanism for ligand discrimination in H-NOX domains has been distilled to a critical tyrosine located in the distal heme binding pocket which forms a hydrogen bond with bound O_2 to stabilize the interaction (*51, 52*). In the H-NOX domain from the obligate anaerobe *Thermoanaerobacter tengcongensis*, mutation of this key tyrosine residue to a phenylalanine is sufficient to inhibit O_2 binding. Conversely, such hydrogen bond donors are absent from the distal heme binding pockets of H-NOX domains in facultative aerobes, which only bind NO. Introduction of a

tyrosine into the key position of the distal pocket in a H-NOX domain from *Legionella pneumophila* restored stable O_2 binding to the heme by slowing the oxygen off-rate. Furthermore, this key tyrosine has so far proven a successful predictor of oxygen binding in both prokaryotic H-NOX domains (*53*) and in eukaryotic atypical guanylate cyclases (*54, 55*), which are found in some insects and have been biochemically verified to bind O_2.

This elegantly simple rule has demonstrated utility in both prediction of ligand specificity and protein engineering of H-NOX domains; however, it has proven to be a less reliable technique in protein engineering of ligand specificity in full-length sGC. Whereas introduction of the key tyrosine into the β1(1-194) heme domain allowed formation of the ferrous-oxy [Fe((II)- O_2] complex (*52*), this point mutation did not permit full-length sGC to bind O_2 (*56*). These results imply that the other sGC domains contribute to ligand discrimination, potentially by restricting oxygen access to the heme. Although one hydrogen bond donor was insufficient, insertion of an entire hydrogen bonding network into distal heme pocket did, in fact, induce O_2 binding to the sGC heme (*57*). The mechanism of ligand discrimination in sGC is an active area of research.

The Complexities of Enzyme Activation

The resting state of sGC is characterized by a 5-coordinate ferrous-unligated [5C Fe(II)] heme, where β1H105 donates the imidazole to occupy the 5th coordination site of the iron (*20, 37, 58*). NO binds to the heme iron at a diffusion-limited rate and initially forms a 6-coordinate intermediate, where both β1H105 and NO are simultaneously bound to the heme iron (*41*). As the histidine rapidly dissociates from the iron, this short-lived 6-coordinate intermediate converts to a stable 5-coordinate ferrous-nitrosyl [5C Fe(II)-NO] complex (*59*). In addition to this ligation state change of the heme, NO also stimulates the enzymatic activity several hundred fold, and the combination of these data inspired an early model of enzyme activation. Here, the iron-histidine bond allosterically restricts the conformation of the sGC active site to a low-activity state, but when NO binds and the iron-histidine bond ruptures, the sGC active site relaxes into a high activity conformation like a spring loaded trap (Figure 1). This straightforward model adequately applied to many early observations of sGC and it proved valuable in its simplicity; however, the model could not account for an observed bimolecular kinetic dependence of the iron-histidine bond rupture on the concentration of NO, which the model had incorrectly predicted to be unimolecular (*41, 60*). The anomalous kinetics went unresolved until a series of seminal experiments revealed a more complex and intricate mechanism of NO activation.

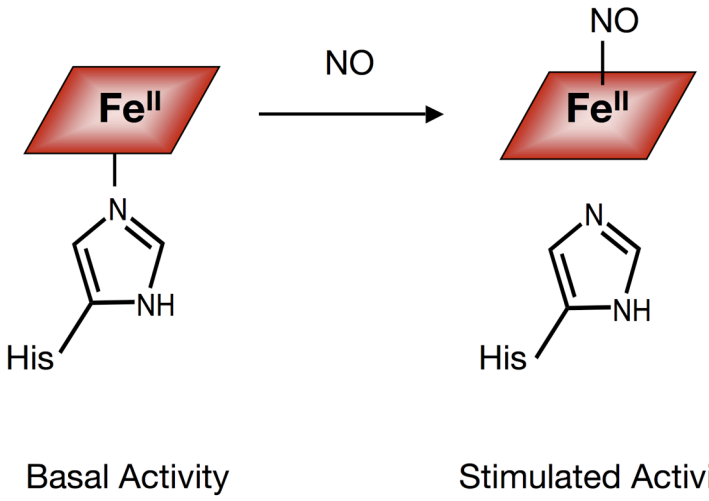

Figure 1: Binary model of NO-activation. sGC activity is allosterically inhibited by an iron-histidine bond between the ferrous heme and β1 His105. NO binding to the heme breaks this bond and induces a conformational change to a high-activity state.

This model ascribes a binary nature to sGC activation: when NO is bound to the heme, the enzyme is predicted to have stimulated activity; when NO dissociates from the heme, the enzyme is predicted to revert to basal activity. Decades of experimental observations supported the correlation between heme coordination of NO and enzyme activation, however the interdependence clearly uncouples for enzyme deactivation. To dissect enzyme deactivation, Cary and colleagues exploited the extremely tight, pM interaction of NO to the sGC heme (Figure 2) (*61*), which is associated with a slow NO off-rate (*42*). Because NO stably binds the sGC heme, free NO in solution and loosely bound NO can be entirely eliminated with an NO trap and subsequent small-molecule removal while maintaining the heme-ligation state. Indeed, under these conditions, sGC was isolated with NO bound to the heme, but it had a dramatically lower activity, roughly 10% of the full NO-stimulated activity. Therefore, contrary to the binary model of sGC activation, ligation of NO at the heme did not correlate with enzyme activation. Importantly, re-stimulation with NO of this low-activity, NO-bound form of sGC fully re-activated the enzyme, ensuring sGC was not subject to non-specific damage during the process of NO removal. This data demonstrates that NO binding to the heme only moderately activates sGC, but additional NO binding to a 2nd site is ultimately responsible for the massive stimulation of enzyme activity. Furthermore, just as each site of NO binding is related to a discrete activation event, each NO-dissociation event correlates with a discrete deactivation. NO dissociation from the 2nd site occurs quickly with a half-life of ~2 seconds and the fast decay of enzyme activity upon removal of the NO stimulus bestows a tight temporal regulation to signal transduction. Furthermore, NO dissociation from the heme occurs slowly with a half-life of ~20 minutes and the slow decay of this partially stimulated enzyme bestows a memory element in the regulation of signal transduction.

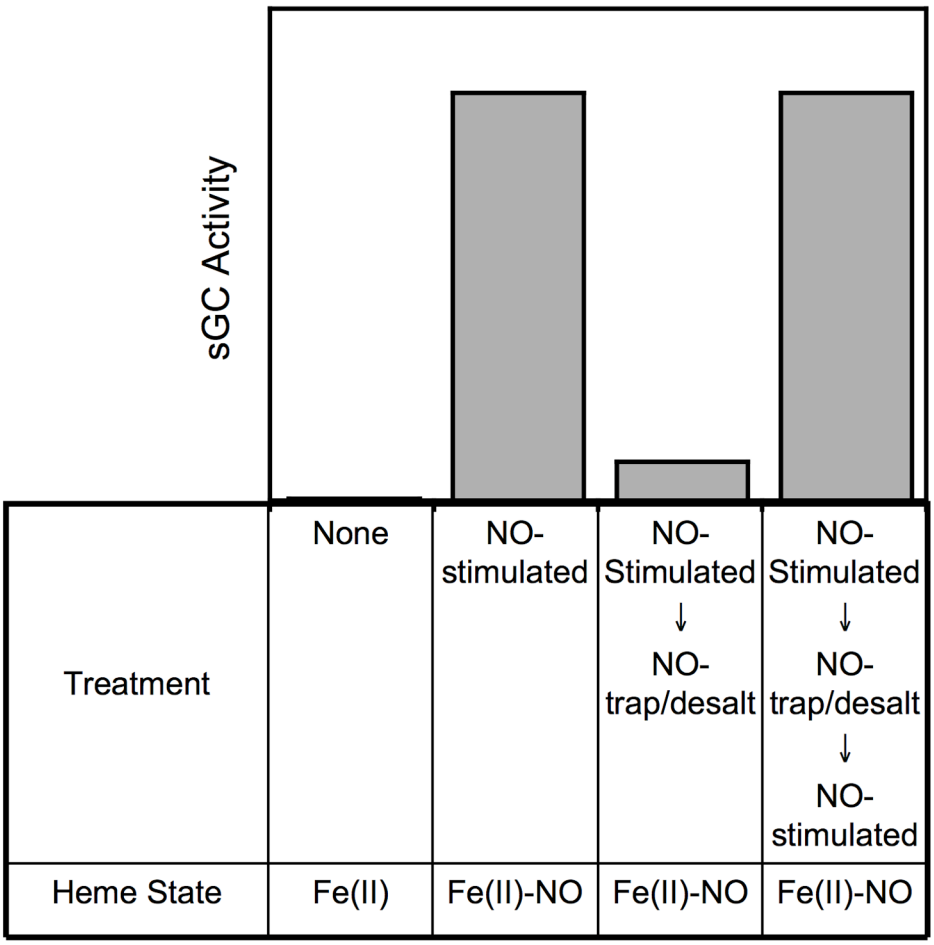

Figure 2: NO-binding to a nonheme site causes the maximal stimulation of sGC. Schematized data obtained by Cary, Winger, and Marletta (*61*). The basal state of sGC is characterized by both a low activity and a ferrous-unligated [Fe(II)] heme. Stimulation with NO activates the enzyme several hundred fold and forms a ferrous-nitrosyl [Fe(II)-NO] complex at the sGC heme. Subsequently, solution NO and (loosely-bound NO) is destroyed via an NO trap, and the decomposition products are removed by anion exchange. This form of the enzyme is deactivated but the heme remains entirely as the ferrous-nitrosyl [Fe(II)-NO] complex, as determined spectrally. Finally, the deactivated enzyme is re-stimulated with NO, and re-activated to full stimulation, thus ensuring the process of NO-removal leaves the enzyme intact. Since enzyme activation and deactivation occurs with solution NO concentration but without a change to the ligation state of the heme, NO binding to a nonheme site is responsible for the full NO stimulation.

The experiments described above coincided with an independent line of investigation that similarly revealed a critical of 2nd site of NO binding for enzyme stimulation. In these experiments, Russwurm and Koesling titrated sub-stoichiometric amounts NO against sGC, creating a mixture of sGC heme bound and unbound to NO (Figure 3) (*62*). They then spectrally determined the fractional ligand occupancy of the sGC heme and simultaneously measured the activity of the mixture. Assuming saturating substrate concentrations, the properties of a binary system are given by the following equations:

$$V_{obs} = V_{basal} \times frac_{unbound} + V_{NO} \times frac_{bound}$$

and since:

$$frac_{unbound} + frac_{bound} = 1$$

then:

$$V_{obs} = V_{basal} + (V_{NO} - V_{basal}) \times frac_{bound}$$

where V_{obs} is the measured activity; V_{basal} is activity of unbound sGC (basal activity); V_{NO} is the activity of NO-bound sGC (NO stimulated activity); $frac_{unbound}$ is the ratio of unbound sGC to total sGC; and $frac_{bound}$ is the ratio of NO-bound sGC to total sGC.

Therefore, the governing equations of a binary system predict that the observed activity is linearly related to the fraction of heme-bound NO, and the slope of this line is equal to the $V_{NO} - V_{basal} \approx V_{NO}$. However, experimentally, the slope was only ~10% of V_{NO}, and the observed activity deviated dramatically from linearity when $frac_{bound} = 1$. In other words, when sGC binds NO at the heme, the enzyme only partially stimulates, but further addition of NO induces full stimulation. These results unequivocally demonstrated that NO binding to the heme induces a conformational change to a state we refer to as 1-NO, and NO binding to a 2nd site induces another conformational change to a state we refer to as xsNO. Therefore, sGC exhibits 3-state behavior in response to NO: basal, 1-NO, and xsNO (Figure 4).

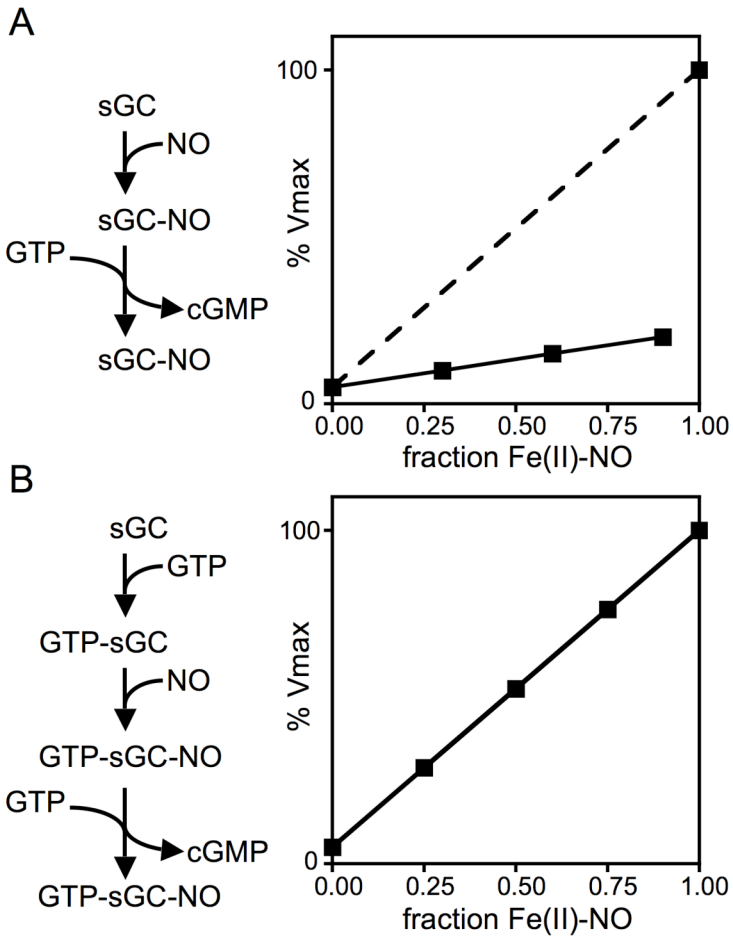

Figure 3: 3-state behavior in NO activation of sGC and a nucleotide switch to 2-state behavior. Schematized data obtained by Russworm and Koesling (*62*). (A) sGC was treated with a substoichiometric amount of NO creating a mixture of heme-bound NO and heme-free sGC (squares). The contribution of each form to the mixture was determined spectrally and the activity was assessed by the addition of GTP. The addition of excess of NO completely forms the ferrous-nitrosyl [Fe(II)-NO] complex at the sGC heme (fraction Fe(II)-NO = 1); however the enzyme is activated well beyond the linear expectation (solid line) from association at the heme. A two-state model predicts a linear transition to full stimulation (dotted line). Therefore, enzyme activation is 3-state: the basal state, a low activity form without a heme-bound ligand; the 1-NO state, a form of intermediate activity and NO coordinated to the heme; and the xsNO state, a high activity state and NO bound to both the heme and a nonheme site. (B) Pre-incubation with GTP allosterically potentiates NO activation by binding the pseudosymmetric site. This form of the enzyme forms a spectrally identical ferrous-nitrosyl [Fe(II)-NO] complex, and NO-binding at the heme induces full stimulation (solid line), in a linear manner. Therefore, when GTP is pre-bound to the pseudosymmetric site, the enzyme activation is a 2-state: the basal state, a low activity form without a heme-bound ligand; and the NO-stimulated state, a high activity state with NO-bound at the heme. The y-intercept in both (A) and (B) indicates basal activity, V_{max} is similar for both 3-state and 2-state behavior with saturating NO.

Subsequent EPR spectroscopy has shown that a change in the heme environment accompanies the transition from 1-NO to xsNO, indicating that binding NO to the 2nd site induces a conformational change in H-NOX domain (*63*). Evidence that the 2nd site of NO binding is distinct from the heme iron was obtained by preventing NO binding to the heme and measuring residual NO-stimulated activity (*44*). In that work, butyl-isocyanide (BIC) was shown to tightly coordinate the sGC heme and effectively compete against NO binding. In the presence of NO, BIC remained bound to the sGC heme but NO further activated the enzyme. Thus, with the heme site blocked, NO still bound at the nonheme site to induce activation. Chapter 2 describes our efforts to further characterize the second site.

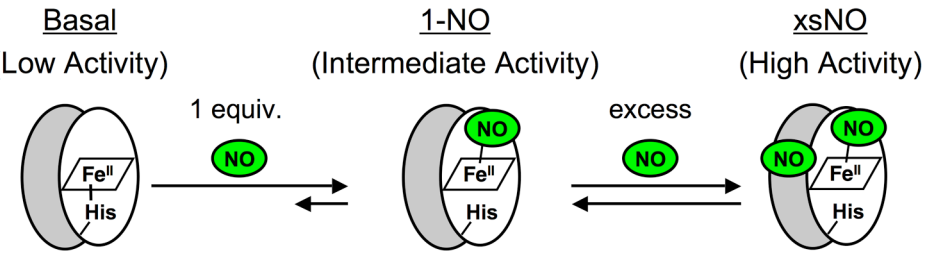

Figure 4: 3-state model of NO activation of sGC. The resting state of sGC is characterized by a low activity and an iron-histidine bond between a 5-coordinate ferrous heme and β1 H105. NO initially binds at the heme and breaks the iron-histidine bond, inducing an intermediate activation. Additional NO binds at a nonheme site and induces a further conformational change that fully stimulates the enzyme.

Superficially, the weak stimulation of 1-NO activity over basal activity casts doubt on the functional relevance of the 1-NO state in physiological NO signaling. However, slight differences in total sGC activity can be magnified *in vivo*, as in the α1 knockout mice described above. While the vasculature of these mice exhibit only 6% of the total sGC activity compared to wild-type, this residual activity prevents the disease phenotype of the complete sGC knockout (*33*). In light of these measurements, the physiological relevance of the 1-NO state, with ~10% of full stimulation, seems a prudent hypothesis. It has been suggested that localization of sGC to the vicinity of a cGMP receptor may account for the signal propagation even with diminished overall activity.

Various small molecules allosterically regulate sGC and modulate the enzymatic response to NO. For instance, ATP is a mixed type inhibitor of sGC exerting both a competitive inhibition at the active site and an allosteric inhibition likely at the pseudo-symmetric site (*64*). The pseudo-symmetric site is inferred based on the high homology between the α and β subunits but it lacks catalytic residues, and its existence is supported by the experimental observation that sGC binds two equivalents of nucleotide (*65*). While ATP binding at this site inhibits turnover, GTP binding at this site primes the enzyme for NO activation (*62*). Specifically, when sGC is treated first with NO to form an sGC-NO complex and then treated with GTP, three distinct states are observed: basal, 1-NO, and xsNO, as discussed above. However, markedly different properties are observed if GTP is first added to the enzyme to form the sGC-GTP complex and then

treated with NO. Only two states are observed, basal and NO-stimulated, and the system may be adequately describe by the equations discussed above (Figure 3). In other words, when GTP is bound in the pseudo-symmetric site, one equivalent of NO bound to the heme is sufficient to fully stimulate the enzyme. ATP competes with GTP for the pseudo-symmetric site and the three-state behavior is restored in the sGC-ATP complex (*61*). Therefore, a complex interplay amongst NO binding at both the heme iron and the nonheme site and nucleotide binding at both the active site and psuedosymmetric site regulates sGC activity. The conditional responses to various allosteric inputs reflects the potential of sGC to tune the magnitude and duration of cGMP output to an appropriate level depending of the physiological application.

YC-1 is a benzyl-indazole derivative that was identified in a pharmaceutical screen for sGC activators (*66*). Crosslinking experiments have shown that YC-1 binds to the α1 H-NOX domain of sGC (*67*) and YC-1 allosterically activates the enzyme in a heme-dependent manner (*61, 68, 69*). Specifically, YC-1 differentially activates sGC only when a ligand is bound to the heme, but has minimal effect on sGC in the basal state when no ligand is bound to the heme. Therefore, YC-1 is a suitable probe for the ligation state of the heme in biological samples, where the complexity of cellular components and the rare abundance of sGC preclude spectroscopic characterization. YC-1 binding to sGC is relatively weak (mid μM, and therefore, second generation molecules like BAY 41-2272 were developed based on the YC-1 scaffold with improved potency (*70*). While this molecule showed early promise in animal models, early phase clinical trials did not meet experimental benchmarks in the treatment of heart failure (*71*). Another derivative of YC-1, BAY 63–2521 has performed well in phase 2 clinical trials for pulmonary hypertension (*72*).

Oxidation of sGC and Subsequent Stimulation with BAY 58-2667

The heme cofactor of sGC is purified in the ferrous [Fe(II)] oxidation state and is remarkably stable. Most hemoproteins are found in the ferric [Fe(III)] oxidation state under aerobic conditions, and only access the ferrous [Fe(II)] state transiently in a reaction cycle (*73*). The ferrous [Fe(II)] heme states are typically unstable aerobically, and readily oxidize to the ferric [Fe(III)] with the concomitant formation of superoxide (*74*). Globins like hemoglobin and myoglobin have tempered the inherent chemical reactivity of ferrous [Fe(II)] heme and exhibit slow oxidation rates with long half-lives ranging from 2 to 12 hours (*74*). sGC is unique in that it does not have an observable oxidation rate in aerobic buffer (*20*), owing to both the H-NOX ligand binding environment and contributions from the other domains, as discussed above. Although molecular oxygen does not oxidize the sGC heme, other oxidants that are produced endogenously like nitrite (NO_2^-), peroxynitrite ($ONOO^-$), and hydrogen peroxide (H_2O_2) can oxidize the heme (*75*). *In vitro*, oxidants like potassium ferricyanide ($K_3Fe^{3+}CN_6$) and ODQ are frequently employed as specific heme oxidants that can be used stoichiometrically to oxidize the sGC heme (*76-78*). As detailed in chapter 3, oxidation of the sGC heme results in enzyme with a blunted response to NO. Since cardiovascular disease is often associated with both increased oxidative stress and decreased sGC activity, the proposal has emerged that ferric [Fe(III)] sGC is the molecular cause for

some symptoms of cardiovascular disease. The molecule BAY 58-2667 was identified to selectively activate the heme-oxidized or the heme-free form of sGC (*79*), although the precise details of the mechanism are unclear (*80*). Selective activation of ferric [Fe(III)] sGC is a promising therapeutic strategy because it may target stimulation of sGC to disease blood vessels. BAY 58-2667 has shown promising results in animal models and is currently in phase 2b clinical trials for acute decompensated heart failure (*81*).

References

1. Lloyd-Jones, D., Adams, R. J., Brown, T. M., Carnethon, M., Dai, S., De Simone, G., Ferguson, T. B., Ford, E., Furie, K., Gillespie, C., Go, A., Greenlund, K., Haase, N., Hailpern, S., Ho, P. M., Howard, V., Kissela, B., Kittner, S., Lackland, D., Lisabeth, L., Marelli, A., McDermott, M. M., Meigs, J., Mozaffarian, D., Mussolino, M., Nichol, G., Roger, V. L., Rosamond, W., Sacco, R., Sorlie, P., Stafford, R., Thom, T., Wasserthiel-Smoller, S., Wong, N. D., and Wylie-Rosett, J. Heart disease and stroke statistics--2010 update: a report from the American Heart Association, *Circulation 121*, e46-e215.
2. Marletta, M. A., Yoon, P. S., Iyengar, R., Leaf, C. D., and Wishnok, J. S. (1988) Macrophage oxidation of L-arginine to nitrite and nitrate: nitric oxide is an intermediate, *Biochemistry 27*, 8706-8711.
3. Palmer, R. M., Ferrige, A. G., and Moncada, S. (1987) Nitric oxide release accounts for the biological activity of endothelium-derived relaxing factor, *Nature 327*, 524-526.
4. Alderton, W. K., Cooper, C. E., and Knowles, R. G. (2001) Nitric oxide synthases: structure, function and inhibition, *Biochem J 357*, 593-615.
5. Nathan, C., and Xie, Q. W. (1994) Regulation of biosynthesis of nitric oxide, *J Biol Chem 269*, 13725-13728.
6. MacMicking, J., Xie, Q. W., and Nathan, C. (1997) Nitric oxide and macrophage function, *Annu Rev Immunol 15*, 323-350.
7. Poltorak, A., He, X., Smirnova, I., Liu, M. Y., Van Huffel, C., Du, X., Birdwell, D., Alejos, E., Silva, M., Galanos, C., Freudenberg, M., Ricciardi-Castagnoli, P., Layton, B., and Beutler, B. (1998) Defective LPS signaling in C3H/HeJ and C57BL/10ScCr mice: mutations in Tlr4 gene, *Science 282*, 2085-2088.
8. Miersch, S., and Mutus, B. (2005) Protein S-nitrosation: biochemistry and characterization of protein thiol-NO interactions as cellular signals, *Clin Biochem 38*, 777-791.
9. Hampton, M. B., Kettle, A. J., and Winterbourn, C. C. (1998) Inside the neutrophil phagosome: oxidants, myeloperoxidase, and bacterial killing, *Blood 92*, 3007-3017.
10. Lowenstein, C. J., Dinerman, J. L., and Snyder, S. H. (1994) Nitric oxide: a physiologic messenger, *Ann Intern Med 120*, 227-237.
11. Moncada, S., Palmer, R. M., and Higgs, E. A. (1991) Nitric oxide: physiology, pathophysiology, and pharmacology, *Pharmacol Rev 43*, 109-142.
12. Walter, U., and Gambaryan, S. (2009) cGMP and cGMP-dependent protein kinase in platelets and blood cells, *Handb Exp Pharmacol*, 533-548.
13. Moncada, S., and Higgs, E. A. (2006) The discovery of nitric oxide and its role in vascular biology, *Br J Pharmacol 147 Suppl 1*, S193-201.
14. Burnett, A. L., Lowenstein, C. J., Bredt, D. S., Chang, T. S., and Snyder, S. H. (1992) Nitric oxide: a physiologic mediator of penile erection, *Science 257*, 401-403.
15. Stark, M. E., and Szurszewski, J. H. (1992) Role of nitric oxide in gastrointestinal and hepatic function and disease, *Gastroenterology 103*, 1928-1949.

16. Jeremy, J. Y., Ballard, S. A., Naylor, A. M., Miller, M. A., and Angelini, G. D. (1997) Effects of sildenafil, a type-5 cGMP phosphodiesterase inhibitor, and papaverine on cyclic GMP and cyclic AMP levels in the rabbit corpus cavernosum in vitro, *Br J Urol 79*, 958-963.
17. Desai, K. M., Sessa, W. C., and Vane, J. R. (1991) Involvement of nitric oxide in the reflex relaxation of the stomach to accommodate food or fluid, *Nature 351*, 477-479.
18. Chung, K. K., and David, K. K. Emerging roles of nitric oxide in neurodegeneration, *Nitric Oxide 22*, 290-295.
19. Burnett, A. L. (1997) Nitric oxide in the penis: physiology and pathology, *J Urol 157*, 320-324.
20. Stone, J. R., and Marletta, M. A. (1994) Soluble guanylate cyclase from bovine lung: activation with nitric oxide and carbon monoxide and spectral characterization of the ferrous and ferric states, *Biochemistry 33*, 5636-5640.
21. Stone, J. R., and Marletta, M. A. (1995) Heme stoichiometry of heterodimeric soluble guanylate cyclase, *Biochemistry 34*, 14668-14674.
22. Ignarro, L. J., Cirino, G., Casini, A., and Napoli, C. (1999) Nitric oxide as a signaling molecule in the vascular system: an overview, *J Cardiovasc Pharmacol 34*, 879-886.
23. Somlyo, A. P., and Somlyo, A. V. (1994) Signal transduction and regulation in smooth muscle, *Nature 372*, 231-236.
24. Wei, X. Q., Charles, I. G., Smith, A., Ure, J., Feng, G. J., Huang, F. P., Xu, D., Muller, W., Moncada, S., and Liew, F. Y. (1995) Altered immune responses in mice lacking inducible nitric oxide synthase, *Nature 375*, 408-411.
25. Huang, P. L., Huang, Z., Mashimo, H., Bloch, K. D., Moskowitz, M. A., Bevan, J. A., and Fishman, M. C. (1995) Hypertension in mice lacking the gene for endothelial nitric oxide synthase, *Nature 377*, 239-242.
26. Huang, P. L., Dawson, T. M., Bredt, D. S., Snyder, S. H., and Fishman, M. C. (1993) Targeted disruption of the neuronal nitric oxide synthase gene, *Cell 75*, 1273-1286.
27. Nelson, R. J., Demas, G. E., Huang, P. L., Fishman, M. C., Dawson, V. L., Dawson, T. M., and Snyder, S. H. (1995) Behavioural abnormalities in male mice lacking neuronal nitric oxide synthase, *Nature 378*, 383-386.
28. Gyurko, R., Leupen, S., and Huang, P. L. (2002) Deletion of exon 6 of the neuronal nitric oxide synthase gene in mice results in hypogonadism and infertility, *Endocrinology 143*, 2767-2774.
29. Son, H., Hawkins, R. D., Martin, K., Kiebler, M., Huang, P. L., Fishman, M. C., and Kandel, E. R. (1996) Long-term potentiation is reduced in mice that are doubly mutant in endothelial and neuronal nitric oxide synthase, *Cell 87*, 1015-1023.
30. Morishita, T., Tsutsui, M., Shimokawa, H., Sabanai, K., Tasaki, H., Suda, O., Nakata, S., Tanimoto, A., Wang, K. Y., Ueta, Y., Sasaguri, Y., Nakashima, Y., and Yanagihara, N. (2005) Nephrogenic diabetes insipidus in mice lacking all nitric oxide synthase isoforms, *Proc Natl Acad Sci U S A 102*, 10616-10621.

31. Mergia, E., Russwurm, M., Zoidl, G., and Koesling, D. (2003) Major occurrence of the new alpha2beta1 isoform of NO-sensitive guanylyl cyclase in brain, *Cell Signal 15*, 189-195.
32. Friebe, A., Mergia, E., Dangel, O., Lange, A., and Koesling, D. (2007) Fatal gastrointestinal obstruction and hypertension in mice lacking nitric oxide-sensitive guanylyl cyclase, *Proc Natl Acad Sci U S A 104*, 7699-7704.
33. Mergia, E., Friebe, A., Dangel, O., Russwurm, M., and Koesling, D. (2006) Spare guanylyl cyclase NO receptors ensure high NO sensitivity in the vascular system, *J Clin Invest 116*, 1731-1737.
34. Winger, J. A., and Marletta, M. A. (2005) Expression and characterization of the catalytic domains of soluble guanylate cyclase: interaction with the heme domain, *Biochemistry 44*, 4083-4090.
35. Zhao, Y., and Marletta, M. A. (1997) Localization of the heme binding region in soluble guanylate cyclase, *Biochemistry 36*, 15959-15964.
36. Karow, D. S., Pan, D., Davis, J. H., Behrends, S., Mathies, R. A., and Marletta, M. A. (2005) Characterization of functional heme domains from soluble guanylate cyclase, *Biochemistry 44*, 16266-16274.
37. Zhao, Y., Schelvis, J. P., Babcock, G. T., and Marletta, M. A. (1998) Identification of histidine 105 in the beta1 subunit of soluble guanylate cyclase as the heme proximal ligand, *Biochemistry 37*, 4502-4509.
38. Ma, X., Beuve, A., and van den Akker, F. Crystal structure of the signaling helix coiled-coil domain of the beta1 subunit of the soluble guanylyl cyclase, *BMC Struct Biol 10*, 2.
39. Ma, X., Sayed, N., Baskaran, P., Beuve, A., and van den Akker, F. (2008) PAS-mediated dimerization of soluble guanylyl cyclase revealed by signal transduction histidine kinase domain crystal structure, *J Biol Chem 283*, 1167-1178.
40. Winger, J. A., Derbyshire, E. R., Lamers, M. H., Marletta, M. A., and Kuriyan, J. (2008) The crystal structure of the catalytic domain of a eukaryotic guanylate cyclase, *BMC Struct Biol 8*, 42.
41. Stone, J. R., and Marletta, M. A. (1996) Spectral and kinetic studies on the activation of soluble guanylate cyclase by nitric oxide, *Biochemistry 35*, 1093-1099.
42. Winger, J. A., Derbyshire, E. R., and Marletta, M. A. (2007) Dissociation of nitric oxide from soluble guanylate cyclase and heme-nitric oxide/oxygen binding domain constructs, *J Biol Chem 282*, 897-907.
43. Stone, J. R., and Marletta, M. A. (1995) The ferrous heme of soluble guanylate cyclase: formation of hexacoordinate complexes with carbon monoxide and nitrosomethane, *Biochemistry 34*, 16397-16403.
44. Derbyshire, E. R., and Marletta, M. A. (2007) Butyl isocyanide as a probe of the activation mechanism of soluble guanylate cyclase. Investigating the role of non-heme nitric oxide, *J Biol Chem 282*, 35741-35748.
45. Derbyshire, E. R., Tran, R., Mathies, R. A., and Marletta, M. A. (2005) Characterization of nitrosoalkane binding and activation of soluble guanylate cyclase, *Biochemistry 44*, 16257-16265.

46. Blomberg, L. M., Blomberg, M. R., and Siegbahn, P. E. (2004) A theoretical study of myoglobin working as a nitric oxide scavenger, *J Biol Inorg Chem 9*, 923-935.
47. Dou, Y., Maillett, D. H., Eich, R. F., and Olson, J. S. (2002) Myoglobin as a model system for designing heme protein based blood substitutes, *Biophys Chem 98*, 127-148.
48. Iyer, L. M., Anantharaman, V., and Aravind, L. (2003) Ancient conserved domains shared by animal soluble guanylyl cyclases and bacterial signaling proteins, *BMC Genomics 4*, 5.
49. Boon, E. M., and Marletta, M. A. (2005) Ligand discrimination in soluble guanylate cyclase and the H-NOX family of heme sensor proteins, *Curr Opin Chem Biol 9*, 441-446.
50. Price, M. S., Chao, L. Y., and Marletta, M. A. (2007) Shewanella oneidensis MR-1 H-NOX regulation of a histidine kinase by nitric oxide, *Biochemistry 46*, 13677-13683.
51. Pellicena, P., Karow, D. S., Boon, E. M., Marletta, M. A., and Kuriyan, J. (2004) Crystal structure of an oxygen-binding heme domain related to soluble guanylate cyclases, *Proc Natl Acad Sci U S A 101*, 12854-12859.
52. Boon, E. M., Huang, S. H., and Marletta, M. A. (2005) A molecular basis for NO selectivity in soluble guanylate cyclase, *Nat Chem Biol 1*, 53-59.
53. Boon, E. M., Davis, J. H., Tran, R., Karow, D. S., Huang, S. H., Pan, D., Miazgowicz, M. M., Mathies, R. A., and Marletta, M. A. (2006) Nitric oxide binding to prokaryotic homologs of the soluble guanylate cyclase beta1 H-NOX domain, *J Biol Chem 281*, 21892-21902.
54. Huang, S. H., Rio, D. C., and Marletta, M. A. (2007) Ligand binding and inhibition of an oxygen-sensitive soluble guanylate cyclase, Gyc-88E, from Drosophila, *Biochemistry 46*, 15115-15122.
55. Gray, J. M., Karow, D. S., Lu, H., Chang, A. J., Chang, J. S., Ellis, R. E., Marletta, M. A., and Bargmann, C. I. (2004) Oxygen sensation and social feeding mediated by a C. elegans guanylate cyclase homologue, *Nature 430*, 317-322.
56. Martin, E., Berka, V., Bogatenkova, E., Murad, F., and Tsai, A. L. (2006) Ligand selectivity of soluble guanylyl cyclase: effect of the hydrogen-bonding tyrosine in the distal heme pocket on binding of oxygen, nitric oxide, and carbon monoxide, *J Biol Chem 281*, 27836-27845.
57. Derbyshire, E. R., Deng, S., and Marletta, M. A. Incorporation of tyrosine and glutamine residues into the soluble guanylate cyclase heme distal pocket alters NO and O2 binding, *J Biol Chem*. (*in press*)
58. Wedel, B., Humbert, P., Harteneck, C., Foerster, J., Malkewitz, J., Bohme, E., Schultz, G., and Koesling, D. (1994) Mutation of His-105 in the beta 1 subunit yields a nitric oxide-insensitive form of soluble guanylyl cyclase, *Proc Natl Acad Sci U S A 91*, 2592-2596.
59. Stone, J. R., Sands, R. H., Dunham, W. R., and Marletta, M. A. (1995) Electron paramagnetic resonance spectral evidence for the formation of a pentacoordinate nitrosyl-heme complex on soluble guanylate cyclase, *Biochem Biophys Res Commun 207*, 572-577.

60. Ballou, D. P., Zhao, Y., Brandish, P. E., and Marletta, M. A. (2002) Revisiting the kinetics of nitric oxide (NO) binding to soluble guanylate cyclase: the simple NO-binding model is incorrect, *Proc Natl Acad Sci U S A 99*, 12097-12101.
61. Cary, S. P., Winger, J. A., and Marletta, M. A. (2005) Tonic and acute nitric oxide signaling through soluble guanylate cyclase is mediated by nonheme nitric oxide, ATP, and GTP, *Proc Natl Acad Sci U S A 102*, 13064-13069.
62. Russwurm, M., and Koesling, D. (2004) NO activation of guanylyl cyclase, *EMBO J 23*, 4443-4450.
63. Derbyshire, E. R., Gunn, A., Ibrahim, M., Spiro, T. G., Britt, R. D., and Marletta, M. A. (2008) Characterization of two different five-coordinate soluble guanylate cyclase ferrous-nitrosyl complexes, *Biochemistry 47*, 3892-3899.
64. Derbyshire, E. R., Fernhoff, N. B., Deng, S., and Marletta, M. A. (2009) Nucleotide regulation of soluble guanylate cyclase substrate specificity, *Biochemistry 48*, 7519-7524.
65. Yazawa, S., Tsuchiya, H., Hori, H., and Makino, R. (2006) Functional characterization of two nucleotide-binding sites in soluble guanylate cyclase, *J Biol Chem 281*, 21763-21770.
66. Ko, F. N., Wu, C. C., Kuo, S. C., Lee, F. Y., and Teng, C. M. (1994) YC-1, a novel activator of platelet guanylate cyclase, *Blood 84*, 4226-4233.
67. Stasch, J. P., Becker, E. M., Alonso-Alija, C., Apeler, H., Dembowsky, K., Feurer, A., Gerzer, R., Minuth, T., Perzborn, E., Pleiss, U., Schroder, H., Schroeder, W., Stahl, E., Steinke, W., Straub, A., and Schramm, M. (2001) NO-independent regulatory site on soluble guanylate cyclase, *Nature 410*, 212-215.
68. Stone, J. R., and Marletta, M. A. (1998) Synergistic activation of soluble guanylate cyclase by YC-1 and carbon monoxide: implications for the role of cleavage of the iron-histidine bond during activation by nitric oxide, *Chem Biol 5*, 255-261.
69. Friebe, A., Schultz, G., and Koesling, D. (1996) Sensitizing soluble guanylyl cyclase to become a highly CO-sensitive enzyme, *EMBO J 15*, 6863-6868.
70. Stasch, J. P., and Hobbs, A. J. (2009) NO-independent, haem-dependent soluble guanylate cyclase stimulators, *Handb Exp Pharmacol*, 277-308.
71. Boerrigter, G., and Burnett, J. C., Jr. (2009) Soluble guanylate cyclase: not a dull enzyme, *Circulation 119*, 2752-2754.
72. Mittendorf, J., Weigand, S., Alonso-Alija, C., Bischoff, E., Feurer, A., Gerisch, M., Kern, A., Knorr, A., Lang, D., Muenter, K., Radtke, M., Schirok, H., Schlemmer, K. H., Stahl, E., Straub, A., Wunder, F., and Stasch, J. P. (2009) Discovery of riociguat (BAY 63-2521): a potent, oral stimulator of soluble guanylate cyclase for the treatment of pulmonary hypertension, *ChemMedChem 4*, 853-865.
73. Zhu, Y., and Silverman, R. B. (2008) Revisiting heme mechanisms. A perspective on the mechanisms of nitric oxide synthase (NOS), Heme oxygenase (HO), and cytochrome P450s (CYP450s), *Biochemistry 47*, 2231-2243.
74. Faivre, B., Menu, P., Labrude, P., and Vigneron, C. (1998) Hemoglobin autooxidation/oxidation mechanisms and methemoglobin prevention or reduction processes in the bloodstream. Literature review and outline of autooxidation reaction, *Artif Cells Blood Substit Immobil Biotechnol 26*, 17-26.

75. Reeder, B. J. The redox activity of hemoglobins: From physiological functions to pathological mechanisms, *Antioxid Redox Signal*.
76. Stone, J. R., Sands, R. H., Dunham, W. R., and Marletta, M. A. (1996) Spectral and ligand-binding properties of an unusual hemoprotein, the ferric form of soluble guanylate cyclase, *Biochemistry 35*, 3258-3262.
77. Zhao, Y., Brandish, P. E., DiValentin, M., Schelvis, J. P., Babcock, G. T., and Marletta, M. A. (2000) Inhibition of soluble guanylate cyclase by ODQ, *Biochemistry 39*, 10848-10854.
78. Schrammel, A., Behrends, S., Schmidt, K., Koesling, D., and Mayer, B. (1996) Characterization of 1H-[1,2,4]oxadiazolo[4,3-a]quinoxalin-1-one as a heme-site inhibitor of nitric oxide-sensitive guanylyl cyclase, *Mol Pharmacol 50*, 1-5.
79. Stasch, J. P., Schmidt, P., Alonso-Alija, C., Apeler, H., Dembowsky, K., Haerter, M., Heil, M., Minuth, T., Perzborn, E., Pleiss, U., Schramm, M., Schroeder, W., Schroder, H., Stahl, E., Steinke, W., and Wunder, F. (2002) NO- and haem-independent activation of soluble guanylyl cyclase: molecular basis and cardiovascular implications of a new pharmacological principle, *Br J Pharmacol 136*, 773-783.
80. Roy, B., Mo, E., Vernon, J., and Garthwaite, J. (2008) Probing the presence of the ligand-binding haem in cellular nitric oxide receptors, *Br J Pharmacol 153*, 1495-1504.
81. Lapp, H., Mitrovic, V., Franz, N., Heuer, H., Buerke, M., Wolfertz, J., Mueck, W., Unger, S., Wensing, G., and Frey, R. (2009) Cinaciguat (BAY 58-2667) improves cardiopulmonary hemodynamics in patients with acute decompensated heart failure, *Circulation 119*, 2781-2788.

Chapter 2
A Nitric Oxide/Cysteine Interaction Mediates Activation of sGC

Introduction

Cardiovascular disease is the leading cause of death in the United States and the enzyme soluble guanylate cyclase (sGC) is a therapeutic target for treatment of the disease. sGC is the central protein in the nitric oxide (NO)/cyclic GMP signaling cascade, a pathway that mediates diverse physiological functions including vasodilation, platelet aggregation, and neurotransmission (1-3). While over 20 years have passed since sGC was identified as the primary eukaryotic NO receptor (4), our understanding of the molecular details of sGC activation by NO continues to evolve.

sGC is a heterodimeric hemoprotein consisting of an 80 kDa α subunit and a 70 kDa β subunit. In mammals, there are two isoforms for each subunit, and the N-terminal domain (~200 residues) of the β subunit binds a heme cofactor. The unliganded enzyme exhibits a low level of cGMP production and is referred to as the basal state. NO coordination to the sGC heme has been thoroughly investigated and was presumed to cause the conversion of the unactivated basal enzyme to the activated NO-bound enzyme. Indeed, coordination of NO to the sGC heme cofactor correlates with a large increase of sGC activity (5, 6); however, we and others have recently demonstrated that NO ligation to the heme is not sufficient to fully activate sGC (7, 8).

NO initially binds to the sGC heme with picomolar affinity (9, 10), inducing a moderate activation of the enzyme (7, 8). This low activity form of the enzyme maintains a 1:1 stoichiometry of NO to sGC, and we refer to it henceforth as the 1-NO state. This 1-NO state exhibits a slow rate of NO dissociation (11, 12) and, as a consequence, this form of the enzyme can be stably isolated away from free NO in solution (7, 8, 13). The subsequent addition of excess NO to the 1-NO state further stimulates sGC to a high activity form that we refer to as the xsNO state. The xsNO state is spectrally identical to the 1-NO state, but it only persists in the presence of excess NO. When NO is removed from solution, the high activity of the xsNO state rapidly reverts to the low activity of the 1-NO state. Thus, all three sGC states (basal, 1-NO and xsNO) can be prepared and studied *in vitro* (7, 8). Importantly, these results define two different states of purified sGC with heme bound NO (7, 8); one with a high activity and one with a low activity.

Further evidence for a non-heme NO binding site was obtained by blocking the heme site with the tight-binding ligand butyl isocyanide, and then showing that NO still activated the enzyme (14). The dependence of sGC function on the non-heme NO binding site draws specific attention to its nature. There is precedent for reversible gaseous ligand binding in proteins involving a non-heme metal (15) or a hydrophobic binding pocket (16); however, sGC is isolated with only the heme iron, and other hydrophobic diatomic gasses such as N_2, CO, and O_2 fail to stimulate the enzyme. A plausible mechanism that could account for the selectivity of NO is through a transient reaction with a cysteine thiol.

In this work, we investigate the function of cysteines in the mechanism of non-heme NO activation, and demonstrate a physiological role for non-heme NO activation. These results suggest that oxidative damage can block the non-heme NO binding site, consequently inhibiting NO stimulation of sGC *in vivo*. These results provide a mechanistic explanation for observations of sGC inhibition by thiol modifying reagents and oxidants (17-19), and it is therefore relevant towards addressing the molecular mechanism of NO tolerance (19, 20), a disease state characterized by a decreased sensitivity to NO in cardiovascular tissue. Additionally, each sGC state (basal, 1-NO and xsNO) may be a unique target for therapeutic intervention in diseases involving sGC dysfunction. This work was done in collaboration with Emily Derbyshire, in Michael Marletta's lab (University of California, Berkeley).

Results and Discussion

Kinetic Characterization of sGC states.

It is known that the 1-NO state exhibits a low level of activity compared to the xsNO state (7, 8); however, a kinetic characterization of these different states has not been reported. Therefore, to further investigate the mechanism of non-heme NO activation of sGC, the V_{max} and K_m for GTP turnover was determined for the basal, 1-NO, and xsNO sGC states (Table 1). In the 1-NO state, NO coordination only to the heme leads to an increase V_{max} and a reduction in the K_m when compared to the basal state. Non-heme NO binding to the 1-NO state further increases V_{max} with no change in the K_m. This increase in V_{max} from the 1-NO state to the xsNO state indicates a shift to a more catalytically competent form of the enzyme upon NO binding to the non-heme site. Since the 1-NO state is activated above basal state, NO may be classified as a non-essential activator for the binding to both the heme and non-heme site. Therefore, each NO binding event induces a distinct conformational change in the active site.

Table 1. Kinetic Parameters of NO-Stimulated sGC States[a]

sGC state	V_{max} (nmol min^{-1} mg^{-1})	K_m (μM)
Basal	14.7 ± 1.3	360 ± 130
xsNO	3610 ± 90	46 ± 6
1-NO	64.1 ± 3.2	46 ± 13

[a]Activities acquired at 25 °C. Each state was prepared as described the materials and methods.

Non-Heme NO Activation is Mediated by Cysteine(s).

To examine the involvement of sGC cysteines in the mechanism of NO activation, the effect of a thiol reactive reagent on enzyme activity was tested. In these experiments rat α1β1 sGC was recombinantly expressed in a Sf9/baculovirus system and purified to homogeneity. Purified protein was then treated with the thiol reactive probe methyl methanethiosulfonate (MMTS), which modifies thiols through the formation of methyl disulfides (Scheme 1).

Scheme 1: The reaction of MMTS with thiols.

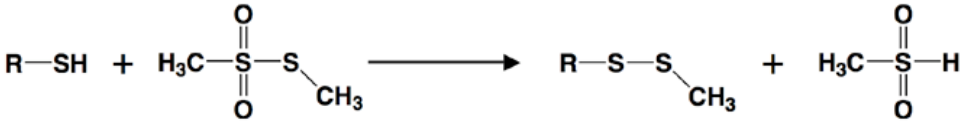

Since this reaction yields a disulfide product, it is reversible with thiol reductants like DTT. We found that MMTS inhibited NO stimulated sGC activity (Figure 1*A*), but electronic absorption spectroscopy showed that MMTS did not prevent the formation of the ferrous-nitrosyl complex (Figure 2). This MMTS-treated ferrous-nitrosyl complex was not stimulated by treatment with additional NO, but the allosteric activator YC-1 was able to activate the protein. YC-1 is an indazole derivative that weakly activates the basal enzyme, but strongly stimulates sGC activity when a ligand is coordinated to the heme (14, 21, 22). The observation of a MMTS-treated ferrous-nitrosyl complex demonstrates that thiol modification does not interfere with NO binding to the heme. Additionally, MMTS (≤ 100 μM) did not inhibit basal sGC activity (Figure 1*B*), which shows that the protein did not denature with MMTS treatment and that essential catalytic residues were not modified. MMTS inhibition of sGC was fully reversible by DTT (Figure 1*C*), demonstrating that the protein structure is not irreversibly damaged by the reaction. These results show that MMTS specifically inhibits the activation of sGC that results from NO binding.

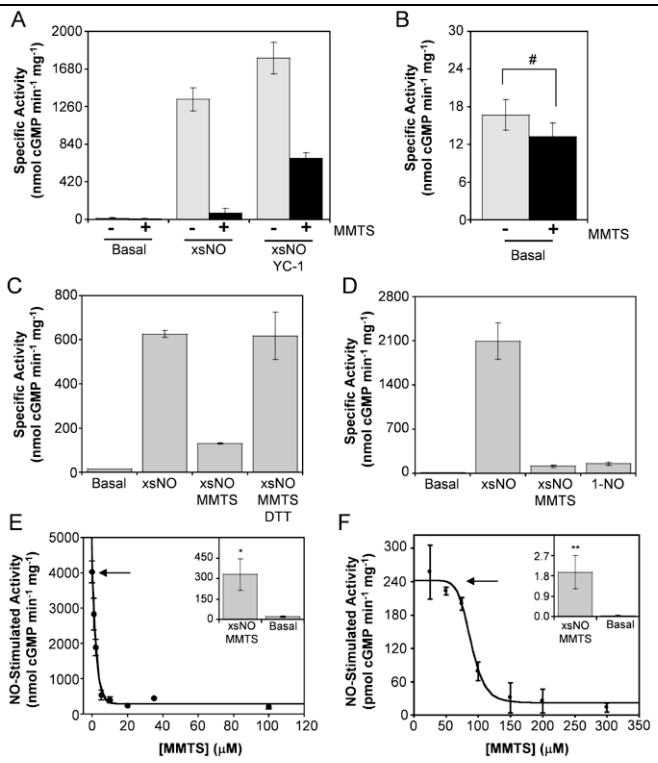

Figure 1: MMTS inhibition of NO-stimulation sGC activity *in vitro* and *in vivo*. (**A**) MMTS inhibits cGMP synthesis of NO-stimulated sGC (xsNO), but YC-1 activates the MMTS-treated protein in the presence of excess NO. (**B**) MMTS does not inhibit basal sGC activity to a statistically significant extent. (**C**) MMTS inhibition of sGC is reversible by DTT. (**D**) MMTS treated sGC is stimulated by NO to a level comparable to the activity of the 1-NO state. (**E**) Titration of MMTS against NO-stimulated sGC activity shows MMTS inhibition saturates at a level that is statistically greater than basal sGC activity (**E**, inset). (**F**) Titration of MMTS against NO-stimulated sGC activity shows inhibition in PC12 cells and this inhibition saturates at a level that is statistically greater than the GC activity in the absence of NO (**F**, inset). The arrow indicates maximal sGC activity in the presence of excess NO (**E** and **F**). Data are presented as means ± SD. #, $P = 0.27$; *, $P < 0.00015$; **, $P < 0.025$ in comparison to basal activity with purified protein (**E**) or PC12 cells (**F**), assessed by an unpaired *t*-test.

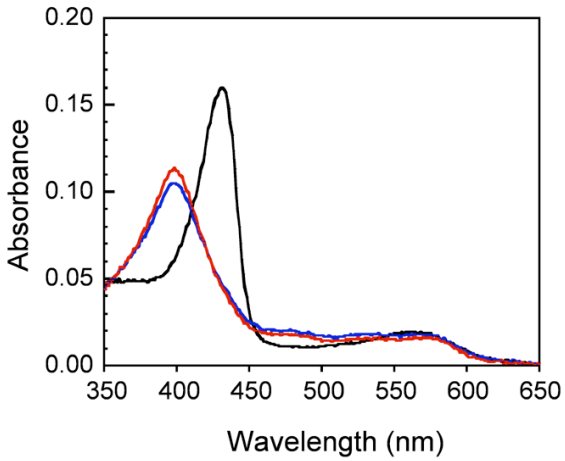

Figure 2: Electronic absorption spectra of the sGC-NO complex in the absence and presence of MMTS. Ferrous unligated sGC (black line) was treated with 30 μM MMTS and then exposed to 50 μM PROLI/NO (blue line). The MMTS-treated protein forms a ferrous-nitrosyl complex that is identical to the spectrum of the ferrous-nitrosyl complex formed in the absence of MMTS (red line).

Interestingly, NO stimulation of MMTS-treated sGC resulted in activity that is similar to that of the low-activity 1-NO form of the enzyme (Figure 1*D*). The observation that MMTS specifically inhibits NO stimulation led us to investigate whether cysteine modification by MMTS inhibits non-heme NO binding. To address this question, MMTS was titrated against sGC and NO stimulated activity was measured (Figure 1*E*). NO stimulated activity is inhibited at low μM MMTS and is zero order in MMTS between 15–100 μM. At concentrations greater than 100 μM, an irreversible loss in both basal and NO stimulated activity was observed. Therefore, high concentrations of MMTS lead to a general, non-specific inhibition of sGC (17). However, the observation of a saturated range of MMTS inhibition implicates a discrete set of cysteines in the mechanism of non-heme NO activation. This saturating effect of MMTS leaves the enzyme synthesizing cGMP at a rate that matches that of the 1-NO species. If modification caused a non-specific disruption of catalysis, the protein would be completely inhibited at saturating concentrations of MMTS. Also, since MMTS-treated sGC was stimulated by the combination of both NO and YC-1 (Figure 1*A*), MMTS does not sterically hinder the transition to the high activity state. Therefore, our observation that MMTS-treated sGC maintains partial NO stimulation, combined with the observation that MMTS-treated sGC binds NO at the heme, suggests that the transition from the 1-NO state to the xsNO state is impaired by cysteine modification. Thus MMTS blocks the cysteine(s) that constitute the non-heme NO binding site.

To assess the role of cysteines in regulating NO activation *in vivo*, MMTS inhibition of sGC activity in PC12 cells, a rat tumor cell line that endogenously expresses

sGC (23) was examined (Figure 1*F*). Similar to purified protein, the NO stimulated sGC activity exhibited a zero order dependence on MMTS between 100–300 μM. This indicates that reduced cysteines are necessary for activation beyond the 1-NO level of stimulation *in vivo*. The range of zero order activity differs from purified protein, likely owing to endogenous intracellular reductants. Additionally, since thiol modification with MMTS inhibits NO stimulated activity *in vivo*, it is possible that other reactants (more specifically intracellular oxidants) may inhibit cGMP production by reaction with the same cysteine. In fact, we have observed sGC inhibition *in vitro* with molecular oxygen as well as the thiol alkylating reagent N-ethyl maleimide (NEM) (Figure 3). Since both reactive oxygen species and decreased sGC activity are associated with cardiovascular disease (24), it is an attractive hypothesis that cysteine oxidation of the non-heme NO binding site causes symptoms in some forms of the disease. This cysteine oxidation would not affect cGMP production in either the basal or 1-NO sGC states, but would significantly impair that derived from the xsNO state. These results provide a causative molecular mechanism to observations that cysteine oxidation correlates with reduced sGC activity (17-19).

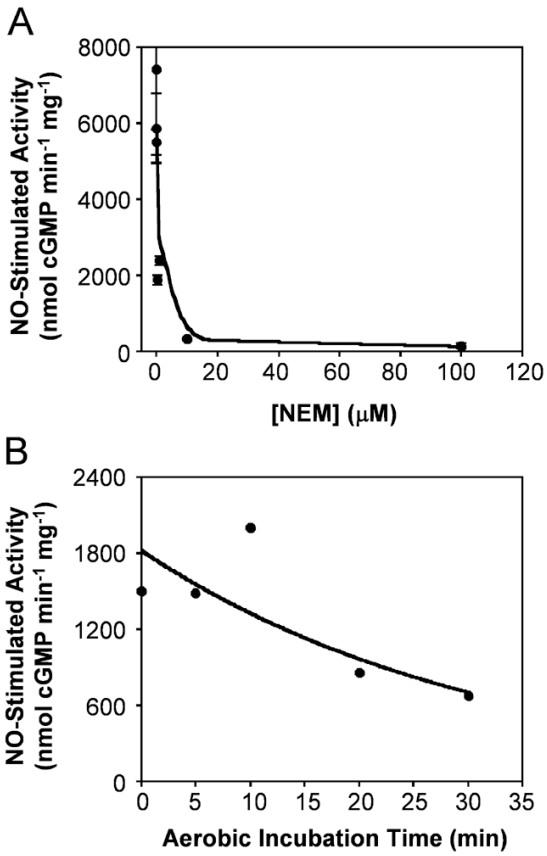

Figure 3. Inhibition of NO-stimulated sGC by thiol modification and oxidation. (**A**) Titration of NEM against NO-stimulated sGC activity shows NEM inhibition saturates at a level that is greater than basal sGC activity. (**B**) NO-stimulated sGC activity decreases when the enzyme is incubated in the absence of DTT in an aerobic buffer at 25 ºC

Characterization of sGC Cysteines Labeled by MMTS.

Since the reaction of MMTS with sGC restricts activation beyond the 1-NO state, we sought to estimate the stoichiometry of this reaction. By labeling sGC cysteines with MMTS and then exchanging the methyl disulfide modification for a biotin tag, the extent of the MMTS reaction can be readily visualized (Figure 4*A*) and quantified (Figure 4*B*). The MMTS reaction with sGC saturates ($\alpha1$ EC_{95} = 34 ± 7 μM; $\beta1$ EC_{95} = 36 ± 5 μM) and the labeling intensity can be used to estimate the number of MMTS-reactive cysteines by standardizing the labeling intensity to that of denatured sGC reacted with excess MMTS, where all cysteine residues are expected to react [20 cysteines in $\alpha1$ and

14 in β1 (Figure 5)]. This analysis projects that 16 ± 3 cysteines on α1 and 10 ± 1 cysteines on β1 react with MMTS under native conditions. Furthermore, at the minimally sufficient MMTS concentration to fully inhibit sGC (IC_{95} = 16 ± 2 μM, dotted vertical line Figure 4*B*), MMTS has reacted with 12 ± 2 cysteines on α1 and 8 ± 1 cysteines on β1. Saturation of NO stimulated activity occurs at a lower concentration than the saturation of labeling, suggesting that the cysteine(s) of the non-heme NO binding site is more reactive to MMTS. To map the cysteines that are reactive to MMTS, the MMTS-treated sGC was proteolyzed with trypsin. Analysis of the digests by mass spectrometry identified several MMTS-reactive residues (Table 2). The key residue(s) comprising the non-heme NO binding site is likely contained within this set of MMTS-modified cysteines.

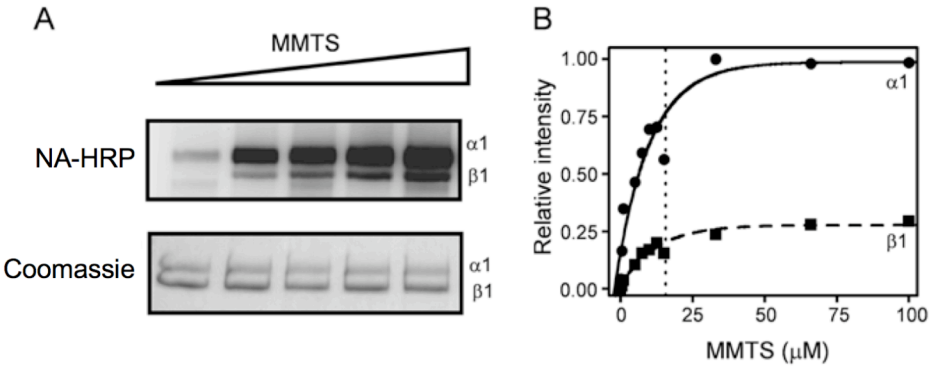

Figure 4: MMTS labeling of sGC subunits. (**A**) MMTS labeling of sGC cysteines was visualized by Western blot analysis. Cysteines on both α1 and β1 react with MMTS. (**B**) Densitometry of labeled bands reveals a linear relationship between labeling and the concentration of MMTS until labeling saturates [α1 EC_{95} = 34 ± 7 μM (circles); β1 EC_{95} = 36 ± 5 μM (squares)]. The dotted vertical line indicates the saturation of MMTS inhibition of NO-stimulated activity (IC_{95} = 16 ± 2 μM).

Table 2. sGC Cysteines Modified by MMTS[a]

Subunit	Residue	Observed Peptide[b]
α1	175	QSSHC*QEAER[c]
α1	609	FESC*SVPR[cd]
α1	628	DC*PGFVFTPR[cd]
β1	174	SEEC*DHTQFLIEEK[cd]
β1	214	ISPYTFC*K[cd]
β1	292	LEC*EDELTGAEISC*LR[d]
β1	303	LEC*EDELTGAEISC*LR[d]

[a]The concentration of MMTS was 20 μM and the numbering corresponds to rat α1β1; [b]C* indicates MMTS-modified cysteine; [c]Identified by MALDI-TOF/TOF; [d] Identified by 2-dimensional LC MS/MS.

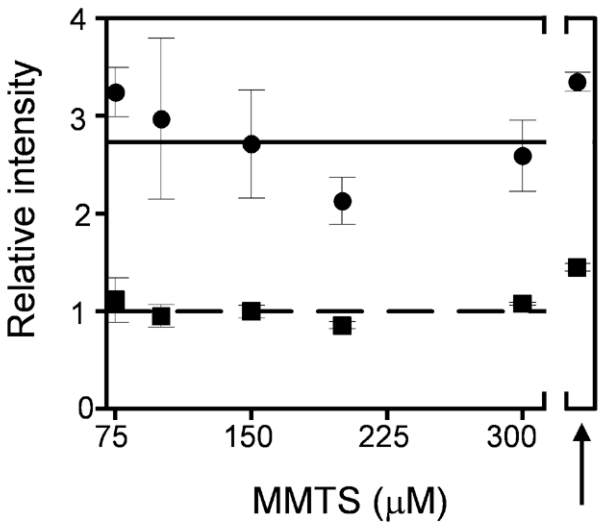

Figure 5: MMTS labeling of sGC. At high MMTS concentrations, the labeling observed on the α1 subunit (circles) and the β1 subunit (squares) saturates. This level of saturation is below the intensity observed when denatured protein reacts with excess MMTS (indicated by arrow). Densitometry analysis estimates the maximum number of cysteines that can react with MMTS in the folded protein to be 16 ± 3 cysteines on α1 and 10 ± 1 cysteines on β1. Data are presented as means ± SD.

The NO/Cysteine Interaction is Reversible With and Without Redox Active Reagents.

In the cellular milieu, there is an abundance of both oxidants and reductants, and, as a consequence, instances of cysteine oxidation are frequently reversed by endogenous reductants. Likewise, commonly used assay buffers for *in vitro* experiments also contain oxidants in the form of O_2 and reductants in the form of DTT. To test the redox chemistry of the NO/cysteine interaction in sGC, the effect of these redox active reagents on NO-mediated cysteine oxidation and on enzyme activation was examined.

Nitrosothiols are gaining recognition as biologically relevant post-translational modifications (25). We sought to determine if *S*-nitrosation could be responsible for NO induced sGC activation. As mentioned above, *S*-nitrosation is an oxidative addition of NO to a thiol that requires a redox partner to act as an electron sink, and most often oxygen serves this role *in vitro* (Scheme 2).

Scheme 2: Nitrosothiol formation and decomposition

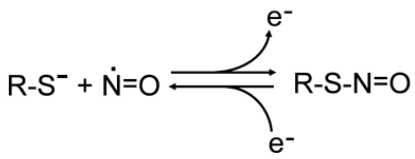

Indeed, the aerobic addition of NO to sGC produces nitrosothiols (Figure 6*A*) (19) while concurrently stimulating the enzyme several hundred fold (Figure 6*B*). If the activating species were a nitrosothiol, then conditions that prevent *S*-nitrosation must also prevent NO stimulation. However, under anaerobic conditions and in the absence of reductant, NO-stimulated sGC was neither *S*-nitrosated nor inhibited (Figure 6*A* and 6*B*). Furthermore, since NO activated sGC to the same extent with and without O_2, the mechanism of enzyme activation is likely the same under anaerobic and aerobic conditions. Thus, the observation of maximal NO stimulation of sGC without *S*-nitrosation excludes a nitrosothiol as the cysteine modification involved in sGC activation by NO.

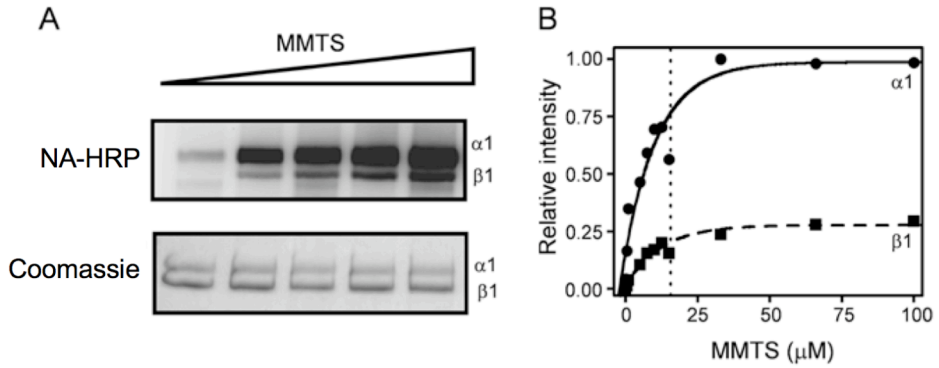

Figure 6: The effect of redox active reagents on NO-stimulated sGC activity. (**A**) The biotin-switch method shows that cysteines on the α1 and β1 subunits are only *S*-nitrosated in the presence of both NO and O_2. (**B**) sGC activity was examined in the presence and absence of O_2. (**C**) The sGC Fe^{II}-NO complex was formed with excess NO (xsNO) in the absence of reducing agent. Excess NO was removed from the Fe^{II}-NO complex (1-NO) and the sample was retreated with excess NO (1-NO + NO). Data are presented as means ± SD.

The observation of full NO stimulation with concomitant *S*-nitrosation under aerobic conditions presents an apparent discrepancy with literature reports that *S*-nitrosation of specific sGC cysteines (β1C122 and α1C243) inhibits sGC activity (19). This discrepancy can be reconciled by noting the difference in assay conditions between the work reported here and the previously published report. The experiments presented here were designed to study the molecular events of NO stimulation of sGC and, accordingly, a short reaction with the NO donor DEA/NO was used. However, the experiments that identified an inhibitory action of *S*-nitrosation were designed to simulate conditions of physiological NO tolerance; therefore a relatively long reaction with *S*-nitrosoglutathione (GSNO) was used (19). Furthermore, GSNO acts primarily through trans-nitrosation whereas the mechanism of *S*-nitrosation by NO typically proceeds through the reaction with O_2. Due to the difference in nitrosating reagents and reaction conditions, different cysteine residues will react to different extents in each experiment. Therefore, while our data eliminates a role for a nitrosothiol in the activation of sGC, it does not conflict with the proposal that *S*-nitrosation is involved in the mechanism of NO tolerance (19, 26, 27).

To further explore the role of redox chemistry in the NO/cysteine interaction, the reversibility of sGC activity in the absence of commonly used redox reactive reagents, such as O_2 and DTT was studied. As discussed above, sGC can be fully activated by NO in the absence of O_2 and DTT (Figure 6*B*). If NO activation was caused by an NO-induced oxidation, NO stimulation would not be reversible without a reductant. To

assess the reversibility of this reaction anaerobically, the xsNO species was formed and then excess NO was removed from solution to form the low-activity 1-NO species (Figure 6*C*). The activity of both the xsNO and 1-NO species with or without O_2 and DTT is similar (Figure 1*D* and Figure 6*C*). The 1-NO sGC species was then re-stimulated with NO, and the enzyme regained full activation (1-NO + NO in Figure 6*C*). Thus, just as activation by NO did not require an oxidation of sGC, deactivation and re-stimulation did not require a reduction of sGC. Because sGC activation is rapidly reversible in the absence of redox mediators, we conclude that the activating species does not alter the oxidation state of the key cysteine(s). Furthermore, since the level of activity of each sGC state is unaffected by anaerobic conditions, we propose that the mechanism of activation and deactivation is O_2-independent. Additionally, the necessity for a reduced thiol in the non-heme NO binding site provides a specific mechanism for the inhibition of NO stimulated activity by thiol oxidation (17, 18, 20) and *S*-nitrosation (19, 26). A chemical species that could account for these observations is the direct nucleophilic addition of a thiol to NO, which yields $RSNO^{\bullet -}$. This species differs from a nitrosothiol by only one electron, but this small difference imparts radically different properties. As opposed to the relative stability of nitrosothiols, this species has been proposed as a short-lived intermediate in reactions that yield disulfides, sulfenic acids, and nitrosothiols (28-30) and has been characterized as a reversible adduct on hemoglobin (31). The characteristic of rapid reversibility is consistent with the rapid deactivation of sGC from the xsNO state to the 1-NO state.

Investigation of cGMP Regulation by NO in HUVECs.

Decades of *in vitro* experiments have established that sGC activation requires the coordination of NO to the heme; however, a NO-bound species has not been directly observed *in vivo*. Spectroscopy is the standard method of detection for the ligation state of a hemoprotein (32), but the complexity of cellular constituents and the low abundance of sGC *in vivo* severely limit the utility of spectroscopy in cells. Therefore, to observe the sGC heme coordination state *in vivo,* we have employed an alternative assay which capitalizes on the small molecule sGC activator YC-1 (22). YC-1 activates sGC to different degrees depending on the heme ligation (21, 33). Although the precise mechanism of YC-1 activation is still under investigation, YC-1 can be used to distinguish sGC heme ligation states by the differential activation of the 1-NO state compared to the basal state or xsNO state (Figure 7*A*) (7).

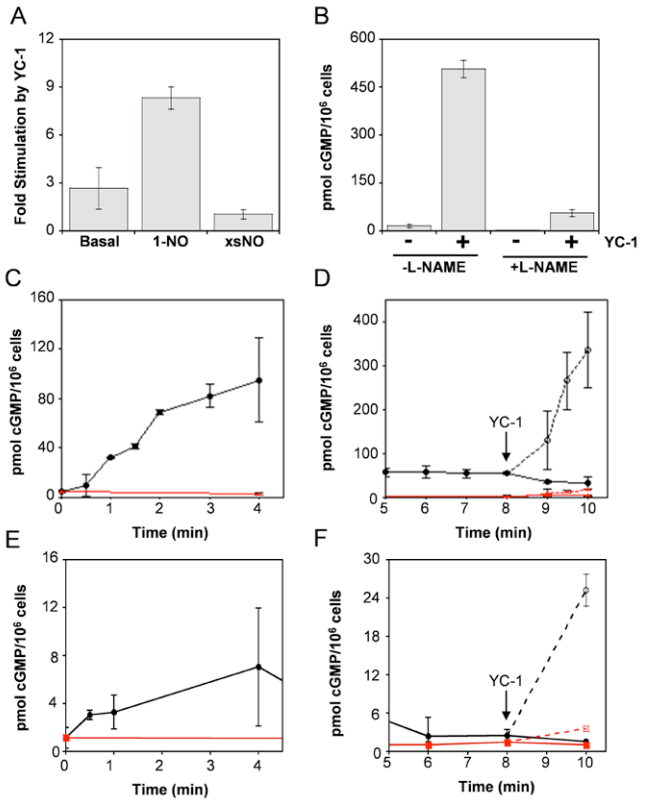

Figure 7: Characterization of three different sGC states in HUVECs. (**A**) Fold activation induced by YC-1 of the basal, 1-NO, and xsNO states of purified sGC. (**B**) YC-1 activation of HUVECs in the absence and presence of L-NAME. (**C** - **F**) Time course of cGMP levels in HUVECS in the presence (**C** and **D**) and absence (**E** and **F**) of IBMX. Plots display both the early (**C** and **E**) and late (**D** and **F**) phases with (black) and without (red) 1 μM PROLI/NO addition at 0 minutes. Basal (red closed squares) and NO-stimulated (black closed circles) cells are shown before and after 150 μM YC-1 addition at 8 minutes, as indicated by an arrow. YC-1 treatment at 8 minutes significantly activates the cells that had been exposed to NO at 0 minutes (open black circles), but not the control cells (open red circles). Data are presented as means ± SD.

To assess the heme ligation state of sGC *in vivo*, cGMP formation in human umbilical vein endothelial cells (HUVECs) was examined. These cells constitutively express both sGC and nitric oxide synthase (NOS) and exhibit a low level of basal cGMP. Upon YC-1 treatment of HUVECs, a large increase in cGMP formation was observed. This YC-1-dependent increase in cGMP levels was prevented by a 2 hour preincubation with N^{ω}-nitro-L-arginine methyl ester (L-NAME), a cell permeable NOS inhibitor (Figure 7*B*). This demonstrates a requirement for NO in the YC-1 mediated activation of sGC *in vivo* and others have observed similar phenomena in porcine aortic endothelial cells (PAECs) (34), implicating a generality of this property in endothelial cells. Both the high fold activation of cGMP production induced by YC-1 and the inhibition of this activation by an extended pretreatment with L-NAME are consistent with the 1-NO state; however, the uncertainty of the local concentration of NO complicates this interpretation.

The kinetics of NO stimulation *in vivo* have been studied extensively (35, 36). In response to NO, cells expressing sGC exhibit a rapid elevation in intracellular cGMP levels, followed by a fast decline in the rate of cGMP synthesis. This rapid deactivation has been previously assumed to reflect the simple dissociation of NO from the sGC heme. This would limit sGC to two defined states; an active NO-bound state and a basal NO-free state. However, experiments with purified protein suggest that the high activity, xsNO state may deactivate to the 1-NO state rather than the basal state (7). This possibility was tested in a cellular context with a time course assay in L-NAME treated HUVECs that were exposed to a burst of NO (delivered by PROLI/NO) in the presence of a phosphodiesterase (PDE) inhibitor, (3-isobutyl-1- methylxanthine, IBMX). The sGC activity was then measured in both the early phase of NO stimulation (0-4 min) (Figure 7*C*) and the late phase of NO stimulation (5-10 min) (Figure 7*D)* (Table 3). In the early phase, HUVECs displayed a well-documented accumulation of cGMP in response to NO, whereas untreated control HUVECs maintained a low, basal level of cGMP (~1 pmol/10^6 cells) (Figure 7*C*). This accounts for the two well-established states of sGC, one with high activity and one with low activity that interconvert depending on the concentration of NO. In the late phase, the intracellular cGMP level reached a plateau indicative of the deactivated, low-activity sGC state (Figure 7*D*). In the late phase, both NO stimulated and untreated HUVECs exhibited low sGC activity which has been assumed to be the activity of basal sGC, i.e. no ligand bound to the heme. However, YC-1 treatment only stimulates sGC activity in the NO treated cells, and the specific and prominent activation of only these cells discriminates between two long-lived, low-activity species with differing propensities towards YC-1 *in vivo*.

Table 3. YC-1 Stimulation of Multiple sGC States in HUVECs[a]

NO Treatment[b]	YC-1	Phase[c]	Velocity[d] (pmol/min/10^6 cells)
none	-	Early	0[e]
	+	Early	ND
none	-	Late	0
	+	Late	8.79 ± 1.60
1 μM	-	Early	32.28 ± 12.83
	+	Early	96.92 ± 32.03
1 μM	-	Late	0
	+	Late	125.45 ± 46.69

[a]Rates acquired at 37 °C. [b]Addition 1 μM PROLI/NO at t=0 min. [c]Early phase between 0-3 min and late phase between 5-10 min. [d]Velocity determined by global analysis of mean measurements. [e]Velocity not statistically different from zero. ND, not determined.

In order to simplify data analysis, the experiments described above were performed in the presence of a PDE inhibitor; however, *in vivo* PDEs are intimately linked to cGMP signaling and shape temporal changes in NO-induced intracellular cGMP levels (37). Therefore, similar experiments were performed in the absence of IBMX, where we found that PDE activity did not affect the cellular responses under investigation (Figure 7*E* and 7F). Importantly, under the conditions of this experiment, NO rapidly decays such that none was detected in solution after 4 minutes (Figure 8), eliminating the uncertainty in local NO concentration.

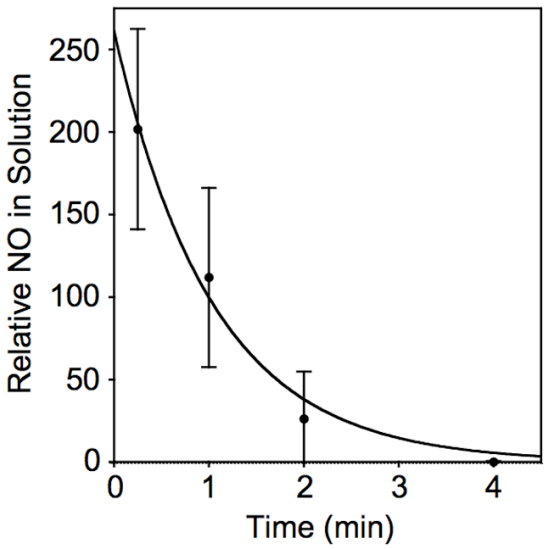

Figure 8. Quantification of NO in solution. Time course of NO in solution after addition of 1 μM PROLI/NO to buffer at 37 ºC. By 4 minutes NO has decayed such that it is no longer detectable by the NOA. Data are presented as means ± SD.

These experiments suggest that sGC exists in three states *in vivo*: a low-activity state that is weakly stimulated by YC-1 (basal), a short-lived, high-activity state that is weakly stimulated by YC-1 (xsNO), and a longer-lived, low-activity state that is highly stimulated by YC-1 (Table 3). Because this closely mirrors the activities of the spectroscopically defined states of sGC *in vitro*, this would appear to be the first clear observation of the 1-NO state *in vivo*. With this evidence we propose a model of sGC activation where a reduced cysteine(s) stabilizes NO binding and produces a highly active sGC state (Figure 9). The rapid dissociation of the cysteine/NO complex deactivates the enzyme to the 1-NO state, which persists until NO slowly dissociates from the sGC heme and the enzyme reverts to the basal state.

Conclusion

In summary, our findings establish the importance of an sGC cysteine(s) in the regulation of sGC by NO (Figure 9). Multiple NO binding sites impart a complexity of regulation to sGC which could be useful for the NO/cGMP signal transduction pathway, as it intersects a great variety of physiological processes. It is noteworthy that both sites of NO interaction on sGC, a reduced thiol and a ferrous iron, are susceptible to oxidation. Therefore, in physiological instances of oxidative stress, it is possible that both cysteine oxidation and heme oxidation contribute to sGC dysfunction by preventing NO binding to each respective site. The interplay between these multiple sGC states and the

molecular causes of dysfunction may offer an opportunity for the design of state-specific sGC activators to target diseased tissue (38, 39).

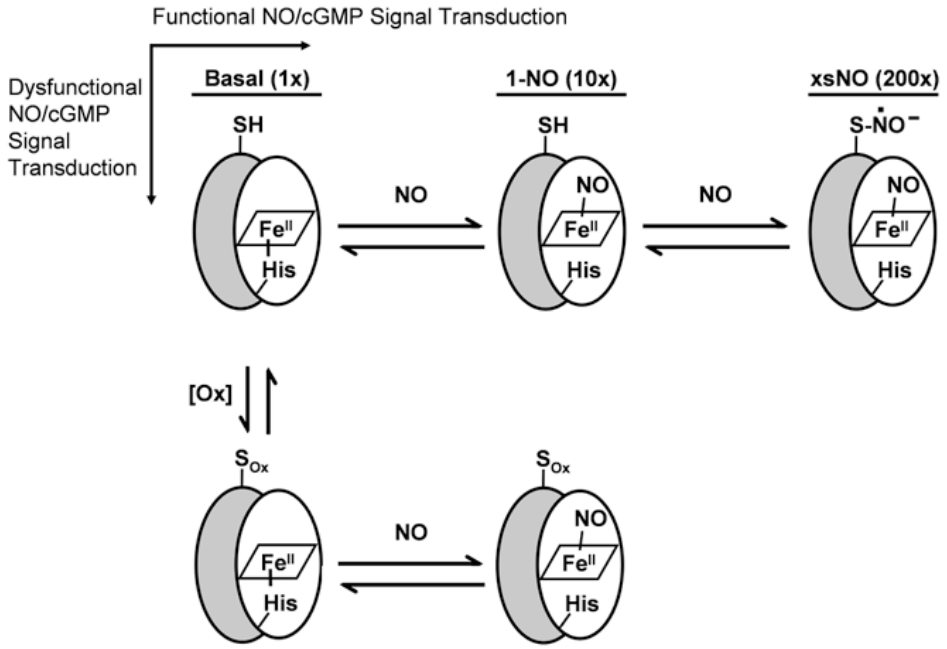

Figure 9: Model for the role of cysteine(s) in the mechanism of sGC activation. NO initially binds to the heme and activates the enzyme about 10-fold. In the presence of excess NO (xsNO), a putative thiol-NO adduct forms and this activates the enzyme roughly 200-fold above the basal level. Although the exact chemical identity is unknown, a thionitroxide is proposed. This species is consistent with the observed properties of activation and deactivation. Under oxidative stress, the non-heme NO binding site oxidizes which prevents NO binding and, therefore, maximal activation. For simplicity, oxidation is only shown to affect the basal state; however oxidation of the non-heme NO binding site in any state would desensitize sGC to NO.

Materials and Methods

sGC *in vitro* Assays. Recombinant rat sGC was purified as described (14) and then dithiothreitol (DTT) was removed from the sGC storage buffer using an anion exchange column. sGC was assayed in the presence and absence of MMTS (50 μM), PROLI/NO (50 μM) and YC-1 (150 μM) where indicated, at room temperature. Assays were initiated with substrate, quenched after 3 minutes and cGMP was quantified. MMTS inhibition of sGC was directly compared to sGC activation by 1 equivalent of NO. sGC with NO only at the heme was formed by addition of sub-stoichiometric amounts of PROLI/NO and spectrally monitoring the formation of the sGC-NO complex. Samples (sGC and sGC-NO) were then incubated with MMTS (30 μM) and assays were initiated by addition of substrate at room temperature. Samples were quenched after 3 min and cGMP was quantified. Reversibility of MMTS inhibition was examined by adding DTT (5 mM) to MMTS-treated sGC, and quantifying cGMP production. To determine the inhibition profile of MMTS on NO-stimulated activity the concentration of MMTS was varied from 0-100 μM. All assays were initiated by addition of $MgCl_2$ (1.5 mM) and GTP (1.5 mM) and cGMP was quantified. All statistic results are given as means ± SD, and significance was evaluated using unpaired *t*-tests (Microsoft Software).

Effect of Oxidants on sGC Activity. The effect of redox active reagents on sGC activity was investigated. The reversibility of NO activation in the absence of DTT was examined by treating sGC with PROLI/NO followed by desalting into a NO-free and DTT-free buffer. The NO-bound enzyme was then assayed in the absence and presence of PROLI/NO (50 μM) at room temperature. The protein was examined with activity assays and electronic absorption spectroscopy after each manipulation. NO-stimulated activity was also examined in the presence and absence of O_2 (237 μM) in a DTT-free buffer at 37 ºC. Assays were initiated with $MgCl_2$ (3 mM) and GTP (1.5 mM), quenched after 3 minutes, and cGMP was analyzed.

Cell Culture. Pooled human umbilical vascular endothelial cells (HUVECs) were obtained from Lonza and maintained in EGM-2 media supplemented with a bulletkit (Lonza) according to the manufacturer's instructions. Semi-adherent PC12 cells were obtained from the American Type Culture Collection (ATCC) and were maintained in a humidified atmosphere of 95% air and 5% CO_2 at 37 °C in Dulbecco's Modified Eagle's medium (Invitrogen) supplemented with 10% fetal bovine serum (FBS), L-glutamine (200 μg/mL), penicillin (100 U/mL), and streptomycin (100 μg/mL). Cells were counted with a hemocytometer and viability was routinely assessed by trypan blue staining and found to be >90%.

HUVEC Activity Assays. Confluent HUVECs in either 6-well plates or 100 x 15 mm Petri dishes were pre-incubated, where indicated, with 300 μM L-NAME in growth media for 2 hours. After pre-treatment, media was replaced with 50 mM Hepes (pH 7.4), 100 mM NaCl, 5 mM KCl, 2.5 mM $CaCl_2$, 1 mM $MgCl_2$, 1 mM IBMX and, where

indicated, 300 μM L-NAME. Samples were incubated for 15 minutes, and then reactions were initiated with additions of 1 μM PROLI/NO (Cayman Chemicals) and/or 150 μM YC-1 (Sigma). End-point assays proceeded for 4 minutes, whereas time course kinetics proceeded for the indicated duration. Reactions were terminated by aspiration of the assay buffer and immediate addition of 100 mM HCl. Quenched reactions were incubated at 4 °C for 30 minutes, scraped with a rubber policeman, transferred to a 1.5 mL Eppendorf tube, and stored at -80 °C until cGMP quantification was carried out using a cGMP enzyme immunoassay kit, Format A (Assay Designs), per the manufacturer's instructions. All manipulations prior to quenching were performed at 37 °C and HUVECs used for cGMP measurements were between passages 3–10. Each assay point was done in duplicate or triplicate and all experiments were repeated 3-4 times to ensure reproducibility.

sGC *in vitro* Assays. sGC was purified as described previously (14). MMTS inhibition of sGC was directly compared to sGC activation by 1 equivalent of NO. In all experiments, MMTS (Pierce) was prepared fresh in assay buffer before each assay. sGC with NO only at the heme was formed by addition of sub-stoichiometric amounts of PROLI/NO and monitored spectrally for the formation of the sGC-NO complex. Samples (sGC and sGC-NO) were then incubated with MMTS (30 μM) for 30 min on ice. Duplicate end-point assays were initiated by addition of 3 mM $MgCl_2$ and 1.5 mM GTP at 25 ºC. Samples were quenched after 3 min by the addition of 400 μL of 125 mM $Zn(CH_3CO_2)_2$ and 500 μL of 125 mM Na_2CO_3. cGMP was quantified using a cGMP enzyme immunoassay kit, Format B (Biomol), per the manufacturer's instructions. All experiments were repeated 3-4 times to ensure reproducibility.

sGC activity was measured in the presence of MMTS. sGC (22 nM) was incubated with 13 μM MMTS in 50 mM Hepes (pH 7.4), 50 mM NaCl on ice for 60 min. Samples were then incubated in the presence or absence of 5 mM DTT for an additional 60 min on ice. sGC activity was measured in duplicate in the presence and absence of DEA/NO (100 μM) and YC-1 (150 μM) by addition of 3 mM $MgCl_2$ and 1.5 mM GTP at 25 ºC.

To determine the inhibition profile of MMTS on NO-stimulated activity, the concentration of MMTS was varied from 0-100 μM. In these experiments, sGC (133 nM) was incubation with MMTS at the indicated concentration for 5 min at 25 ºC before 10-fold dilution and DEA/NO (50 μM) addition. Duplicate 3 min end-point assays were initiated with 3 mM $MgCl_2$ and 1.5 mM GTP at 25 ºC. Data analysis and figure generation were carried out using Kaleidagraph (Synergy Software). All statistic results are given as means ± SD, and significance was evaluated using unpaired *t*-tests (Microsoft Software).

MMTS Labeling of sGC. To visualize MMTS labeling of sGC the following method was developed based on existing protocols (40, 41). Specifically, after sGC was incubated with MMTS, reactions were quenched with 1 equivalent of 250 mM Hepes (pH 7.2), 1 mM EDTA, 0.1 mM neocuproine, 10% SDS, 80 mM N-ethylmaleimide (NEM)

for 30 minutes at 65 ºC. Samples were acetone precipitated and protein pellets were then resuspended in 62 mM Hepes (pH 7.2), 0.25 mM, EDTA, 0.025 mM neocuproine, 5% SDS, 20 mM DTT and incubated at 37 ºC for 30 minutes. Samples were again acetone precipitated and then resuspended in 62 mM Hepes (pH 7.2), 0.25 mM EDTA, 0.025 mM neocuproine, 5% SDS, 5 mM maleimide-PEO_2-biotin (Pierce) and incubated for 1 hour at 37 ºC. This reaction was quenched by addition of 50 mM DTT and SDS-PAGE loading buffer, and the samples were split and evaluated by SDS-PAGE using pre-cast 10% Tris-glycine gels (Invitrogen). One gel was stained with Coomassie to control for loading, while another gel was transferred to nitrocellulose, stained with a Neutravidin-HRP conjugate (Pierce), and imaged with West Femto imaging solutions (Pierce) on a FluorS imaging station (Bio-Rad Laboratories). Densitometry analysis was carried out with QuantityOne software (Bio-Rad Laboratories).

Peptide Mapping. MMTS-treated sGC (15 μg) was blocked with 40 mM NEM and acetone precipitated. The protein pellet was resuspended in 10 μL of 50 mM Hepes (pH 7.2), 20 mM NEM, 6 M guanidinium HCl and heated to 55 °C for 30 minutes. The reaction was then diluted 10-fold with 50 mM Tris (pH 7.6), 1 mM $CaCl_2$ and 150 ng of Trypsin Gold (Promega) was added. Digests proceeded for 12 hours at 37 °C and were concentrated by Speed Vac to ~30 μL. Samples were then prepared for either mudPIT or MALDI-TOF/TOF.

MudPIT analysis was performed by the Proteomics/Mass Spectrometry Laboratory at UC Berkeley. Sample was first desalted using a C18 spec tip (Varian). A nano LC column was packed in a 100 μm inner diameter glass capillary with an emitter tip. The column consisted of 10 cm of Polaris C18 (5 μm) packing material (Varian), followed by 4 cm of PartiSphere 5 SCX (Whatman). The column was loaded by use of a pressure bomb and washed extensively with buffer A (42). The column was then directly coupled to an electrospray ionization source mounted on a Thermo-Fisher LTQ XL linear ion trap mass spectrometer. An Agilent 1200 HPLC equipped with a split line to deliver a flow rate of 30 nl/min was used for chromatography. Peptides were eluted using a 4-step MudPIT procedure (4). The program DTASelect was used to identify modified peptides from the rat sGC sequence.

For MALDI-TOF/TOF, peptides from the digest solution were adsorbed onto a C18 ZipTip and eluted with 5 μL of 60% acetonitrile/ 0.5% TFA saturated with HCCA. Samples were spotted and allowed to dry on the MALDI target. A fullscan mass spectrum of the digest was recorded on an Applied Biosystems 4800 MALDI tandem TOF instrument in reflector mode. The ions at *m*/*z* corresponding to protonated modified peptides were then isolated in MS1, and individual CID spectra were acquired with air used as the collision gas at 1.0 keV collision energy.

Effect of *S*-nitrosation on sGC Activity. sGC activity and nitrosothiol formation were monitored in the presence and absence of O_2 to determine if *S*-nitrosation activates sGC. In an anaerobic chamber (Coy), residual DTT was removed from sGC by 2 cycles of dilution/concentration using a 10K Ultrafree-0.5 centrifugal filter device (Vivaspin).

sGC (0.2 μg) was then assayed in the presence and absence of 40 μM DEA/NO in duplicate at 37 ºC. This set of assays was done both in the absence and presence of O_2 (237 μM). Assay mixtures contained 50 mM Hepes (pH 7.4), 50 mM NaCl, 3 mM $MgCl_2$, 1.5 mM GTP and were in a final volume of 100 μL. Assays were quenched after 3 minutes and analyzed as described above. To evaluate cysteine *S*-nitrosation, identically prepared sGC samples were examined by the biotin-switch method (40) with minor modification. Briefly, *S*-nitrosation was allowed to proceed for 5 minutes, and reactions were then quenched aerobically with an equal volume of 250 mM Hepes (pH 7.2), 1 mM EDTA, 0.1 mM neocuproine, 10% SDS, 120 mM NEM. Reactions were transferred to 65 ºC for 30 minutes and vortexed frequently. Samples were then acetone precipitated and the protein pellets were subsequently dissolved in 30 μl of 62 mM Hepes (pH 7.2), 0.25 mM EDTA, 0.025 mM neocuproine, 5% SDS, 1 mM maleimide-PEO_2-biotin (Pierce), 10 mM sodium ascorbate, and incubated for 1 hour at 25 ºC. The reactions were quenched by addition of SDS-PAGE loading buffer containing 50 mM DTT. The samples were then split and analyzed by both Coomassie blue staining and Neutravidin-HRP Western blot, as described above. The total protein loaded into each well was 2.6 μg from the biotin-switch method and 1.3 μg for the Coomassie gel.

PC12 Cells Activity Assays. Semi-adherent PC12 cells in 150 x 15 mm Petri dishes were washed extensively with ice-cold assay buffer (50 mM Hepes (pH 7.4), 50 mM NaCl) and harvested with a rubber policeman. Cells were collected by centrifugation at 4 °C and gently resuspended in ice-cold assay buffer. Cells were then incubated with MMTS (0-300 μM) on ice for 10 minutes. Reactions were then transferred to 37 °C for 10 seconds before addition of 1 μM PROLI/NO. After 5 seconds, reactions were quenched with 1 volume of 133 mM HCl. Protein concentration was measured in each sample using the Bradford Microassay (Bio-Rad Laboratories) against a bovine serum albumin standard, and cGMP quantification was carried out using a cGMP enzyme immunoassay kit, Format A (Assay Designs), per the manufacturer's instructions. Each assay point was done in duplicate and all experiments were repeated 3-4 times to ensure reproducibility. Data analysis and figure generation were carried out using Kaleidagraph (Synergy Software). All statistic results are given as means ± SD, and significance was evaluated using unpaired *t*-tests (Microsoft Software).

Direct Detection of Solution NO. The concentration of NO in solution was quantified after addition of PROLI/NO at various times points. A solution of 50 mM Hepes (pH 7.4), 100 mM NaCl, 5 mM KCl, 2.5 mM $CaCl_2$, 1 mM $MgCl_2$ (1 mL total volume) was deposited in a 6-well plate at 37 ºC. NO decomposition was initiated by addition of 1 μM PROLI/NO to the solution. At the indicated times, aliquots (200 μL) were withdrawn and immediately sealed in a 1.25 mL reacti-vial. After vortexing the vial, 5 mL of headspace was removed with a gas-tight Hamilton syringe and injected into a Sievers Nitric Oxide Analyzer NOA™ 280i. The NO detection limit of the NOA is ~1 ppb. Peak area was quantified with the manufacturer's software. Data shown are representative of eight independent trials.

References

1. Munzel, T, Feil, R, Mulsch, A, Lohmann, SM, Hofmann, F, Walter, U (2003) Physiology and pathophysiology of vascular signaling controlled by guanosine 3',5'-cyclic monophosphate-dependent protein kinase. *Circulation* 108: 2172-2183.
2. Sanders, KM, Ward, SM, Thornbury, KD, Dalziel, HH, Westfall, DP, Carl, A (1992) Nitric-oxide as a nonadrenergic, noncholinergic neurotransmitter in the gastrointestinal-tract. *Jpn J Pharmacol* 58: 220-225.
3. Warner, TD, Mitchell, JA, Sheng, H, Murad, F (1994) Effects of cyclic GMP on smooth muscle relaxation. *Adv Pharmacol* 26: 171-194.
4. Arnold, WP, Mittal, CK, Katsuki, S, Murad, F (1977) Nitric-oxide activates guanylate cyclase and increases guanosine 3'-5'-cyclic monophosphate levels in various tissue preparations. *P Natl Acad Sci USA* 74: 3203-3207.
5. Gerzer, R, Hofmann, F, Schultz, G (1981) Purification of a soluble, sodium-nitroprusside-stimulated guanylate-cyclase from bovine lung. *Eur J Biochem* 116: 479-486.
6. Wolin, MS, Wood, KS, Ignarro, LJ (1982) Guanylate-cyclase from bovine lung - a kinetic-analysis of the regulation of the purified soluble enzyme by protoporphyrin-IX, heme, and nitrosyl-heme. *J Biol Chem* 257: 3312-3320.
7. Cary, SP, Winger, JA, Marletta, MA (2005) Tonic and acute nitric oxide signaling through soluble guanylate cyclase is mediated by nonheme nitric oxide, ATP, and GTP. *P Natl Acad Sci USA* 102: 13064-13069.
8. Russwurm, M, Koesling, D (2004) NO activation of guanylyl cyclase. *EMBO J* 23: 4443-4450.
9. Stone, JR, Marletta, MA (1996) Spectral and kinetic studies on the activation of soluble guanylate cyclase by nitric oxide. *Biochemistry* 35: 1093-1099.
10. Zhao, Y, Brandish, PE, Ballou, DP, Marletta, MA (1999) A molecular basis for nitric oxide sensing by soluble guanylate cyclase. *P Natl Acad Sci USA* 96: 14753-14758.
11. Kharitonov, VG, Russwurm, M, Magde, D, Sharma, VS, Koesling, D (1997) Dissociation of nitric oxide from soluble guanylate cyclase. *Biochem Biophys Res Commun* 239: 284-6.
12. Winger, JA, Derbyshire, ER, Marletta, MA (2006) Dissociation of nitric oxide from soluble guanylate cyclase and H-NOX domain constructs. *J Biol Chem* 282: 897-907.
13. Derbyshire, ER, Gunn, A, Ibrahim, M, Spiro, TG, Britt, RD, Marletta, MA (2008) Characterization of two different five-coordinate soluble guanylate cyclase ferrous-nitrosyl complexes. *Biochemistry* 47: 3892-9.
14. Derbyshire, ER, Marletta, MA (2007) Butyl isocyanide as a probe of the activation mechanism of soluble guanylate cyclase: investigating the role of non-heme nitric oxide. *J Biol Chem* 282: 35741-35748.
15. Aono, S (2008) Metal-containing sensor proteins sensing diatomic gas molecules. *Dalton Trans*: 3137-3146.

16. Chen, L, Lyubimov, AY, Brammer, L, Vrielink, A, Sampson, NS (2008) The binding and release of oxygen and hydrogen peroxide are directed by a hydrophobic tunnel in cholesterol oxidase. *Biochemistry* 47: 5368-77.
17. Brandwein, HJ, Lewicki, JA, Murad, F (1981) Reversible inactivation of guanylate-cyclase by mixed disulfide formation. *J Biol Chem* 256: 2958-2962.
18. Braughler, JM (1983) Soluble guanylate cyclase activation by nitric oxide and its reversal. Involvement of sulfhydryl group oxidation and reduction. *Biochem Pharmacol* 32: 811-818.
19. Sayed, N, Baskaran, P, Ma, X, van den Akker, F, Beuve, A (2007) Desensitization of soluble guanylyl cyclase, the NO receptor, by S-nitrosylation. *P Natl Acad Sci USA* 104: 12312-12317.
20. Maron, BA, Zhang, YY, Handy, DE, Beuve, A, Tang, SS, Loscalzo, J, Leopold, JA (2009) Aldosterone increases oxidant stress to impair guanylyl cyclase activity by cysteinyl thiol oxidation in vascular smooth muscle cells. *J Biol Chem* 284: 7665-7672.
21. Friebe, A, Schultz, G, Koesling, D (1996) Sensitizing soluble guanylyl cyclase to become a highly CO-sensitive enzyme. *EMBO J* 15: 6863-6868.
22. Ko, FN, Wu, CC, Kuo, SC, Lee, FY, Teng, CM (1994) YC-1, a novel activator of platelet guanylate cyclase. *Blood* 84: 4226-4233.
23. Bal-Price, A, Gartlon, J, Brown, GC (2006) Nitric oxide stimulates PC12 cell proliferation via cGMP and inhibits at higher concentrations mainly via energy depletion. *Nitric Oxide-Biol Chem* 14: 238-246.
24. Boerrigter, G, Burnett, JC (2007) Nitric oxide-independent stimulation of soluble guanylate cyclase with BAY 41-2272 in cardiovascular disease. *Cardiovasc Drug Rev* 25: 30-45.
25. Hess, DT, Matsumoto, A, Kim, SO, Marshall, HE, Stamler, JS (2005) Protein S-nitrosylation: purview and parameters. *Nat Rev Mol Cell Bio* 6: 150-166.
26. Mayer, B, Kleschyov, AL, Stessel, H, Russwurm, M, Munzel, T, Koesling, D, Schmidt, K (2009) Inactivation of soluble guanylate cyclase by stoichiometric S-nitrosation. *Mol Pharmacol* 75: 886-891.
27. Sayed, N, Kim, DD, Fioramonti, X, Iwahashi, T, Duran, WN, Beuve, A (2008) Nitroglycerin-induced S-nitrosylation and desensitization of soluble guanylyl cyclase contribute to nitrate tolerance. *Circ Res* 103: 606-14.
28. DeMaster, EG, Quast, BJ, Redfern, B, Nagasawa, HT (1995) Reaction of nitric oxide with the free sulfhydryl group of human serum albumin yields a sulfenic acid and nitrous oxide. *Biochemistry* 34: 11494-11499.
29. Gow, AJ, Buerk, DG, Ischiropoulos, H (1997) A novel reaction mechanism for the formation of S-nitrosothiol in vivo. *J Biol Chem* 272: 2841-2845.
30. Pryor, WA, Church, DF, Govindan, CK, Crank, G (1982) Oxidation of thiols by nitric-oxide and nitrogen-dioxide - synthetic utility and toxicological implications. *J Org Chem* 47: 156-159.
31. Zhao, YL, Houk, KN (2006) Thionitroxides, RSNHO center dot: The structure of the SNO moiety in "S-nitrosohemoglobin", a possible NO reservoir and transporter. *J Am Chem Soc* 128: 1422-1423.
32. Antonini, E, Brunori, M (1971) *Hemoglobin and myoglobin in their reactions with ligands* (North-Holland Pub. Co., Amsterdam).

33. Martin, E, Lee, YC, Murad, F (2001) YC-1 activation of human soluble guanylyl cyclase has both heme-dependent and heme-independent components. *P Natl Acad Sci USA* 98: 12938-12942.
34. Schmidt, K, Schrammel, A, Koesling, D, Mayer, B (2001) Molecular mechanisms involved in the synergistic activation of soluble guanylyl cyclase by YC-1 and nitric oxide in endothelial cells. *Mol Pharmacol* 59: 220-224.
35. Bellamy, TC, Garthwaite, J (2002) Pharmacology of the nitric oxide receptor, soluble guanylyl cyclase, in cerebellar cells. *Brit J Pharmacol* 136: 95-103.
36. Roy, B, Garthwaite, J (2006) Nitric oxide activation of guanylyl cyclase in cells revisited. *P Natl Acad Sci USA* 103: 12185-12190.
37. Soderling, SH, Beavo, JA (2000) Regulation of cAMP and cGMP signaling: new phosphodiesterases and new functions. *Curr Opin Cell Biol* 12: 174-179.
38. Boerrigter, G, Costello-Boerrigter, LC, Cataliotti, A, Lapp, H, Stasch, JP, Burnett, JC (2007) Targeting heme-oxidized soluble guanylate cyclase in experimental heart failure. *Hypertension* 49: 1128-1133.
39. Stasch, JP, Schmidt, PM, Nedvetsky, PI, Nedvetskaya, TY, H, SA, Meurer, S, Deile, M, Taye, A, Knorr, A, Lapp, H, Muller, H, Turgay, Y, Rothkegel, C, Tersteegen, A, Kemp-Harper, B, Muller-Esterl, W, Schmidt, HH (2006) Targeting the heme-oxidized nitric oxide receptor for selective vasodilatation of diseased blood vessels. *J Clin Invest* 116: 2552-61.
40. Jaffrey, SR, Snyder, SH (2001) The biotin switch method for the detection of S-nitrosylated proteins. *Science STKE* 2001: PL1.
41. Leichert, LI, Jakob, U (2006) Global methods to monitor the thiol-disulfide state of proteins in vivo. *Antioxid Redox Signal* 8: 763-772.
42. Washburn, M. P., Wolters, D. & Yates, J. R., 3rd (2001) Large-scale analysis of the yeast proteome by multidimensional protein identification technology. *Nat Biotechnol* 19**:** 242-247.

Chapter 3
Heme-assisted *S*-nitrosation causes the NO-desensitization of heme-oxidized sGC

Introduction:

Cardiovascular disease is often associated with both increased oxidative stress and reduced sGC activity (*1, 2*). This association bears potential significance towards the development of novel therapeutics in light of the biochemical response of sGC to oxidative stress. Specifically, the heme iron of sGC is typically reduced, or in the ferrous [Fe(II)] oxidation state, and the enzymatic response to NO depends critically on this state, as loss of one electron from the heme iron to the ferric [Fe(III)] oxidation state dramatically inhibits NO stimulation (*3, 4*). Consequently, the ferric [Fe(III)] oxidation state of sGC is considered NO-desensitized because NO only partially stimulates this form of the enzyme as compared to the ferrous [Fe(II)] oxidation state. These observations have provoked the hypothesis that ferric [Fe(III)] sGC is the molecular cause of some instances of cardiovascular disease (*5*). In this proposal, reactive oxygen species (ROS) which are upregulated in disease are thought to oxidize the sGC heme, rendering the enzyme NO-insensitive and preventing normal vasodilatory signal transduction. The potential merit of this idea has led to the development of small molecule sGC activators that selectively activate the heme-oxidized form of the enzyme and are postulated to target sGC in disease tissue (*6*). One such molecule, BAY 58-2667, has shown promising results in animal models and Phase IIb clinical trials (*5, 7, 8*). Because of the burgeoning physiological role of ferric [Fe(III)] sGC, the biochemical characterization of NO-desensitization of ferric [Fe(III)] sGC warrants further investigation.

Extensive studies on the interaction between NO and either small molecule iron porphyrins or hemoproteins points to the general principle that ferric [Fe(III)] heme typically binds NO much weaker than ferrous [Fe(II)] heme (*9*). Trivially then, a weaker affinity of the hemoprotein for NO would result in less hemoprotein-bound NO at a given concentration of NO, which would manifest as an apparent enzyme inhibition. To test this proposal, we quantitatively evaluated ligand occupancy but found that it does not contribute to NO-desensitization of sGC *in vitro*.

Certain ferric [Fe(III)] hemoproteins are subject to a complicating reaction with NO that precludes direct determination of a dissociation constant with NO. Specifically, the ferric-nitrosyl [Fe(III)-NO] complex of these hemoproteins is only stable under acidic conditions, and in mildly alkaline solutions, the complex converts to a ferrous-nitrosyl [Fe(II)-NO] by a base catalyzed mechanism (Scheme 1) (*10*). Here, the ferric-nitrosyl [Fe(III)-NO] complex is in resonance with the ferrous-nitroso [Fe(II)-NO^+] form. The reactive nitroso group is susceptible to nucleophilic attack by hydroxide, which yields nitrite (formally nitrous acid) and the reduced, ferrous [Fe(II)] heme. Finally, the newly regenerated ferrous [Fe(II)] heme binds an additional equivalent of NO to yield a ferrous-nitrosyl [Fe(II)-NO] complex. This reaction is frequently called reductive nitrosylation because the overall change to the heme includes both a one-electron reduction and the coordination of a molecule of NO.

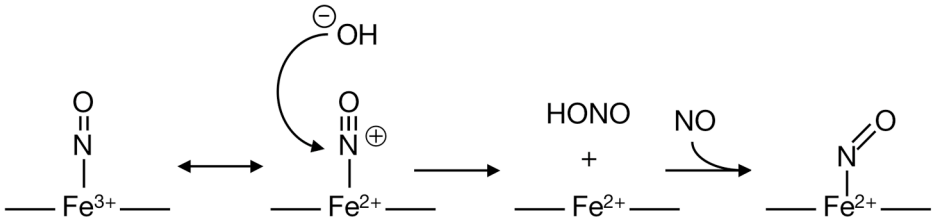

Scheme 1: Hydroxide-mediated reductive nitrosylation of ferric [Fe(III)] heme

Under alkaline conditions, myoglobin, hemoglobin, and cytochrome *c* undergo hydroxide-mediated reductive nitrosylation (*10*), and the same mechanism has been suggested for neuroglobin (*11*) and sGC (*3*). However, thiol-mediated reductive nitrosylation, where a thiol replaces hydroxide as the nucleophile in the mechanism above, has been suggested to account for reductive nitrosylation in nitrophorins (*12*) and partially in hemoglobin (*13*). Furthermore, glutathione (GSH) can replace hydroxide as the active nucleophile in the reductive nitrosylation of cytochrome *c* (*14*), and the thiol-mediated reductive nitrosylation reactions produce corresponding nitrosothiols. In fact, the reductive nitrosylation of biological molecules was known long before the discovery of the physiological relevance of NO, as Keilin and Hartree found in 1937 that identical electronic absorption spectra develop from exposure of NO to either ferrous [Fe(II)] or ferric [Fe(III)] hemoglobin (*15*). Sancier and colleagues later confirmed these findings by EPR assignment of a ferrous-nitrosyl [Fe(II)-NO] complex from NO-treated ferric [Fe(III)] hemoglobin (*16*).

The reductive nitrosylation of sGC appears to further convolute the mechanism of NO-desensitization, as regeneration of the ferrous [Fe(II)] heme presents an apparent paradox: whether the initial heme state is ferrous [Fe(II)] or ferric [Fe(III)], the final heme state of sGC after treatment with NO is ferrous-nitrosyl [Fe(II)-NO]; however, the activity between these two spectrally identical species markedly differs (Figure 1). Despite regeneration of the ferrous [Fe(II)] heme in the reductive nitrosylation reaction, the NO-stimulated activity of the ferric-derived ferrous-nitrosyl [Fe(III)→Fe(II)-NO] is significantly inhibited. Because the heme ligation state is identical in both instances, we infer that the protein must be modified during the reductive nitrosylation reaction and this modification must prevent the full stimulation of sGC by NO.

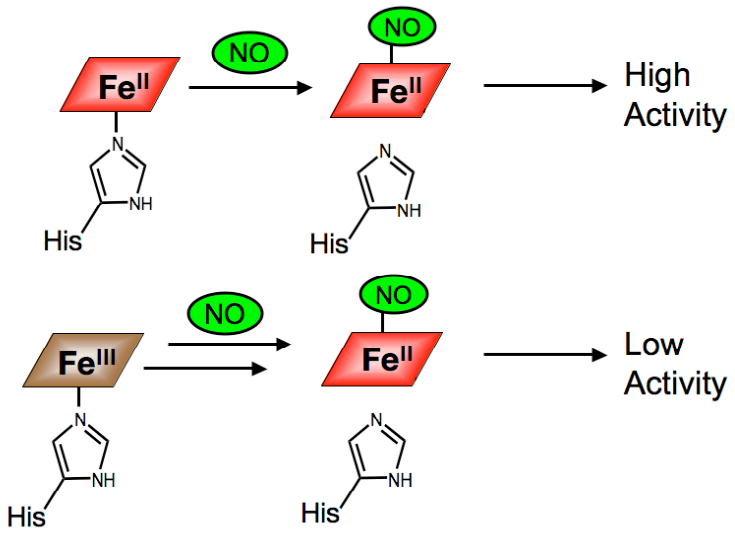

Figure 1: The paradox of reductive nitrosylation in sGC. Heme-reduced, ferrous [Fe(II)] sGC binds NO in a simple bimolecular interaction to form a ferrous-nitrosyl [Fe(II)-NO] complex that leads to full enzyme activation (*top*). Heme-oxidized, ferric [Fe(III)] sGC reacts with NO to form an identical ferrous-nitrosyl [Fe(II)-NO] complex, but has a low activity (*bottom*).

In this chapter, these observations are further investigated. To reconcile the simultaneous NO-desensitization and reductive nitrosylation of ferric [Fe(III)] sGC, we have discovered that a protein thiol, Cysteine 78, assumes the role of the chemically active nucleophile, instead of the hydroxide ion as shown in Scheme 1. This reaction yields a nitrosothiol, a one electron oxidized adduct of NO to a thiol, and we conclude that sGC couples heme iron reduction to thiol oxidation. Furthermore, the nitrosothiol formed in this reaction ultimately prevents the activation of sGC by NO. Therefore, the imprint of the heme oxidation is maintained by S-nitrosation, and this provides a chemical mechanism for NO-desensitization of ferric [Fe(III)] sGC. Part of this work was done in collaboration with Emily Derbyshire, in Michael Marletta's Lab (UC Berkeley)

Results and discussion*:*

The Reduced Stimulation of Ferrous-Nitrosyl Derived from Ferric sGC.

Using electronic absorption spectroscopy and EPR spectroscopy, Zhao and colleagues previously reported that the ferric [Fe(III)] heme cofactor of sGC undergoes reductive nitrosylation to the ferrous-nitrosyl [Fe(II)-NO] complex when exposed to NO, but NO only partially activates ferric [Fe(III)] sGC (*3*). To explain this partial stimulation, it was suggested that NO treatment may cause only a partial conversion to a fully active ferrous-nitrosyl [Fe(II)-NO]. To test this ligand occupancy hypothesis, an anaerobic sample of ferric [Fe(III)] sGC was treated with 100 μM of the NO donor

DEA/NO at 37 °C and allowed to completely convert to the ferrous-nitrosyl [Fe(II)-NO] complex. This reaction was monitored spectrally, as the Soret band of ferric [Fe(III)] sGC (λ_{max} = 392 nm) is readily differentiated from the Soret band of the ferrous-nitrosyl [Fe(II)-NO] complex (λ_{max} = 398 nm) (*17*) (Figure 2A). After 30 minutes, the reductive nitrosylation reaction was complete and the activity of the ferric-derived ferrous-nitrosyl [Fe(III)→Fe(II)-NO] complex was measured and compared to identically treated ferrous-derived ferrous-nitrosyl [Fe(II)→Fe(II)-NO] complex (Figure 2B). In direct contradiction to the ligand occupancy hypothesis, the fully formed ferrous-nitrosyl complex derived from ferric sGC [Fe(III)→Fe(II)-NO] is significantly inhibited relative to ferrous-nitrosyl complex derived from ferrous sGC [Fe(II)→Fe(II)-NO]. Therefore, during the process of reductive nitrosylation, a concomitant protein modification must occur to inhibit NO-stimulation of the enzyme. Similar results were observed under aerobic conditions.

Figure 2: The effect of NO on ferrous [Fe(II)] and ferric [Fe(III)] sGC at the heme and the active site. (**A**) Electronic absorption spectroscopy of ferrous [Fe(II)] sGC (grey dotted line) and the conversion to ferrous-nitrosyl [Fe(II)-NO] complex (grey solid line) in the presence of 50 μM DEA/NO, an NO donor, at 37 °C. Upon identical treatment, ferric [Fe(III)] sGC (black dotted line) converts to a spectrally identical ferrous-nitrosyl [Fe(II)-NO] complex (black solid line). (**B**) sGC activity was measured at 37 °C of the indicated treatments after completion of reductive nitrosylation, as assessed by a kinetically stable electronic absorption spectra.

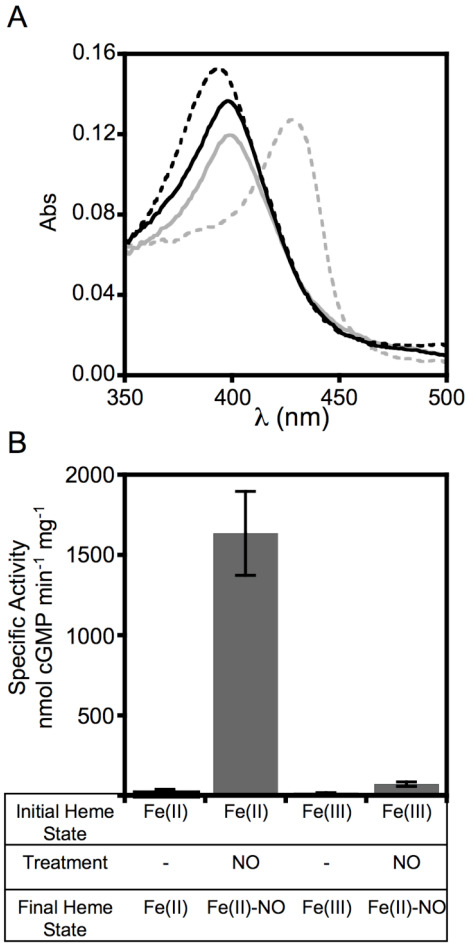

Previous reports have noted the constant activity of NO-stimulated ferric [Fe(III)] sGC over time (*4*). If the ferric-derived ferrous-nitrosyl [Fe(III)→Fe(II)-NO] complex had a high activity but slow rate of formation, then the NO stimulated activity of ferric [Fe(III)] sGC would increase over time. However, enzyme inhibition is constant during the active formation of the ferrous-nitrosyl [Fe(II)-NO] complex, and so the difference of initial heme oxidation state of must translate to another modification elsewhere on the protein during NO-stimulation.

Thiol Dependence of Reductive Nitrosylation in sGC.

The reductive nitrosylation reaction necessitates a one-electron reduction of the heme iron, and logically, an electron source must be simultaneously oxidized. Solvent mediated reduction is unlikely, since activity measurements indicate the protein itself is modified and because the experiments were performed without exogenous reductant. Cysteine thiols are redox active and cysteine modification frequently affects enzyme activity.

To test this proposal, we utilized the H-NOX domain of sGC consisting of β1(1-194). This domain has been shown to be the minimally sufficient portion of sGC to bind heme (*18*). β1(1-194) maintains similar ligand properties to full-length sGC and it can be recombinantly expressed in high yields from *Escherichia coli*. As such, it is a convenient model for ligand binding in full-length sGC. One pertinent discrepancy between the heme domain β1(1-194) and full-length sGC concerns the resting ferric [Fe(III)] state. Ferric [Fe(III)] full-length sGC exhibits a λ_{max} at 392 nm (Figure 2A) which has been unambiguously characterized by EPR as a high-spin 5-coordinate ferric heme state (*19*). Conversely, the heme domain truncations β1(1-194) and β1(1-385) do not maintain a stable ferric [Fe(III)] Soret band with a λ_{max} at 392 nm; rather the ferric [Fe(III)] forms of these domains readily convert to a species with a λ_{max} at 414 nm (Figure 3A) indicative of a low-spin 6-coordinate ferric heme, possibly in coordination with HO^-. For simplicity, we refer to this state as ferric [Fe(III)] with the implicit caveat that water or hydroxide may be bound at the heme in the resting state.

To assess the influence of cysteine thiols in reductive nitrosylation, the ferric [Fe(III)] form of β1(1-194) was treated with 500 μM DEA/NO for 12 minutes at 25 °C. Similar to full-length sGC, reductive nitrosylation proceeded with a spectral transition wherein the Soret band shifted from 414 nm to 399 nm, indicating a heme-state transition from the ferric [Fe(III)] state to the ferrous-nitrosyl [Fe(II)-NO] complex (Figure 3A). However, when cysteine thiols were alkylated with N-ethylmaleimide (NEM), the ferric [Fe(III)] β1(1-194) maintained a Soret band with a λ_{max} of 414 nm even after addition of 500 μM DEA/NO in identical conditions, indicating the heme state persisted as ferric [Fe(III)] (Figure 3B). The decrease in absorbance at 414 nm of NEM-treated protein signifies heme loss and implies a reduced affinity of thiol-alkylated β1(1-194) for heme. Similar heme loss was observed without the addition of NO. In summary, thiol alkylation completely prevented reductive nitrosylation, implicating cysteine thiols as the sole electron source in the reaction, and that hydroxide mediated reductive nitrosylation does not occur.

Figure 3: Thiol dependence of reductive nitrosylation in β1(1-194). (**A**) Native ferric [Fe(III)] β1(1-194) (solid grey line) was treated with 500 μM DEA/NO at 25 °C and converted to the ferrous-nitrosyl [Fe(II)-NO] complex. Electronic absorption spectra were acquired at 0.5, 1.5, 4, 8, (dotted black line) and 12 minutes (solid black line). (**B**) Thiol-alkylated β1(1-194) (solid grey line) was treated with 500 μM DEA/NO at 25 °C and no reductive nitrosylation was observed. Electronic absorption spectra were acquired at 0.5, 1.5, 4, 8, (dotted black line) and 12 minutes (solid black line). In the presence of 1 mM DTT and 500 μM DEA/NO at 25 °C, thiol-alkylated β1(1-194) fully formed the ferrous nitrosyl [Fe(II)-NO] complex in the same time interval (bold solid black line).

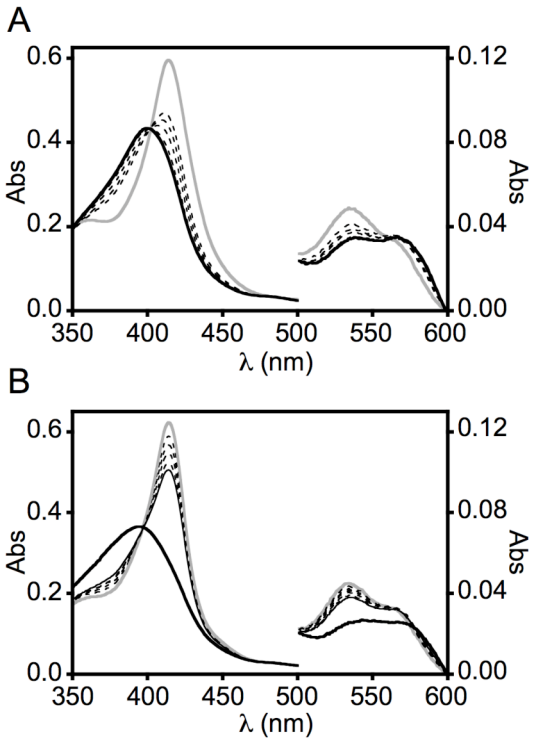

Chemical modification of a protein risks a broad impact on protein function, and therefore our results must be carefully investigated to demonstrate specific effects. Heme loss is observed upon incubation of NEM treated protein at 25 °C, even without addition of NO. Therefore, the effect of NEM treatment on general ligand binding was characterized to test the specificity of defective reductive nitrosylation in heme-bound alkylated β1(1-194) (Table 1). Thiol-alkylated ferric [Fe(III)] β1(1-194) competently bound cyanide, and underwent a similar spectral shift to cyanide-bound native ferric [Fe(III)] β1(1-194). This indicated that the NEM treatment does not block ligand access to the ferric [Fe(III)] heme or significantly alter the structure of the heme binding pocket. Importantly, just as [Fe(II)] ferrous native β1(1-194) bound CO and NO, thiol-alkylated ferrous [Fe(II)] β1(1-194) bound CO and NO, which demonstrates the stable formation of the ferrous-nitrosyl [Fe(II)-NO] complex. Because the ultimate product of the reductive nitrosylation reaction, namely a ferrous-nitrosyl [Fe(II)-NO] complex, can be stably formed by a different synthetic route in alkylated β1(1-194), a protein thiol must be involved in the actual chemistry of reductive nitrosylation. These data show that thiol alkylation specifically inhibits reductive nitrosylation, but does not inhibit ligand binding or the overall fold of the heme pocket.

Table 1: The Effect of Thiol Alkylation by N-ethylmaleimide on the Ligand Binding Properties of β1(1-194)[a]

Thiol State[b]	Initial Heme State	Treatment	Soret (nm)	α / β (nm)	Final Heme State
Native	Fe(III)	None[c]	414	565 / 535	Fe(III)
Native	Fe(III)	NO	399	570 / 538	Fe(II)-NO
Native	Fe(III)	NO / DTT	399	570 / 538	Fe(II)-NO
Native	Fe(III)	KCN	418	567 / 538	Fe(III)-CN
Native	Fe(II)	None[d]	427	560 / 531	Fe(II)
Native	Fe(II)	NO	398	568 / 539	Fe(II)-NO
Native	Fe(II)	CO	422	567 / 540	Fe(II)-CO
Alkylated	Fe(III)	None[c]	414	566 / 534	Fe(III)
Alkylated	Fe(III)	NO	414	566 / 534	Fe(III)
Alkylated	Fe(III)	NO / DTT	396	570 / 539	Fe(II)-NO
Alkylated	Fe(III)	KCN	417	567 / 538	Fe(III)-CN
Alkylated	Fe(II)	None[d]	427	560 / 531	Fe(II)
Alkylated	Fe(II)	NO	396	568 / 539	Fe(II)-NO
Alkylated	Fe(II)	CO	422	567 / 540	Fe(II)-CO

[a]Ligand binding assessed by electronic absorption spectroscopy with 5 – 10 μM β1(1-194) at 25 °C. [b]protein was either treated with 10 mM NEM (alkylated) or without (native) for 10 minutes at 25 °C and then desalted into 50 mM HEPES (pH 7.4) 50 mM NaCl. [c]β1(1-194) initially oxidized to a high-spin species which readily converts to a low-spin species as discussed in (*3*). This stable low-spin species was used in these experiments. [d]Due to an extremely rapid oxidation of the alkylated β1(1-194), dithionite was kept in excess to measure the spectral properties of ferrous β1(1-194).

Addition of exogenous thiol chemically rescues reductive nitrosylation of thiol alkylated β1(1-194). Upon treatment with 1 mM DTT and 500 μM DEA/NO, the Soret band of thiol-alkylated ferric [Fe(III)] β1(1-194) shifted from 415 nm to 399 nm, indicating a heme state transition from ferric [Fe(III)] to the ferrous-nitrosyl [Fe(II)-NO] complex (Figure 3B and 4). This data conclusively demonstrates that alkylated β1(1-194) is structurally competent to undergo reductive nitrosylation, but lacks the reduced thiol necessary to drive the reaction. Therefore, under native conditions, a protein thiol serves as an intramolecular reductant for the reductive nitrosylation of β1(1-194).

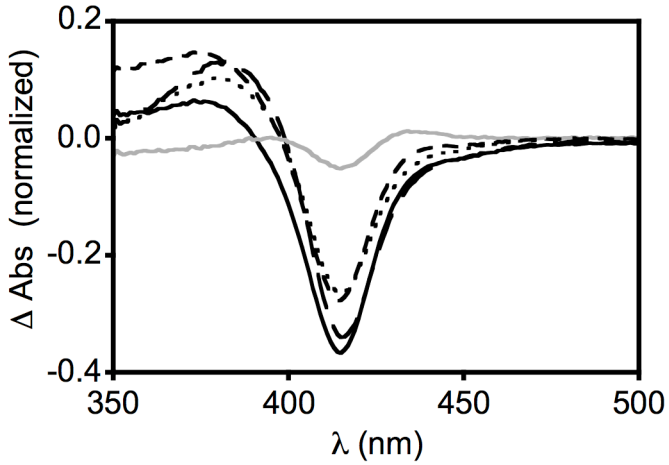

Figure 4: Chemical rescue of reductive nitrosylation in NEM-treated β1(1-194). Thiol-alkylated β1(1-194) was incubated with 250 μM DEA/NO and either 1 mM β-ME (solid black line), 1 mM DTT (long dashed line), 1 mM GSH (medium dashed line), 10 μM Trx (dotted black line), or 1 mM TCEP (solid grey line) for 15 minutes at 25 °C. For comparison, data is presented as a difference spectrum from the sample before NO addition, corrected for heme loss based on untreated thiol-alkylated β1(1-194), and normalized by the initial λ_{max} of the initial Soret band.

To further characterize the potential of exogenous thiol to drive reductive nitrosylation, thiol-alkylated β1(1-194) was incubated with various thiols and then treated with 250 μM DEA/NO for 10 minutes at 25 °C (Figure 4). As evidenced by the normalized difference spectra, co-incubation of NO with 1 mM glutathione (GSH), 1 mM β-mercaptoethanol (β-ME), 1 mM DTT, or 10 μM thioredoxin (Trx) all enable conversion to the ferrous-nitrosyl [Fe(II)-NO] complex. While β-ME, DTT, and GSH are small molecule thiol reductants (78 Da, 155 Da, and 307 Da, respectively), Trx (~14 000 Da) is much larger, suggestive of a size independence for thiol based chemical rescue. In contrast, the phosphine based reductant 1 mM tris(2-carboxyethyl)phosphine (TCEP) was not able to restore reductive nitrosylation, suggesting that either TCEP can not gain access to the heme or that the phosphine moiety is not capable of driving reductive nitrosylation chemistry. The spectral change associated with TCEP treatment is consistent with slightly accelerated rate of heme loss.

To assess the thiol dependence of reductive nitrosylation in full-length sGC, ferric sGC was alkylated with NEM. Interestingly, thiol alkylation induces a spectral shift in the Soret band from 392 nm to 413 nm, suggesting that the mechanism of water exclusion from the heme binding pocket in ferric [Fe(III)] sGC is disrupted with thiol alkylation. Whereas 50 μM DEA/NO at 37 °C reductively nitrosylated native ferric [Fe(III)] sGC (Figure 5A), identical treatment elicits no reaction of NEM-treated ferric [Fe(III)] sGC (Figure 5B). In response to NO, the Soret band of thiol-alkylated ferric [Fe(III)] sGC converted from 413 nm to 411 nm, indicating that reductive nitrosylation is entirely dependent on a free thiol in full-length sGC. Interestingly, the reductive nitrosylation of native ferric [Fe(III)] sGC shows clear isosbestic points (Figure 5C), demonstrating that reductive nitrosylation proceeds from the ferric [Fe(III)] form to ferrous-nitrosyl [Fe(II)-NO] complex with no accumulation of an observable intermediate. The relevance of this finding to the mechanism of reductive nitrosylation is discussed below.

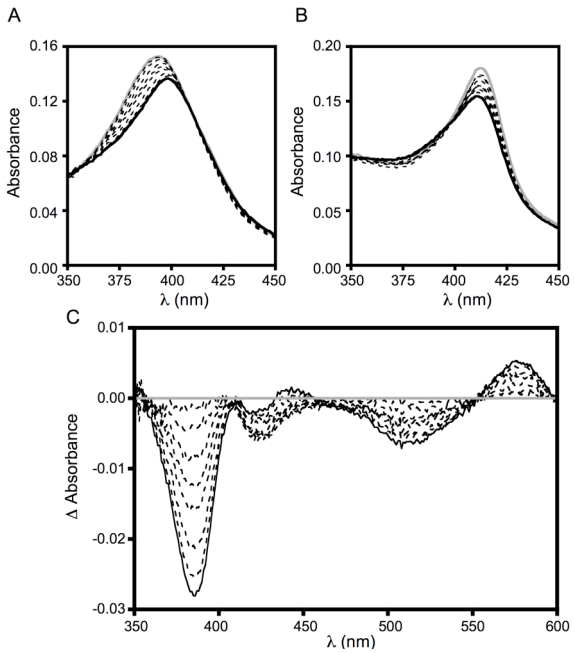

Figure 5: Thiol dependence of reductive nitrosylation in sGC. (**A**) Native ferric [Fe(III)] sGC (solid grey line) was treated with 50 μM DEA/NO at 37 °C and converted to the ferrous-nitrosyl [Fe(II)-NO] complex. Electronic absorption spectra were acquired at 0.5, 1.5, 3, 6, 8, 12, 16 (dotted black line) and 20 minutes (solid black line). (**B**) Thiol-alkylated ferric [Fe(III)] sGC (solid grey line) was treated with 50 μM DEA/NO at 37 °C and no reductive nitrosylation occurred. Electronic absorption spectra were acquired at 0.5, 1.5, 3, 6, 8, 12, 16 (dotted black line) and 20 minutes (solid black line). (**C**) Difference spectra of the reductive nitrosylation in (**A**).

The subtle spectral change observed after NO treatment of thiol-alkylated ferric [Fe(III)] sGC is most likely heme loss due to the thiol alkylation, as was similarly observed for β1(1-194). Furthermore, the observed change is consistent with a mixture between free heme and ferric [Fe(III)] sGC, however an alternate ferric conformation of the heme pocket can not be categorically dismissed. In either case, these studies reveal that reductive nitrosylation of ferric [Fe(III)] sGC is entirely dependent on a protein thiol.

Reductive Nitrosylation of the Heme is Coupled to S-nitrosation of an sGC Thiol.

Thiols can be oxidized by ROS and RNS to a variety of adducts including disulfides (R-S-S-R), sulfenic acids (R-SOH), sulfinic acids ($R\text{-}SO_2H$), sulfonic acids ($R\text{-}SO_3H$), and nitrosothiols (R-SNO). Because reductive nitrosylation requires a one-electron reduction of the heme, a chemical species that is a one-electron oxidation product of a reduced thiol, like a nitrosothiol, represents an intuitive candidate for the thiol modification. Furthermore, S-nitrosation has been shown to occur with the reductive nitrosylation of nitrophorin from *Cimex lectularius* (*12*). Therefore, we assessed the concomitant nitrosothiol formation on protein thiols during reductive nitrosylation of the heme.

The ferrous [Fe(II)] state of the sGC heme binds NO in a simple bimolecular association, and therefore the reaction proceeds without redox chemistry. Furthermore, thiol modification does not affect NO binding to the ferrous [Fe(II)] heme in full-length sGC (*20*) or the heme domain (Table 1), confirming the logical extension that thiol oxidation is not required to form the ferrous derived ferrous-nitrosyl [Fe(II)→Fe(II)-NO] complex. On the other hand, the thiol dependence of reductive nitrosylation strongly supports a concomitant thiol oxidation during the reductive nitrosylation of ferric [Fe(III)] sGC. A required coupling of *S*-nitrosation to reductive nitrosylation predicts that NO-stimulated ferric sGC would be differentially *S*-nitrosated over ferrous sGC.

To assess *S*-nitrosation coupled reductive nitrosylation, we employed the heme domain construct β1(1-385) which has a more stable ferrous [Fe(II)] oxidation state than β1(1-194). Furthermore, to detect nitrosothiols, we used the biotin switch method, which selectively replaces nitrosothiols with a biotin tag that can be used for subsequent analysis (*21*). Ferrous [Fe(II)] and ferric [Fe(III)] β1(1-385) were treated with increasing amounts of DEA/NO at 37 °C for 20 minutes in aerobic buffer and subjected to the biotin switch method (Figure 6A), however, nitrosothiols were formed irrespective of the initial heme oxidation state. The specificity of this assay relies on the absence of a direct reaction between NO and a thiol; however solution NO can react with oxygen to form higher nitrogen oxides, like N_2O_3, which potently reacts with thiols to form nitrosothiols (*22*). To increase the specificity of this assay, ferrous and ferric β1(1-385) were treated with increasing amounts of DEA/NO at 37 °C for 20 minutes in anaerobic buffer and subjected to the biotin switch method (Figure 6B). Here, nitrosothiol formation was only observed when ferric [Fe(III)] β1(1-385) was treated with NO but not when ferrous [Fe(II)] β1(1-385) was treated with NO. This differential *S*-nitrosation shows that reductive nitrosylation of the heme is coupled to *S*-nitrosation of a protein thiol. In aerobic conditions, this coupling still occurs, as *S*-nitrosation is observed on ferric β1(1-385), but the specificity over the ferrous [Fe(II)] state is masked by a background of *S*-nitrosation that occurs via the reaction between NO and O_2.

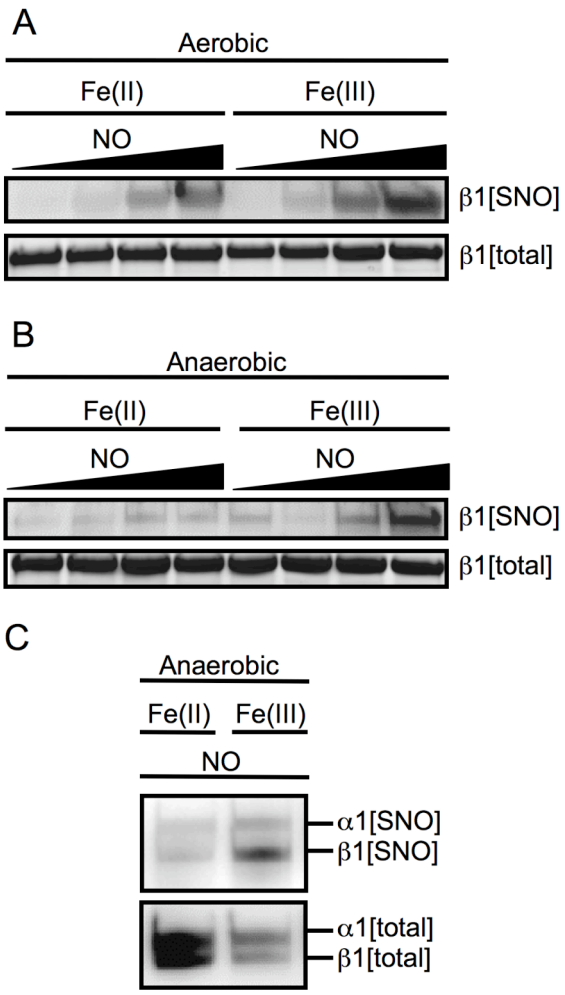

Figure 6: Selective S-nitrosation of ferric [Fe(III)] β1(1-385) and sGC. (**A**) Ferrous [Fe(II)] and ferric [Fe(III)] β1(1-385) were treated aerobically with (from left to right) 0, 10, 50, or 150 μM DEA/NO for 20 minutes at 37 °C and subjected to the biotin switch method. (*above*) Western blot detection of biotinylation, a surrogate for S-nitrosation. (*below*) Coomassie loading control. Both oxidation states were significantly S-nitrosated. (**B**) Ferrous [Fe(II)] and ferric [Fe(III)] β1(1-385) were treated as in (**A**) except anaerobically, but only the ferric [Fe(III)] form is S-nitrosated. (C) Ferrous [Fe(II)] and ferric [Fe(III)] sGC were treated as in (**A**) except anaerobically and the loading control is an anti-sGC western blot. Only the ferric form of sGC is S-nitrosated.

To investigate the coupled mechanism in full-length sGC, both ferric [Fe(III)] and ferrous [Fe(II)] sGC were treated with 150 μM DEA/NO at 37 °C for 20 minutes anaerobically (Figure 6C). As with the heme domain, ferric [Fe(III)] sGC was differentially *S*-nitrosated, indicating that reductive nitrosylation occurs concomitantly with *S*-nitrosation in the full-length enzyme. Therefore, the reduction of the heme iron is achieved through a coupled oxidation of the protein thiol, and this net electron transfer stably transforms a protein thiol into a nitrosothiol. Because NO causes both selective *S*-nitrosation and reduced activation of ferric [Fe(III)] sGC, this data evokes a strong correlation and suggests causation between S-nitrosation of an sGC cysteine and the NO-desensitization of ferric [Fe(III)] sGC.

S-nitrosation Causes Inhibition of Ferric [Fe(III)] sGC.

Despite the requirement of S-nitrosation for reductive nitrosylation in sGC, these results have not yet unequivocally identified a nitrosothiol as the inhibitory modification. Theoretically, the nitrosothiol need not directly inhibit enzyme activation, and one alternative explanation is a conformational kinetic trap of ferric [Fe(III)] sGC (Scheme 2). In this hypothesis, upon heme oxidation, the active site allosterically locks in a catalytically incompetent conformation that only slowly reverts to catalytic competence after reductive nitrosylation restores the ferrous-nitrosyl [Fe(II)-NO] complex. This hypothetical mechanism renders the nitrosothiol an artifactual bystander in the redox reaction, rather than an active role in inhibition. Heme oxidation can be reversed with dithionite and has been shown to restore full NO-sensitivity (*3, 19*), which argues against this hypothesis by demonstrating a conformational reversibility. However this reaction accesses the ferrous-unligated [Fe(II)] state of sGC whereas reductive nitrosylation of ferric [Fe(III)] sGC need not stably access this state in the formation of the ferrous-nitrosyl [Fe(II)-NO] complex. Because the routes differ from the ferric [Fe(III)] sGC state to the ferrous-nitrosyl [Fe(II)-NO] complex, the kinetic rates of interconversion may also differ even though the equilibria between the two states must be constant.

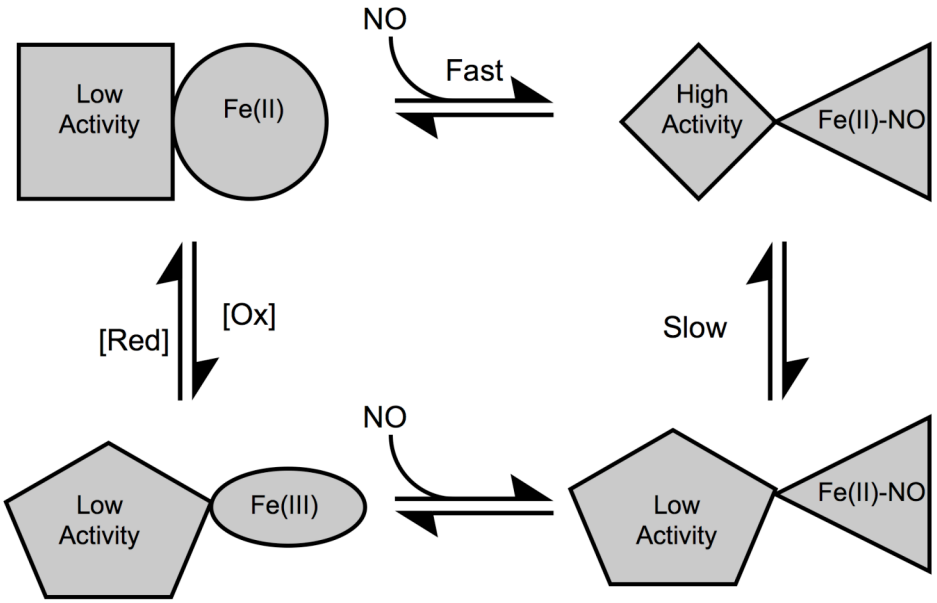

Scheme 2: Kinetic trap to cause an apparent NO-desensitization of ferric [Fe(III)] sGC

In light of this argument, the role of *S*-nitrosation in the inhibition of ferric [Fe(III)] sGC warrants further inquiry to differentiate a causative role from an artifactual role. Nitrosothiols are labile to thiol reductants, and the importance of this modification can be assessed by the chemical regeneration of the reduced protein thiol with DTT. The activity of ferric [Fe(III)] sGC was measured in the presence of both 150 μM DEA/NO and 1 mM DTT and compared to the NO-stimulated activities of ferrous [Fe(II)] and ferric [Fe(III)] sGC. As previously reported, the NO-stimulated activity of ferric [Fe(III)] sGC was inhibited relative to the NO-stimulated activity of ferrous [Fe(II)] sGC; however, DTT restored NO-sensitivity to ferric [Fe(III)] sGC (Figure 7). Similar results were obtained under anaerobic conditions. These data cumulatively demonstrate both that nitrosothiol formation correlates with enzyme inhibition and that nitrosothiol depletion correlates with an increase in enzyme activation. Therefore, these experiments reveal a causative role for *S*-nitrosation in the inhibition of ferric [Fe(III)] sGC.

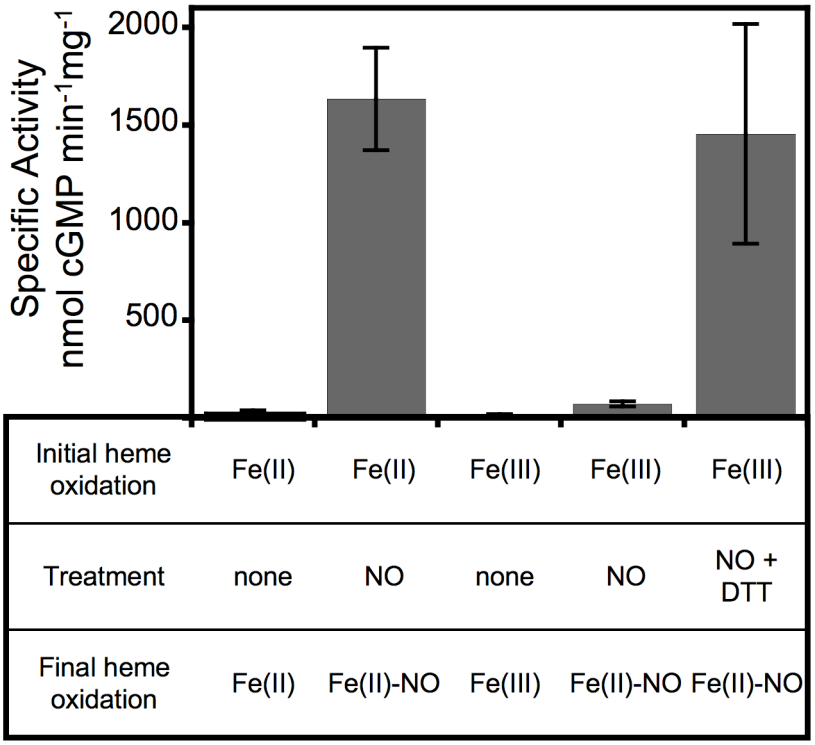

Figure 7: Thiol reductant restores NO-sensitivity to ferric [Fe(III)] sGC. sGC activity was measured as in Figure 1, however the addition of 1 mM DTT to ferric-derived ferrous-nitrosyl [Fe(III)→Fe(II)-NO], as indicated, permits full NO-activation.

Mapping the S-nitrosated Cysteine in β1(1-194).

sGC is a large and complex protein, containing 34 cysteine residues within two peptide chains that have a total combined molecular weight of ~150 kDa. The heme domain β1(1-194) is significantly simpler, with only 3 cysteine residues distributed in a single peptide chain that has a molecular weight of ~22 kDa. Since both sGC and the heme domain undergo reductive nitrosylation, we employed β1(1-194) as a model to identify which cysteine is responsible for reductive nitrosylation. Each of the cysteine residues (C78, C122, and C174) was systematically mutated to alanine in β1(1-194), and each mutant protein was expressed, purified, and characterized. Each was subjected to 250 μM DEA/NO at 25 °C and spectra were acquired over time to assess the kinetics of reductive nitrosylation. As previously discussed, native ferric [Fe(III)] β1(1-194) exhibits a transition in the Soret maximum from 414 nm to 399 nm (Figure 8A) when treated with NO, indicating a heme state conversion to the ferrous-nitrosyl [Fe(II)-NO] complex. β1(1-194) C122A and β1(1-194) C174A exhibit a similar spectral conversion, and therefore, C122 and C174 do not have a primary role in reductive nitrosylation. However, under identical treatment, β1(1-194) C78A exhibited a spectral transition in the λ_{max} of the Soret band from 414 nm to 408 nm (Figure 8B), likely indicating a transition between two different ferric Fe(III) states and dysfunctional reductive nitrosylation. Functional reductive nitrosylation was restored to β1(1-194) C78A in the presence of 1

mM DTT and 250 μM DEA/NO (Figure 8B bold line), which induces a Soret band at 399 nM, characteristic of the ferrous-nitrosyl [Fe(II)-NO] complex. The chemically rescued reductive nitrosylation reaction does not have an isosbestic point with the transition from the 414 nm species to the 408 nm species. This is a further indication that the 408 nm species reflects an alternate ferric [Fe(III)] state rather than a mixture of ferric [Fe(III)] heme and the ferrous-nitrosyl [Fe(II)-NO] complex. Since β1(1-194) C78A can undergo intermolecular reductive nitrosylation with DTT, the point mutant specifically inhibits the intramolecular reductive nitrosylation. These results delineate a critical role for C78 in the reductive nitrosylation of β1(1-194).

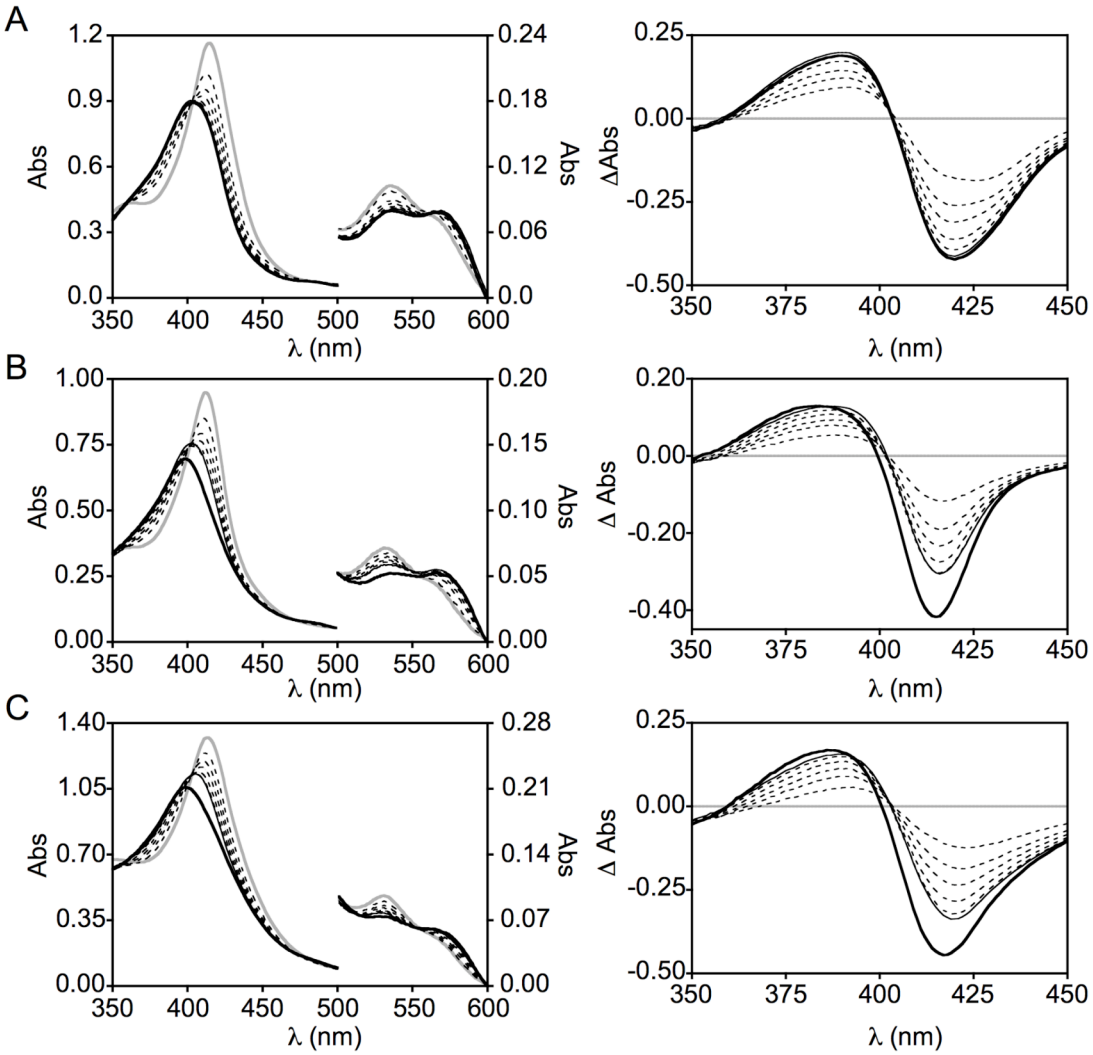

Figure 8: Inhibition of reductive nitrosylation in β1(1-194) C78A mutants. Ferric [Fe(III)] β1(1-194) (**A**) or β1(1-194) C78A (**B**) or β1(1-194) C78/122/174A (**C**) (solid grey line) was treated with 250 μM DEA/NO at 25 °C (*Left)* Electronic absorption spectra were acquired at 0.5, 1.5, 3, 5, 9, (dotted black line) and 17 minutes (solid black line). The identical reaction was run in the presence of 1 mM DTT for 8 minutes (solid bold black line). (*Right)* difference spectra of the reaction.

To further test the influence of C122 and C174, the cysteine-free mutant β1(1-194) C78/122/174A was expressed, purified, and characterized. Upon treatment with 250 μM DEA/NO at 25 °C, ferric [Fe(III)] β1(1-194) C78/122/174A exhibited identical properties as ferric [Fe(III)] β1(1-194) C78A. Specifically, a spectral transition occurred such that the Soret band shifted from 414 nm to 408 nm (Figure 8C), again indicating a transition between two different ferric [Fe(III)] states and dysfunctional reductive nitrosylation. Reductive nitrosylation was similarly rescued in the presence of 1 mM DTT (Figure 8C bold line) and 250 μM DEA/NO, which shifted the Soret maximum to 399 nm. The observation of identical properties of reductive nitrosylation between β1(1-194) C78A and β1(1-194) C78/122/174A C78A strongly suggests that C78 is entirely responsible for reductive nitrosylation of β1(1-194).

Although there is currently no high resolution structure of sGC, structures of homologous H-NOX domains have been solved by X-ray crystallography (*23-25*) and NMR spectroscopy (*26*). Homology modeling of the β1(1-194) protein using these structures shows that the thiol side chain of C78 is prominently exposed in the distal heme binding pocket (Figure 9). This location positions the nucleophilic sulfur of C78 directly next to a ligand bound to the heme iron. Therefore, C78 appears chemically primed for reductive nitrosylation, which we hypothesize to occur via inner sphere electron transfer (Figure 9).

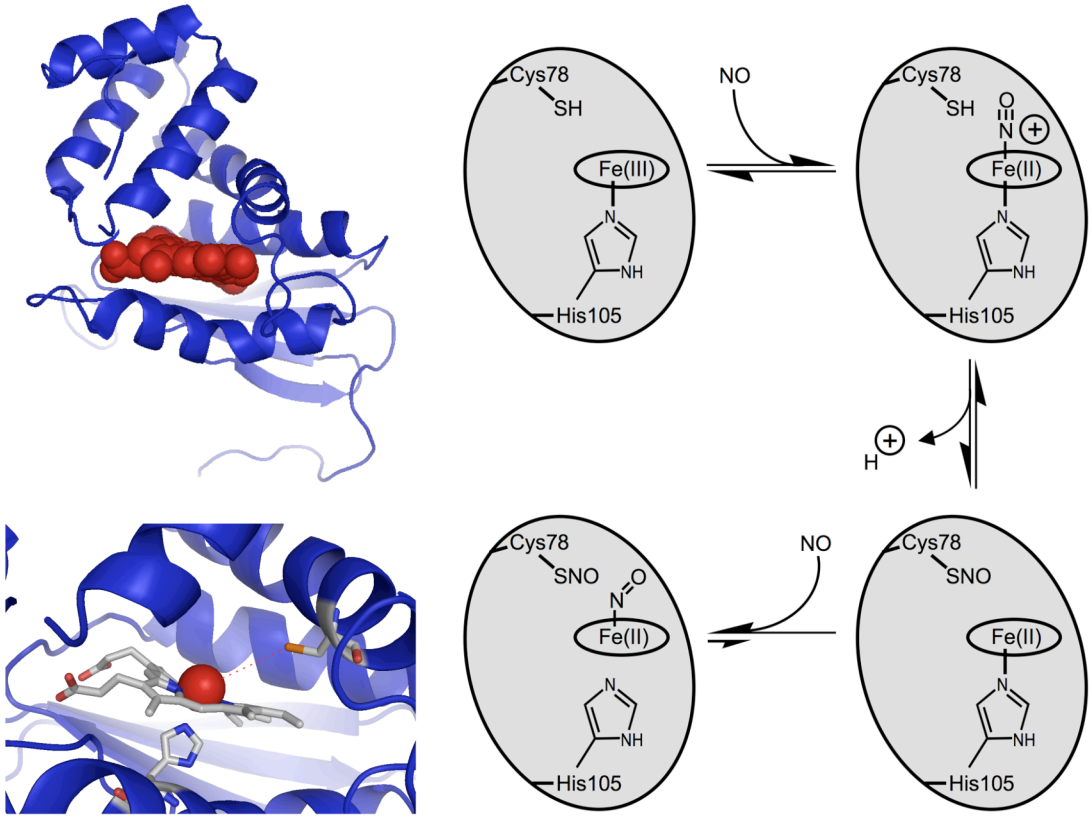

Figure 9: Proposed mechanism of coupling S-nitrosation of C78 to reductive nitrosylation of the heme in β1(1-194). (*Top left*) Homology model of β1(1-194) based on the structure of the H-NOX domain from *T. tengcongensis* with the heme highlighted as red spheres. (*Bottom left*) C78 lies in the distal heme pocket, in proximity to the heme iron. (*Right*) Inner sphere electron transfer from the C78 thiol to the ferric-nitrosyl [Fe(III)-NO] complex forms a nitrosothiol on C78 and reduces the heme, which can bind another equivalent of NO.

The reductive nitrosylation of full-length sGC is more complicated than that of β1(1-194). Preliminary experiments indicated that the C78 mutant undergoes faster reductive nitrosylation than wild-type but maintains NO-insensitivity. Therefore, while C78 may regulate this process in full-length sGC via trans-nitrosation, ultimately, *S*-nitrosation of a different key cysteine causes the inhibition of sGC activity. To ascertain the molecular identity of this key cysteine, peptide mapping for differential cysteine oxidation of NO-treated ferric [Fe(III)] sGC relative to ferrous [Fe(II)] is required and currently underway.

The Effect of Heme Pocket Nucleophiles.

As discussed above, both β1(1-194) C78A and β1(1-194) C78/122/174A undergo a spectral transition in Soret maximum from 414 nm to 408 nm in the presence of NO at 25 °C. This may reflect a spin state change of the heme iron, a protonation difference of

iron-bound water, or a different conformation of the heme pocket. In fact, a Soret shift to ~405 nm is observed in both the C78A and C78/122/174A mutants upon incubation at 25 °C without addition of the NO donor. Heme pocket nucleophiles can alter the coordination geometry of heme ligands and, in turn, affect the spectral properties of the heme-ligand complex (*27*). Therefore, both the absence of the nucleophilic thiol and the open space it would otherwise occupy are likely to promote an alternate coordination angle of bound [H]OH, and the observed instability of the 414 nm ferric [Fe(III)] state in the C78A mutants.

Because thiol nucleophiles were able to chemically rescue reductive nitrosylation of thiol-alkylated β1(1-194) (Figure 3C), the effect of the nucleophiles to restore ligand coordination in β1(1-194) C78/122/174A was assessed. The cysteine-free mutant was used to differentiate from any conformational effects resulting from differential cysteine oxidation states upon treatment with reductant. In the absence of exogenous reductant, the Soret band of β1(1-194) C78/122/174A shifted from 414 nm to a stable species at 405 nm upon incubation at 25 °C for 20 minutes, and various nucleophiles were subsequently incubated with this 405 nm species for an additional 15 minutes at 25 °C (Table 2). 1 mM DTT fully restores the 415 nm species, indicating that the nucleophile induced an identical coordination of the ferric [Fe(III)] ligand as native ferric [Fe(III)] β1 (1-194); whereas 1 mM GSH, 1 mM TCEP, or 10 μM Trx induce a shift to a 410 nm species, indicating an alternate ligand coordination or spin state. Furthermore, the 410 nm species is unlikely an equilibrium mixture of the 415 nm and 405 nm species, as lower concentrations of these nucleophiles maintained similar Soret bands at 410 nm. Interestingly, 1 mM β-ME did not significantly alter the spectral properties of the 405 nm species, however 5 mM β-ME induced the transition to the 410 nm species. Therefore β-ME only weakly binds to the protein, but when bound, it is likely in the same orientation as the other nucleophiles to induce the same spectral changes.

Table 2. The Effect of Various Nucleophiles on the λ_{max} for Either β1(1-194) or the Cysteine-Free Mutant β1(1-194) C78/122/174A[a]

Mutation	Heme Oxidation	Nucleophile	Soret (nm)
Wt	Fe(II)	None	426
Wt	Fe(III)	None	414
Wt	Fe(III)	1 mM DTT	415
C78/122/174A	Fe(II)	None	426
C78/122/174A	Fe(III)	None	405
C78/122/174A	Fe(III)	1 mM β-ME	406
C78/122/174A	Fe(III)	5 mM β-ME	410
C78/122/174A	Fe(III)	1 mM GSH	410
C78/122/174A	Fe(III)	10 μM Trx	410
C78/122/174A	Fe(III)	1 mM TCEP	410
C78/122/174A	Fe(III)	1 mM DTT	415

[a]Spectra were acquired after a 15 minute incubation at 25 °C with the indicated nucleophile.

The comparison of the chemical rescue of reductive nitrosylation to the chemical rescue of ferric ligand coordination yields insight regarding the nature of these reactions. Specifically, 1 mM TCEP was unable to restore reductive nitrosylation to the thiol alkylated β1(1-194), however 1 mM TCEP binds in the heme pocket of β1(1-194) C78/122/174A to alter the orientation of bound [H]OH. Therefore, TCEP accesses the heme, but the phosphine nucleophile is not chemically competent to drive reductive nitrosylation. Conversely, 1 mM β-ME was able to restore reductive nitrosylation to the thiol-alkylated β1(1-194), but 1 mM β-ME does not stably bind β1(1-194) C78/122/174A. Therefore, chemical competence for reductive nitrosylation does not require a stably bound thiol, but instead proceeds through a transient intermediate, as discussed below.

Mechanism of Reductive Nitrosylation in sGC.

Based on the data presented above, three chemically reasonable mechanisms warrant consideration (Scheme 3). The first possible mechanism is an inner sphere electron transfer, where a protein thiol or exogenous thiol reductant in physical proximity to the ferric-nitrosyl [Fe(III)-NO] complex (Scheme 3 Mechanism 1). The ferric-nitrosyl [Fe(III)-NO] complex is in resonance with a ferrous-nitroso [Fe(II)-NO^+] species, which has been suggested to predominate and bestow a linear geometry to this species (*9*). The electrophilicity of the nitroso group makes the N_{NO} susceptible to nucleophilic attack from the adjacent thiolate, a process that forms a transient covalent intermediate. The nitrosothiol product is formed and generates a ferrous Fe(II) heme, which is available for immediate nitrosylation by another equivalent of NO. This mechanism utilizes an inner sphere, two-electron transfer in the nucleophilic attack of the nitroso group, but outer sphere, one-electron transfer mechanisms have also been proposed for reductive nitrosylation reactions (Scheme 3 Mechanisms 2 and 3). These radical-based mechanisms rely on a one electron transfer from the thiolate to the ferric Fe(III) heme,

forming a thiyl radical which reacts quickly via radical recombination with NO to yield a nitrosothiol as the final product. The mechanism has two variations wherein the heme may be theoretically reduced in the ferric Fe(III) state before NO binding to the heme (Scheme 3 Mechanism 2) or in the ferric-nitrosyl Fe(III)-NO state after NO binding to the heme (Scheme 3 Mechanism 3). Because these mechanisms do not form a covalent intermediate between the reductant and the oxidant, there is no spatial requirement *per se* between the thiolate and the heme. Long-range electron transfer is a well studied phenomenon in proteins (*28, 29*), which relies on intervening tryptophans, tyrosines, and peptide bonds to provide local minima in potential energy to facilitate electron transfer. In sGC, the first mechanism (Scheme 3 Mechanism 3) is limited to C78 or a cysteine from another domain that may protrude into the heme binding pocket in the full-length enzyme. Conversely, the second and third mechanisms (Scheme 3 Mechanisms 2 and 3) have no distance constraint and therefore expand the number of potential cysteines involved in reductive nitrosylation.

Scheme 3: Mechanisms of S-nitrosation coupled reductive nitrosylation

Mechanism 1: Inner sphere electron transfer

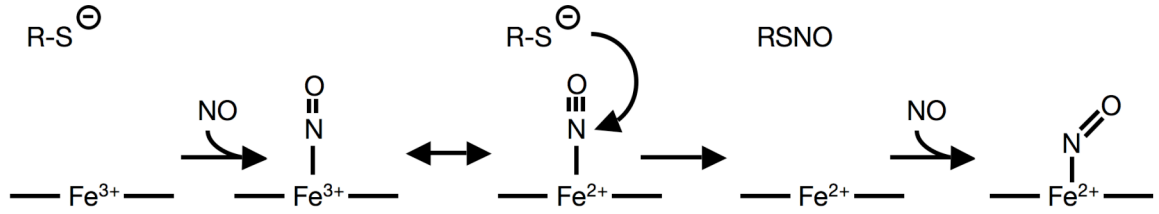

Mechanism 2: Outer sphere electron transfer to the ferric heme

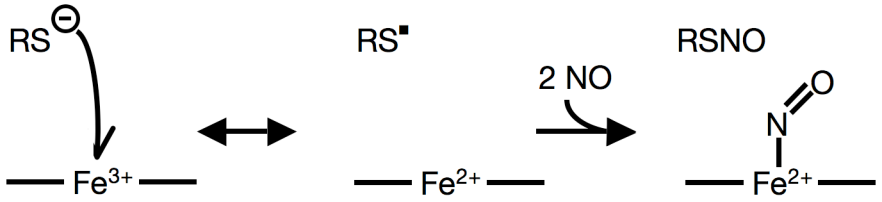

Mechanism 3: Outer sphere electron transfer to the ferric-nitrosyl heme

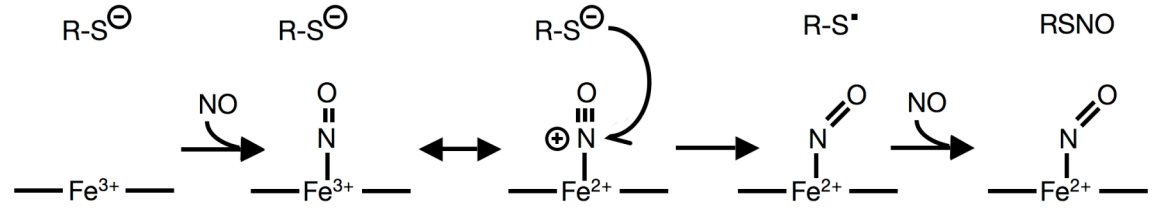

The kinetics of reductive nitrosylation present an apparent discrepancy with all three of these mechanisms. First, there are clear isosbestic points in the spectral transition from ferric [Fe(III)] heme to the ferrous-nitrosyl [Fe(II)-NO] complex for both sGC (Figure 5A) and β1(1-194) (Figure 8A), meaning no intermediate is observed between these two states. This data contrasts the reductive nitrosylation of globins, where a ferric-nitrosyl [Fe(III)-NO] complex forms rapidly and slowly undergoes reductive nitrosylation to the ferrous-nitrosyl [Fe(II)-NO] complex (*10*). The absence of an observable intermediate necessarily implies that the rate limiting step in the overall reaction occurs before the formation of the ferric-nitrosyl [Fe(III)-NO] complex, and that the downstream chemistry of reductive nitrosylation proceeds quickly preventing the accumulation of the intermediate. In the proposed mechanisms, the association between NO and ferric [Fe(III)] sGC is the only step that precedes the formation of ferric-nitrosyl [Fe(III)-NO]; and because it is bimolecular with NO, the observed rate of the overall reaction must depend linearly on the concentration of NO. However, the rate of reductive nitrosylation is zero order in NO (Figure 10), meaning that association of NO and ferric heme is not rate limiting. In summary, these proposed mechanisms uniformly require either a ferric-nitrosyl [Fe(III)-NO] intermediate or a kinetic dependence on [NO]; however, neither is observed.

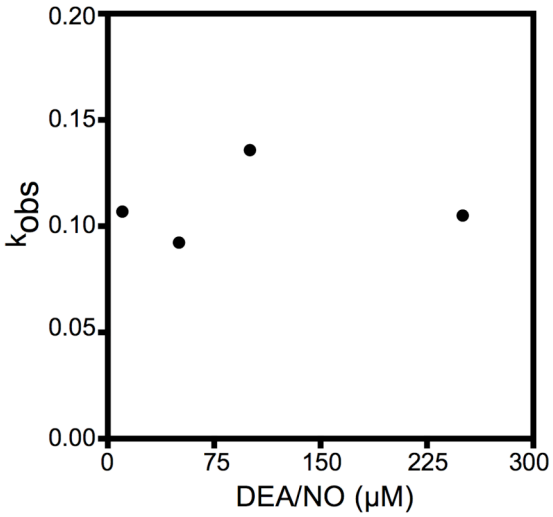

Figure 10: Kinetic saturation of reductive nitrosylation in full-length sGC. Ferric [Fe(III)] sGC was treated with the indicated amount of DEA/NO at 37°C and spectra were acquired over time. The rate of reductive nitrosylation was fit to a single exponential.

To reconcile these data, the simplest explanation invokes open and closed conformations of ferric [Fe(III)] sGC (Scheme 4). Here, only the open conformation of the protein associates with NO to form the ferric-nitrosyl [Fe(III)-NO] complex, whereas the closed form does not bind NO. Therefore, if the rate limiting step is the conformational change from the closed form to the open form, then the subsequent steps of NO binding and reductive nitrosylation will occur before the accumulation of any intermediate; which is consistent with the observed transition from ferric [Fe(III)] heme to the ferrous-nitrosyl [Fe(II)-NO] complex. Furthermore, the model predicts that the bimolecular association rate with NO does not affect the kinetics of reductive nitrosylation until such a low NO concentration that the observed rate of NO binding, k_1[NO], is on the order of the observed rate of the conformational change to the open state, k_{open}. Based on the rate of reductive nitrosylation at saturating NO concentrations (Figure 10), k_{open} is slow for this system (~0.1 min^{-1}) and k_1 is typically fast for heme proteins (> 10^6 min^{-1}) (*9*). Thus, the saturation of the reductive nitrosylation rate is expected at low μM NO, which is consistent with the measurements reported above.

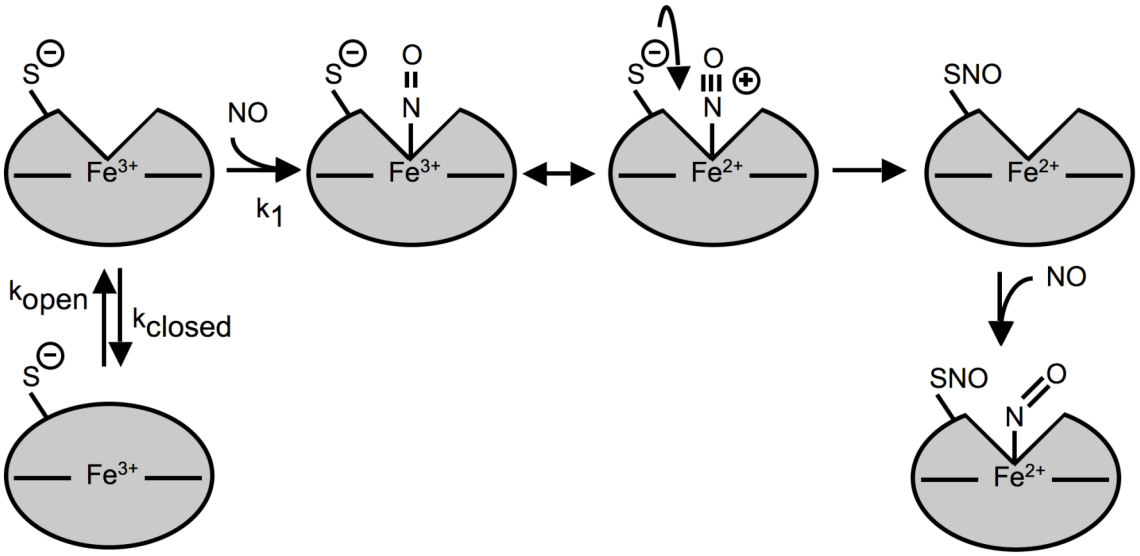

Scheme 4: Conformationally-gated inner sphere reductive nitrosylation in sGC

In further support of a regulatory conformational change, the kinetics of NO dissociation from ferrous sGC and the heme domains also indicate an equilibrium between such an open conformation and closed conformation that influences the NO off-rate (*30*). Additionally, the thermal dependence of the reductive nitrosylation reaction supports the notion of open and closed conformations of sGC. Zhao et al observed that reductive nitrosylation does not occur in sGC even with saturating NO gas at 10 °C (*3*), and we have similarly observed that the reaction does not proceed at 25 °C. However, reductive nitrosylation of sGC occurs at 37 °C in the presence of as little as 2 μM DEA/NO. A temperature dependence between the open and closed conformational states readily explains these results. Here, the closed conformation predominates at 25 °C, restricting access of the key cysteines to chemically competent positions. At 37 °C, the open conformation becomes accessible, and as the key cysteine moves into the appropriate position, and reductive nitrosylation ensues. In light of this model, the observation that reductive nitrosylation of β1(1-194) proceeds at 25 °C suggests that the other domains of sGC stabilize the thermal barrier between the open and closed states. Therefore, the conformationally-gated inner sphere (Scheme 4) represents the mechanism of reductive nitrosylation most consistent for β1(1-194), although other sGC cysteines may react via conformationally-gated outer sphere electron transfer.

Mechanism of sGC Inhibition.

The data unequivocally demonstrate that an sGC cysteine is the electron source for reductive nitrosylation, and that oxidation of this key thiol inhibits the enzymatic response to NO. Although the molecular identity of the key cysteine is currently undetermined, the model corroborates the mechanisms presented in Chapter 2. Specifically, it is reasonable to speculate that the specific cysteine residue which is oxidized in reductive nitrosylation of ferric [Fe(III)] sGC is the same cysteine residue that complexes the additional NO to mediate NO-activation of ferrous [Fe(II)] sGC. *S*-

nitrosation of the cysteine (formally a complex of thiolate and NO^+) blocks the nitrosylation of the cysteine (formally a complex of thiolate and $^{\cdot}NO$), which is required for enzyme activation. Despite the similarity of a nitrosothiol (RSNO) to the proposed addition complex ($RSNO^{\cdot-}$), the difference of one electron results in a dramatically different enzyme activity.

Implications for Human Health.

The data presented here shows that the ferric [Fe(III)] state of sGC is unstable in the presence of NO because of protein thiols, and enzyme inhibition is reversible with thiol reductants. *In vivo*, the production of NO in combination with the thiol redox buffer, in part consisting of GSH and Trx, seems to preclude the persistence of the ferric [Fe(III)] state of sGC in a cellular context. While the physiological relevance warrants further investigation, direct assessment of sGC heme state in a complex biological mixture is not yet possible with existing technology. However, the characteristics of reductive nitrosylation suggest conditions wherein the ferric [Fe(III)] state of sGC may persist. For instance, because the highly activated ferrous-nitrosyl [Fe(II)-NO] form of sGC is regenerated in the presence of exogenous thiol, the equilibrium ratio of high activity, reduced sGC to low activity, oxidized sGC will be a the ratio of the rate of reduction to the rate of oxidation. Therefore, instances of sustained, upregulated oxidant production would maintain the equilibrium population of low activity, oxidized protein. Similarly, decreasing the concentration of exogenous free thiol would decreases the regeneration rate of sGC activity, and so in instances of compromised thiol redox buffer, a temporary burst of oxidants would persistently inhibit sGC activity.

Conclusion

We have shown that the NO-desensitization of ferric [Fe(III)] sGC results from an inhibitory heme-assisted S-nitrosation. However, mechanisms other than heme oxidation have been suggested to disrupt functional sGC activity and cause disease. A recent report from the Beuve laboratory proposes that NO-desensitization of sGC results from the transnitrosation from endogenous small molecule nitrosothiols to specific sGC thiols (*31*). This would seemingly offer an independent corroboration that S-nitrosation of key thiols inhibits NO-stimulation by blocking the nonheme NO binding site. In their experiments however, the intended transnitrosation of an sGC thiol is convoluted by an unintended reaction that actually forms ferric [Fe(III)] heme. Specifically, a ferrous [Fe(II)] heme reacts with a nitrosothiol to yield a ferric [Fe(III)] heme, a free thiol, and NO (*32*) (Scheme 5 (1)). The newly formed NO then rapidly and tightly binds to a ferrous [Fe(II)] heme (Scheme 5 (2)), and the final product is a mixture of two different heme states: 50% ferrous-nitrosyl [Fe(II)-NO] complex and 50% ferric [Fe(III)] heme (Scheme 5 (3)).

(1) $$Hb[Fe(II)] + GSNO + H^+ \rightarrow Hb[Fe(III)] + GSH + NO$$

(2) $$Hb[Fe(II)] + NO \rightarrow Hb[Fe(II)\text{-}NO]$$

(3) $$2\ Hb[Fe(II)] + GSNO + H^+ \rightarrow Hb[Fe(III)] + Hb[Fe(II)\text{-}NO] + GSH + NO$$

Scheme 5: The reaction of nitrosothiols and ferrous [Fe(II)] hemoglobin

We have observed that purified sGC is subject to the same chemistry, and so experiments that involve the treatment of sGC with small molecule nitrosothiols, such as GSNO, must consider the inevitable oxidation of at least half of the sGC heme. This argument readily accounts for the observed ~50% inhibition of NO-stimulated sGC activity with GSNO pretreatment. Therefore, the NO-desensitization after GSNO treatment likely results from the formation of ferric [Fe(III)] sGC and subsequent heme-assisted *S*-nitrosation, rather than the direct transnitrosation from GSNO. While these biochemical characteristics of purified sGC indicate the ferric [Fe(III)] states facile formation, there are not currently methods to specifically detect this form of the enzyme in the complex biological milieu. Therefore, novel methods to quantify ferric sGC in tissue samples will greatly aid our understanding of the molecular causes for disease. Ultimately, this research provides a framework for understanding the capabilities of the enzyme and the mechanism of NO-desensitization of the ferric [Fe(III)] state of sGC.

Materials and Methods

Materials. Rat sGC α1β1, β1(1-194), and β1(1-385) were recombinantly expressed and purified as described previously (*30, 33*). The NO donor diethylammonium (Z)-1-(N,N diethylamino) diazen-1-ium-1,2-diolate (DEA/NO) and 1H-[1,2,4]oxadiazolo[4,3-a]quinoxalin-1-one (ODQ) were from Cayman Chemical Co and stock solutions were made in 10 mM NaOH and DMSO, respectively. NEM was from Sigma, and NO gas and CO gas were from Praxair. Recombinantly expressed human thioredoxin was a generous gift from Dr. Douglas Mitchell (University of Illinois at Urbana-Champaign). Primers were obtained from Elim Biopharmaceuticals. Sf9 cells were obtained from the Department of Molecular and Cell Biology Tissue Culture Facility, University of California, Berkeley.

Electronic Absorption Spectroscopy. Absorption spectra were collected on a Cary 3E spectrophotometer with a Neslab RTE-100 temperature controller. Spectra were collected over the range of 350-600 nm at 600 nm/min with a 1 nm data point interval. Anaerobic samples were prepared in septum-sealed cuvettes (Starna) by 10 cycles of alternate evacuation and purging with 99.999% argon (Praxair) or in an anaerobic chamber (Coy). Gas-tight syringes were used for all subsequent manipulations.

Preparation of ferrous and ferric complexes. Full-length sGC was desalted from DTT in the storage buffer by 4 cycles of dilution/concentration using a 10K Ultrafree-0.5 centrifugal filter device (Millipore) with 50 mM Hepes, pH 7.4, 50 mM NaCl at 4 °C. Ferrous sGC was used directly, and ferric sGC was prepared by further incubation with 100 μM ODQ for 1 hour at 0 °C followed by 2 additional cycles of dilution/concentration in 50 mM Hepes, pH 7.4, 50 mM NaCl. β1(1-194) and β1(1-385) were either treated with 1 mM $K_3Fe^{3+}CN_6$ (ferric) or 1 mM sodium dithionite (ferrous) for 1 hour at 4 °C in an anerobic chamber (Coy) and desalted by 6 cycles of dilution/concentration using a 5K Ultrafree-0.5 centrifugal filter device (Millipore) with 50 mM Hepes, pH 7.4, 50 mM NaCl at 4 °C. Heme states were spectrally assessed after each manipulation. The CO complex was formed by passing CO gas over the headspace of an anaerobic cuvette of ferrous [Fe(II)] β1(1-194) at 25 °C, and the NO complex was formed by subsequent addition of NO gas. The cyanide complex was formed by incubating ferric [Fe(III)] β1(1-194) with 20 mM NaCN for 20 minutes at 25 °C.

Preparation of NEM alkylated protein. Full-length ferric [Fe(III)] sGC was incubated with 500 μM NEM (thiol-alkylated) or sham-treated (native) for 20 minutes at 37 °C. Identical results were obtained whether or not excess NEM was desalted before reductive nitrosylation assays. β1(1-194) was treated with 10 mM NEM (thiol-alkylated) or sham-treated (native) for 15 minutes at 25 °C and excess NEM was removed by 6 rounds of dilution/concentration using a 5K Ultrafree-0.5 centrifugal filter device with 50 mM Hepes, pH 7.4, 50 mM NaCl at 4 °C.

Reductive nitrosylation of ferric proteins. Thiol-alkylated and native full-length ferric [Fe(III)] sGC were treated with 50 μM DEA/NO in 50 mM Hepes, pH 7.4, 50 mM NaCl at 37 °C and the reactions were followed spectrally over time. The kinetic dependence of

the reductive nitrosylation rate on the NO concentration was found by varying the initial concentration of DEA/NO. Electronic absorption spectra were acquired every minute for 60 minutes, as the protein converted from ferric [Fe(III)] to the ferrous-nitrosyl [Fe(II)-NO] complex. The difference in absorbance from 392 nm to 398 nm was plotted versus time, and the data were fit to a single exponential equation, which is reported as the observed rate. Reductive nitrosylation reactions of β1(1-194) were performed at 25 °C in 50 mM Hepes, pH 7.4, 50 mM NaCl and supplemented with reducing agent, where indicated. The amount of DEA/NO for each experiment is specified in the text, but similar properties were observed with concentrations between 10 μM and 500 μM DEA/NO under both aerobic and anaerobic conditions.

Activity assays. Duplicate end-point assays were performed at 37 ºC as previously described (*34*). Anaerobic samples of ferrous [Fe(II)] and ferric [Fe(III)] sGC were treated with and without 100 μM DEA/NO in 50 mM Hepes, pH 7.4, 50 mM NaCl. The ferric [Fe(III)] sample was monitored by electronic absorption spectroscopy in an anaerobic cuvette for 30 minutes. After the formation of the ferrous-nitrosyl [Fe(II)-NO] was confirmed the protein was added to an assay mixture to initiate the enzyme reaction. The final assay contained 0.2 μg of enzyme in 50 mM Hepes, pH 7.4, 3 mM $MgCl_2$, 1.5 mM GTP and, where indicated, 1 mM DTT in a final volume of 100 μL. Reactions were quenched after 2 min by the addition of 400 μL of 125 mM $Zn(CH_3CO_2)_2$ and 500 μL of 125 mM Na_2CO_3. cGMP quantification was carried out using a cGMP enzyme immunoassay kit, Format B (Biomol), per the manufacturer's instructions. All results are given as means ± SD.

Selective S-nitrosation of ferric sGC. Cysteine *S*-nitrosation in the presence and absence of O_2 and NO was examined by the biotin-switch method (*21*) with minor modification. Aerobically or in an anaerobic chamber, sGC or β1(1-385) was incubated with the indicated amount of DEA/NO for 20 minutes at 37 ºC in 50 mM Hepes, pH 7.4, 50 mM NaCl. Reactions were then quenched aerobically with an equal volume of 250 mM Hepes (pH 7.2), 1 mM EDTA, 0.1 mM neocuproine, 10% SDS, 120 mM NEM. Reactions were transferred to 65 ºC for 30 minutes and vortexed frequently. Samples were then acetone precipitated and the protein pellets were subsequently dissolved in 30 μl of 62 mM Hepes (pH 7.2), 0.25 mM EDTA, 0.025 mM neocuproine, 5% SDS, 1 mM maleimide-PEO_2-biotin (Pierce), 10 mM sodium ascorbate, and incubated for 1 hour at 25 ºC. The reactions were quenched by addition of SDS-PAGE loading buffer containing 50 mM DTT. The samples were then split and analyzed by both Neutravidin-HRP Western blot and Coomassie blue staining or anti-sGC Western blot.

Preparation of β1(1-194) mutants. Mutants of β1(1-194) were generated using the QuikChange XL site-directed mutagenesis kit (Stratagene), according to the manufacturer's instructions. Each substitution was verified by sequencing (University of California, Berkeley DNA Sequencing Facility), and recombinant β1(1-194) mutants were expressed and purified according to a previously described (*30*). The protein purity of all sGC mutants was assessed by SDS-PAGE, and was routinely greater than 95%. Protein concentrations were determined using the Bradford Microassay (Bio-Rad

Laboratories). Several mutants were isolated without a bound heme cofactor, and these mutants were reconstituted according to a previously published protocol (*35*).

Nucleophile treatment of β1(1-194) C78/122/174A. The cysteine-free mutant β1(1-194) C78/122/174A was prepared as native β1(1-194), described above. After desalting DTT in the storage buffer, the ferric [Fe(III)] protein was incubated at 25 ºC for 20 minutes such that a stable Soret band formed at 405 nm. This species was subsequently treated with the indicated nucleophile at the indicated concentration for 15 minutes, and assessed by electronic absorption spectroscopy.

References:

1. Ruetten, H., Zabel, U., Linz, W., and Schmidt, H. H. (1999) Downregulation of soluble guanylyl cyclase in young and aging spontaneously hypertensive rats, *Circ Res 85*, 534-541.
2. Harrison, D. G. (1997) Endothelial function and oxidant stress, *Clin Cardiol 20*, II-11-17.
3. Zhao, Y., Brandish, P. E., DiValentin, M., Schelvis, J. P., Babcock, G. T., and Marletta, M. A. (2000) Inhibition of soluble guanylate cyclase by ODQ, *Biochemistry 39*, 10848-10854.
4. Schrammel, A., Behrends, S., Schmidt, K., Koesling, D., and Mayer, B. (1996) Characterization of 1H-[1,2,4]oxadiazolo[4,3-a]quinoxalin-1-one as a heme-site inhibitor of nitric oxide-sensitive guanylyl cyclase, *Mol Pharmacol 50*, 1-5.
5. Stasch, J. P., Schmidt, P. M., Nedvetsky, P. I., Nedvetskaya, T. Y., H, S. A., Meurer, S., Deile, M., Taye, A., Knorr, A., Lapp, H., Muller, H., Turgay, Y., Rothkegel, C., Tersteegen, A., Kemp-Harper, B., Muller-Esterl, W., and Schmidt, H. H. (2006) Targeting the heme-oxidized nitric oxide receptor for selective vasodilatation of diseased blood vessels, *J Clin Invest 116*, 2552-2561.
6. Stasch, J. P., Schmidt, P., Alonso-Alija, C., Apeler, H., Dembowsky, K., Haerter, M., Heil, M., Minuth, T., Perzborn, E., Pleiss, U., Schramm, M., Schroeder, W., Schroder, H., Stahl, E., Steinke, W., and Wunder, F. (2002) NO- and haem-independent activation of soluble guanylyl cyclase: molecular basis and cardiovascular implications of a new pharmacological principle, *Br J Pharmacol 136*, 773-783.
7. Boerrigter, G., Costello-Boerrigter, L. C., Cataliotti, A., Lapp, H., Stasch, J. P., and Burnett, J. C., Jr. (2007) Targeting heme-oxidized soluble guanylate cyclase in experimental heart failure, *Hypertension 49*, 1128-1133.
8. Lapp, H., Mitrovic, V., Franz, N., Heuer, H., Buerke, M., Wolfertz, J., Mueck, W., Unger, S., Wensing, G., and Frey, R. (2009) Cinaciguat (BAY 58-2667) improves cardiopulmonary hemodynamics in patients with acute decompensated heart failure, *Circulation 119*, 2781-2788.
9. Hoshino, M., Laverman, L., and Ford, P. C. (1999) Nitric oxide complexes of metalloporphyrins: an overview of some mechanistic studies, *Coordination Chemistry Reviews 187*, 75-102.
10. Hoshino, M., Maeda, M., Konishi, R., Seki, H., and Ford, P. C. (1996) Studies on the reaction mechanism for reductive nitrosylation of ferrihemoproteins in buffer solutions, *Journal of the American Chemical Society 118*, 5702-5707.
11. Herold, S., Fago, A., Weber, R. E., Dewilde, S., and Moens, L. (2004) Reactivity studies of the Fe(III) and Fe(II)NO forms of human neuroglobin reveal a potential role against oxidative stress, *J Biol Chem 279*, 22841-22847.
12. Weichsel, A., Maes, E. M., Andersen, J. F., Valenzuela, J. G., Shokhireva, T., Walker, F. A., and Montfort, W. R. (2005) Heme-assisted S-nitrosation of a proximal thiolate in a nitric oxide transport protein, *Proc Natl Acad Sci U S A 102*, 594-599.
13. Luchsinger, B. P., Rich, E. N., Gow, A. J., Williams, E. M., Stamler, J. S., and Singel, D. J. (2003) Routes to S-nitroso-hemoglobin formation with heme redox

and preferential reactivity in the beta subunits, *Proc Natl Acad Sci U S A 100*, 461-466.
14. Basu, S., Keszler, A., Azarova, N. A., Nwanze, N., Perlegas, A., Shiva, S., Broniowska, K. A., Hogg, N., and Kim-Shapiro, D. B. A novel role for cytochrome c: Efficient catalysis of S-nitrosothiol formation, *Free Radic Biol Med 48*, 255-263.
15. Keilin, D., and Hartree, E. F. (1937) Reaction of Nitric Oxide with Haemoglobin and Methaemoglobin, *Nature 139*, 548.
16. Sancier, K. M., Freeman, G., and Mills, J. S. (1962) Electron spin resonance of nitric oxide- hemoglobin complexes in solution, *Science 137*, 752-754.
17. Stone, J. R., and Marletta, M. A. (1994) Soluble guanylate cyclase from bovine lung: activation with nitric oxide and carbon monoxide and spectral characterization of the ferrous and ferric states, *Biochemistry 33*, 5636-5640.
18. Karow, D. S., Pan, D., Davis, J. H., Behrends, S., Mathies, R. A., and Marletta, M. A. (2005) Characterization of functional heme domains from soluble guanylate cyclase, *Biochemistry 44*, 16266-16274.
19. Stone, J. R., Sands, R. H., Dunham, W. R., and Marletta, M. A. (1996) Spectral and ligand-binding properties of an unusual hemoprotein, the ferric form of soluble guanylate cyclase, *Biochemistry 35*, 3258-3262.
20. Fernhoff, N. B., Derbyshire, E. R., and Marletta, M. A. (2009) A nitric oxide/cysteine interaction mediates the activation of soluble guanylate cyclase, *Proc Natl Acad Sci U S A 106*, 21602-21607.
21. Jaffrey, S. R., and Snyder, S. H. (2001) The biotin switch method for the detection of S-nitrosylated proteins, *Science STKE 2001*, PL1.
22. Miersch, S., and Mutus, B. (2005) Protein S-nitrosation: biochemistry and characterization of protein thiol-NO interactions as cellular signals, *Clin Biochem 38*, 777-791.
23. Pellicena, P., Karow, D. S., Boon, E. M., Marletta, M. A., and Kuriyan, J. (2004) Crystal structure of an oxygen-binding heme domain related to soluble guanylate cyclases, *Proc Natl Acad Sci U S A 101*, 12854-12859.
24. Ma, X., Sayed, N., Beuve, A., and van den Akker, F. (2007) NO and CO differentially activate soluble guanylyl cyclase via a heme pivot-bend mechanism, *EMBO J 26*, 578-588.
25. Nioche, P., Berka, V., Vipond, J., Minton, N., Tsai, A. L., and Raman, C. S. (2004) Femtomolar sensitivity of a NO sensor from Clostridium botulinum, *Science 306*, 1550-1553.
26. Erbil, W. K., Price, M. S., Wemmer, D. E., and Marletta, M. A. (2009) A structural basis for H-NOX signaling in Shewanella oneidensis by trapping a histidine kinase inhibitory conformation, *Proc Natl Acad Sci U S A 106*, 19753-19760.
27. Soldatova, A. V., Ibrahim, M., Olson, J. S., Czernuszewicz, R. S., and Spiro, T. G. New light on NO bonding in Fe(III) heme proteins from resonance raman spectroscopy and DFT modeling, *J Am Chem Soc 132*, 4614-4625.
28. Stubbe, J., Nocera, D. G., Yee, C. S., and Chang, M. C. (2003) Radical initiation in the class I ribonucleotide reductase: long-range proton-coupled electron transfer?, *Chem Rev 103*, 2167-2201.

29. Purdy, M. M., Koo, L. S., de Montellano, P. R., and Klinman, J. P. (2006) Mechanism of O2 activation by cytochrome P450cam studied by isotope effects and transient state kinetics, *Biochemistry 45*, 15793-15806.
30. Winger, J. A., Derbyshire, E. R., and Marletta, M. A. (2007) Dissociation of nitric oxide from soluble guanylate cyclase and heme-nitric oxide/oxygen binding domain constructs, *J Biol Chem 282*, 897-907.
31. Sayed, N., Baskaran, P., Ma, X., van den Akker, F., and Beuve, A. (2007) Desensitization of soluble guanylyl cyclase, the NO receptor, by S-nitrosylation, *Proc Natl Acad Sci U S A 104*, 12312-12317.
32. Spencer, N. Y., Zeng, H., Patel, R. P., and Hogg, N. (2000) Reaction of S-nitrosoglutathione with the heme group of deoxyhemoglobin, *J Biol Chem 275*, 36562-36567.
33. Derbyshire, E. R., and Marletta, M. A. (2007) Butyl isocyanide as a probe of the activation mechanism of soluble guanylate cyclase. Investigating the role of non-heme nitric oxide, *J Biol Chem 282*, 35741-35748.
34. Derbyshire, E. R., Tran, R., Mathies, R. A., and Marletta, M. A. (2005) Characterization of nitrosoalkane binding and activation of soluble guanylate cyclase, *Biochemistry 44*, 16257-16265.
35. Derbyshire, E. R., Deng, S., and Marletta, M. A. Incorporation of tyrosine and glutamine residues into the soluble guanylate cyclase heme distal pocket alters NO and O2 binding, *J Biol Chem*.